Analysis of three close eclipsing binary systems: BP Velorum, V392 Carinae and V752 Centauri

A thesis submitted in partial fulfilment of the requirements for the degree of Master of Science

Hana Josephine Schumacher

2008

Department of Physics and Astronomy, University of Canterbury, Private Bag 4800, Christchurch, New Zealand

Abstract

This thesis reports photometric and spectroscopic studies of three close binary systems; BP Velorum, V392 Carinae and V752 Centauri.

BP Velorum, a W UMa-type binary, was observed photometrically in February 2007. The light curves in four filters were fitted simultaneously with a model generated in the eclipsing binary modeling software package PHOEBE. The best model was one with a cool star spot on the secondary larger component. The light curves showed additional cycle-to-cycle variations near the times of maximum light which may indicate the presence of star spots that vary in strength and/or location on a time scale comparable with the orbital period, ($P = 0^d.265$). The system was confirmed to belong to the W-type subgroup of W UMa binaries for which the deeper primary minimum is due to an occultation.

V392 Carinae, a detached binary with an orbital period of $3^d.147$, was observed photometrically by Michael Snowden in 1997. These observations were reduced and combined with the published light curve from Debernardi and North (2001). High resolution spectroscopic images were taken using the University of Canterbury's HERCULES spectrograph. The radial velocities measured from these observations were combined with velocities from Debernardi and North (2001). The radial velocity and light curves were fit simultaneously, confirming that V392 Car is a detached system of two main sequence A stars with a mass-ratio of 0.95. The derived systematic velocity is consistent with V392 Car being a member of the open cluster NGC 2516.

The W UMa-type binary V752 Centauri was observed photometrically and spectroscopically during 2007. The high resolution spectra displayed weak sharp lined features superimposed over the strong broad lined spectrum expected from the $0^d.370$ contact binary. Fourier methods were used to separate the broad and sharp spectral features and radial velocities for each were measured by cross-correlation. A fit to the photometry and radial velocities for the contact binary implied a system of two late F stars with a mass-ratio of 3.38 in an over-contact configuration. The derived systematic velocity ($-13.8 kms^{-1}$), has changed significantly from the 1972 value ($29.2 kms^{-1}$). The third (sharp lined) component's radial velocities were measured and found to have a period of $5^d.147$, semi-amplitude of $43.4 kms^{-1}$ and systematic velocity of $-7.3 kms^{-1}$. The likely configuration of the entire system is that of a contact binary in a long period orbit about a lower mass detached binary. V752 Cen is thus a triple lined spectroscopic quadruple.

Contents

List of Figures

List of Tables

Chapter 1

Introduction

1.1 Binary Systems of Stars: Historical overview

William Herschel first coined the phrase 'binary star' in 1802, to name 'a real double star - the union of two stars that are formed together in one system, by the laws of attraction' (Kopal, 1959). The term 'double star' had long been used to describe stars in close pairs. The Greek astronomer Ptolemy used it in his Almagest circa 150 A.D.(Ptolemaeus, 1952). However, not all double stars are gravitationally bound and these are therefore, not binary stars. The visual binary systems that Herschel and others observed marked the beginning of a long era of discovery regarding binary systems.

John Goodricke initiated the field of interacting binary stars with the publication of his paper in the Philosophical Transactions of the Royal Society, London, in 1783 (Sahade and Wood, 1978). In this paper he described his independent discovery and observations of the variations in brightness of Algol. The brightness variations of Algol actually had been detected over a century before by Montenari and Miraldi. There is evidence in the writings of ancient Chinese that these variations were known long before. Goodricke himself determined that the variations were periodic and deduced the period.

From the time Goodricke published this paper until the early twentieth century, the approach to observing eclipsing binaries followed the same patterns as for other variable stars. At the start of the twentieth century the observation techniques available were photography, spectroscopy and photoelectric photometry. Throughout the twentieth century, as the technology of observations improved and fainter objects became observable, the vast occurrence of binary systems became apparent. Recent estimates state that over

80% of all stars may be members of binary systems (Smith, 1995).

The analysis of binary systems can result in the determination of important properties of stars. The fundamental property of mass can be determined without external models from the gravitational effect of some binary systems. Stellar mass is the most intrinsically important property of stars. The knowledge of the initial mass and chemical composition of an isolated star can provide information related to its structure and subsequent evolution (Ramm, 2004).

1.2 Eclipsing Binary Stars

Binary star systems contain two stars gravitationally bound orbiting about their common center of mass. Eclipsing binary systems, EBs, are systems where the orbital plane lies close to, if not aligned with, the plane of the observer, that is the inclination of the orbit is close to 90° (see Figure 1.1). The alignment of the orbital plane with the plane

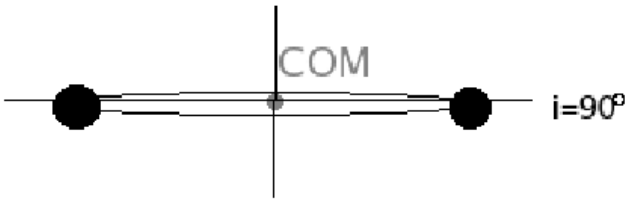

Figure 1.1: *The orbital plane of the objects as seen from the Earth.*

of the Earth means the stars eclipse each other periodically. The angular separation of the components as seen from the Earth is not great enough for the components to be resolved individually. The discovery and detection of eclipsing binary systems comes from measuring the variation of the intensity of light through photometry. The observed light intensity varies as the stars move through their orbits. The light curves clearly show the effects of movement of the components of the system.

Spectroscopic observations of eclipsing binaries show whether the systems are double-lined, SB2, or single-lined, SB1, spectroscopic binaries. When used in conjunction with

light curve data double-lined spectroscopic binaries can be used to determine the individual masses of the stars, their radii, the ratio of their fluxes and hence the ratio of their effective temperatures. Equipped with the photometric and spectroscopic orbital solutions of an eclipsing binary, a star's radius can be estimated to a high precision, indicating the star's evolutionary state (Ramm, 2004).

The components in close binary systems have undergone gravitational stresses which have resulted in circular and synchronous orbits. Stellar rotation through the tidal bulge raised by the companion's gravitational pull, causes the star to pulsate. Orbital and rotational energy are dissipated until the system reaches the state of minimum energy for its constant angular momentum which inspires synchronous rotation and circular orbits (Carroll and D.A. Ostlie, 1996).

In the cases where the binary system's components are well detached, the separate components undergo stellar evolution as one would expect from a single star. The gravitational effect from the companion star does not appreciably alter the shape of the star. However, in the cases where the separation of the components is very little, there is mass exchange between the components, and their evolutionary progress departs that of a single star corresponding to the same position on the main sequence of an H-R diagram (Sahade and Wood, 1978). These are known as *interacting* or *contact* binaries.

Contact binary systems are defined to be systems 'which have both components surrounded by a common envelope lying between the inner and outer Lagrangian zero-velocity equipotential surfaces' (Mochnacki, 1981). Systems which are of spectral type F0 and later are usually referred to as W Ursae Majoris stars (W UMa).

1.3 Classification of Close Binary Systems: The Roche Model

The classification of close binary systems is based on the relationship of the components to the closed equipotential surfaces surrounding each star (Kopal, 1959). The Roche model deals with the restricted three body problem, the two stellar bodies acting as point masses with a third body; a point with infinitesimal mass to ensure no gravitational interference with the stars. The Roche model can be applied to close binaries if it is assumed that the stars' masses are centrally condensed in circular orbits with synchronous rotation. In contact configurations, the Roche model still stands, as stars that share a common envelope (photosphere) have 90% of their mass within half of the radius from the centre

of the star. In this region the equipotential surfaces are nearly spheres so the attraction on a point near the exterior of the star is approximately the same as for the Roche model (Sahade and Wood, 1978). The closer a stellar surface is to an equipotential surface the more it takes the shape of that surface.

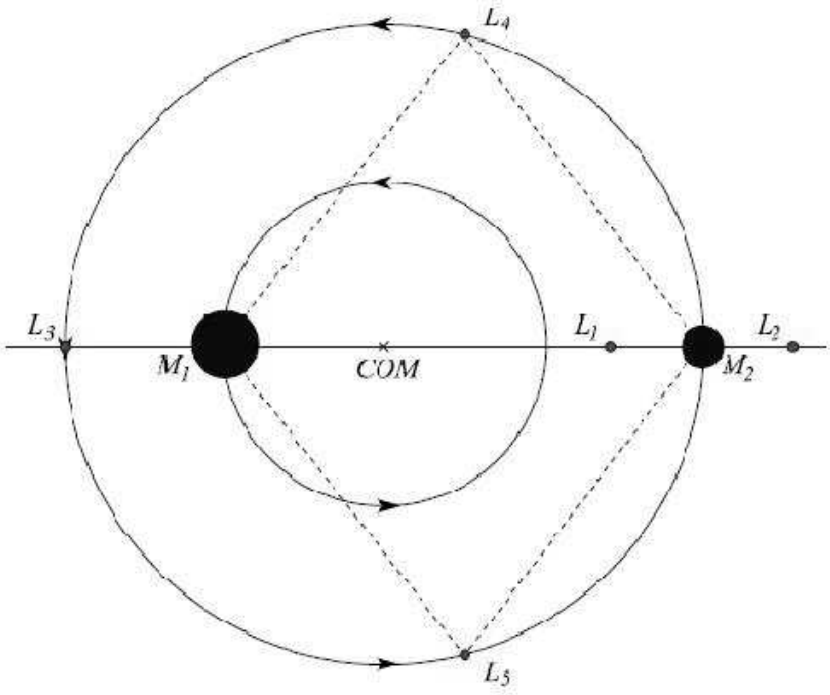

Figure 1.2: *A schematic diagram of the Lagrangian points in the Roche model from PHOEBE Scientific Reference (Prša, 2006).*

The surfaces are also known as the zero-velocity or Roche surfaces, with the shape of these surfaces depending on the Lagrangian points. Lagrange's work established points in the rotating field of the two massive bodies where the third body has zero velocity; these are known as the Lagrangian points. The first of these points is located on the axis between the two massive bodies. This is often called the inner Lagrangian point L_1, and it is an unstable equilibrium point. The Roche surfaces that meet at this point are called the Roche limits. They encompass the Roche lobes, a critical feature in the classification of close binary systems. There are two more Lagrangian points along this axis; L_2 is located beyond the outer surface of the lesser mass, L_3 is similarly located outside the outer surface of the larger mass. There are two other Lagrangian points corresponding to potential maxima, L_4 and L_5. They form equilateral triangles with the two masses. The inner Lagrangian point is the point at which the stars may exchange mass with each other,

depending on whether their respective Roche lobes are filled or not. L_2 and L_3 provide a route to which the system as a whole can lose mass. The filling of the Roche lobes may be determined through the fill-out factor which can be derived from the normalised total potential $\psi(\mathbf{r}, q)$ at point $\mathbf{r}$ (Mochnacki and Doughty, 1972):

$$\psi(\mathbf{r}, q) = \frac{2}{1+q}\frac{1}{r_n} + \frac{2q}{1+q}\frac{1}{r_l} + p^2 = C, \tag{1.1}$$

where q is the mass ratio of the lighter mass m_l, with the heavier mass m_h. The distance from $\mathbf{r}$ to the center of the lighter and heavier components, r_l and r_h respectively, p is the perpendicular distance from the axis of rotation. Equipotential surfaces are classified by the constant C of $\psi(\mathbf{r}, q)$ (Mochnacki and Doughty, 1972). The fill-out ratio F, is used to determine the degree to which the equipotential surface of the photosphere fills its corresponding Roche lobe. C_p is the photospheric potential, $C_1(q)$ is the constant corresponding to the Roche limit, and $C_2(q)$ is the constant for the second Lagrangian surface L_2. For a completely detached binary the fill-out ratio is defined as

$$F = \frac{C_1}{C_p}, \tag{1.2}$$

where $C_p \geq C_1(q)$ and $0 < F \leq 1$. For a contact configuration, the fill-out factor is

$$F = \frac{C_1 - C_p}{C_1 - C_2} + 1, \tag{1.3}$$

where $C_1(q) \geq C_p \geq C_2(q)$ and $1 \leq F \leq 2$. Note for the contact configuration the entire envelope over both components is specified by a single surface potential value, C_p (Mochnacki and Doughty, 1972).

The fill-out factor is a convenient way to determine the configuration of the close binary system. Kopal (1959) specifies 3 categories from the Roche model classification scheme with two additional sub-categories;

1. **Detached systems**: the Roche limit is not exceeded by either component. The components' shapes are determined by inner Roche surfaces and are nearly spherical.

2. **Semi-detached systems**: one component exactly fills its Roche limit. There is mass transfer via the inner Lagrangian point L_1.

3. **Contact systems**: both components fill their Roche lobes.

3a. **Double-contact systems**: 'each component fills a critical lobe. However, one component rotates super synchronously owing to it being spun-up by accreting material. Its critical surface is not bounded by the inner Lagrangian surface, but instead is bounded

by the equipotential that has equatorial material rotating at close to the centrifugal limit.' (Ramm, 2004).

3b. **Over-contact systems**: the systems have the components surrounded by a common convective envelope.

W UMa-type contact binaries fall into the over-contact category. Figure 1.3 illustrates three configurations, the inside dotted line depicts the Roche limit. The top figure is a detached binary, the middle figure is a semi-detached configuration, the bottom illustration shows an over-contact configuration.

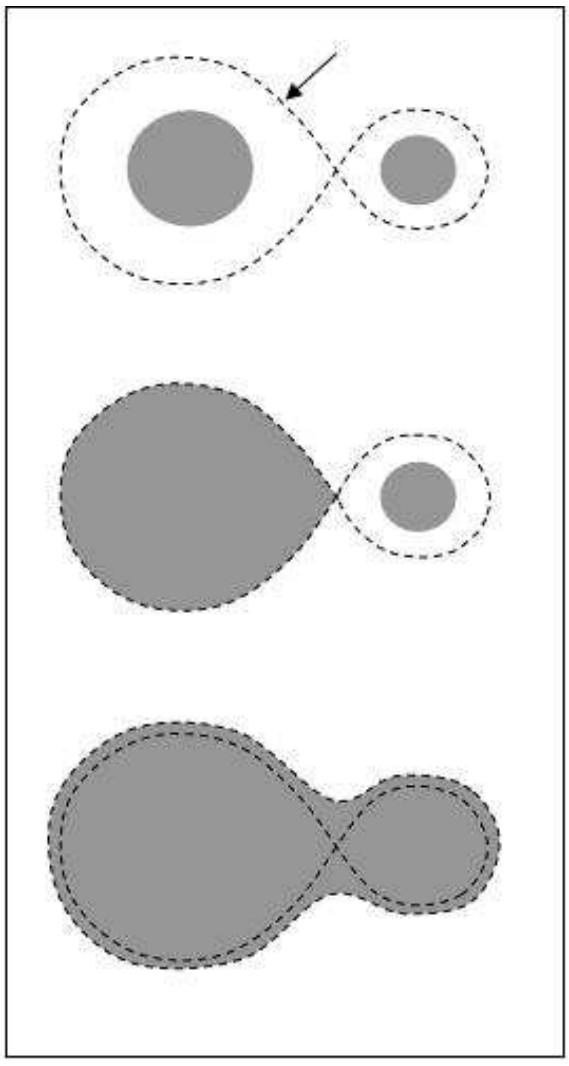

Figure 1.3: *An illustration of the various configurations of close binary stars as given by the Roche Model.*

1.4 W UMa-type Binaries

W Ursae Majoris systems are prolific in the contact binary population, they are of spectral type F0 and later. The large population of W UMa-type binaries indicate that they are not all formed as a result of detached binaries evolving into contact and were therefore created as binaries in contact on the zero-age main sequence, ZAMS (Lucy, 1968b). They typically have very short periods ($\leq$0.5 days), which often makes it possible for complete light curves to be observed in one night. Their light curves show strong characteristics. The light variation is continuous, with the minima nearly equal in depth (Lucy, 1968a).

W UMa-type systems can be further classified into two sub-groups; A-type systems and W-type introduced by Binnendijk (1965). The W-type systems are defined as having the primary minimum resulting from an occultation of the secondary, less massive component; A-type systems have the deeper minimum corresponding to a transit of the secondary in front of the primary, more massive component (Mochnacki, 1981).

Generally A-type systems are of earlier spectral type and more evolved (Mochnacki, 1981). A-type systems generally have lower mass ratios and a higher degree of contact than W-type systems. Light curves of W-type systems often have asymmetries, whereas in light curves from A-type systems asymmetries are more moderate or even absent.

Lucy (1968b) proposed a model with a convective envelope surrounding the two components that allowed W UMa-type binaries to be created on the ZAMS with different initial radii. The convective envelope model successfully interpreted the characteristics of the distinctive light curve of W UMa-type binaries, while simultaneously explaining the near equal temperatures and luminosities of the components even though they can have highly different masses (Csizmadia and P. Klagyivik, 2004).

Hilditch (2001), explains the general consensus surrounding the formation of W UMa-type contact binaries being that they formed from detached systems of low mass and orbital periods of 1 day or less. Orbital angular momentum is lost from the detached system due to magnetic stellar wind causing the orbit to shrink. The shrinking of the orbit leads to the shrinking of the Roche lobes to the extent where overflow of the Roche lobe occurs by the primary onto the secondary. Eventually contact is made, though this can be tenuous as the system alternates about a state of marginal contact for an uncertain length of time before coalescing into a single star (Vilhu, 1982; Bradstreet and Guinan, 1994).

The earlier contact systems of types O, B, and A, are not classified as W UMa-type binaries because their components' radiative properties do not support the common

envelope theory of Lucy (1968a).

1.5 Motivation for this work

The three targets analysed in this work are displayed in table 1.1. They were selected on a criteria comprising of a few complimentary points. Firstly, the targets' observability from the telescope facilities at Mt John University Observatory and the time frame under which the thesis was to be conducted. The suitable candidates from the initial sorting were contemplated and decided upon regarding their exposure in literature.

The target BV Velorum has previously been observed photoelectrically with the results published in Lapasset et al. (1996). The faint magnitude of BP Velorum has made it difficult to study spectroscopically. The photometric observations of this target used in this thesis were undertaken during one week using the Optical Craftsman telescope at Mt John University Observatory mounted with the SBIG ST-9 CCD camera. The solution determined by Lapasset et al. (1996) provides a good check on the methods used throughout this thesis. The faintness of the target meant that no spectroscopic observations were made as it was beyond the limits of the HERCULES instrument.

V392 Carinae, also nominated Cox 38, belongs to the open cluster NGC 2516. It was observed photometrically at the European Southern Observatory, La Silla, Chile from January 1978 to January 1991. Spectroscopic observations were performed at the same sight over two nights during February 1991. The orbital elements of V392 Car were calculated by Debernardi and North (2001) who found the system was indeed a member of NGC 2516 and that the stars were of spectral type A2. The phase coverage of the spectroscopic observations is very poor. We were approached by Michael Snowden to make further spectroscopic observations of this star to combine with imaging photometry he had undertaken in 1997.

V752 Centauri has been analysed both photometrically and spectroscopically. Complete light curves were observed photoelectrically in 1971 by Sisteró and Castore de Sisteró (1973) and radial velocity curves were measured from spectrograph observations taken in 1972 (Sisteró and Castore de Sisteró, 1974). Leung (1976) reanalysed the observations taken by Sisteró and Castore de Sisteró using the Wilson and Devinney code. Barone et al. (1993) reanalysed the archival data for V752 Centauri in 1993 with their Wilson-Price code.

The repeated analysis of V752 Centauri each time used the observations from Sisteró and Castore de Sisteró, made in the early 1970s. New observations of V752 Centauri were

Name	R.A. (J2000)	Dec. (J2000)	V max. mag.	Period
BP Velorum[1]	$08^h18^m05.8^s$	$-45°23'26''$	12.9	$0^d.2649859700$
V392 Car[1]	$07^h58^m10.5^s$	$-60°51'57.2''$	9.48	$3^d.174990^*$
V752 Cen[1]	$11^h42^m48.1^s$	$-35°48'58''$	9.1	$0^d.37022484$

Table 1.1: *The details of the three stars analysed in this thesis.*
[1] *VizieR catalogue information (Viz).*
[*] *Period taken from Debernardi and North (2001).*

completed for this research at the Mt John University Observatory. The photometric observations were obtained with the SBIG ST-9 CCD attached to the O.C. telescope, while the spectroscopic observations were made using the 1m McLellan telescope and the high resolution HERCULES spectrograph. The resulting high resolution spectra provided more information on the system.

Chapter 2

Observations

The photometric and spectroscopic observations used in this work were all taken at Mt John University Observatory (MJUO), Lake Tekapo, New Zealand (170° 27.9′ E, 43° 59.2′ S).

2.1 Photometry

The light curves of the three EB's were obtained from photometric observations conducted with the 0.6m Optical Craftsman telescope.

The photometric observations for BP Velorum and V752 Centauri were taken by the author, using the Optical Craftsman telescope, (O.C.), from February to April 2007. The O.C. is a 0.61m reflector with a cassegrain focus of f/16 equipped with the AAVSO CCD. The CCD camera is a SBIG ST-9e type. It is 512 by 512 pixels, each $20\mu\ m \times 20\mu\ m$ in size, corresponding to a 9′ by 9′ field of view of the sky. The gain is 2.4 electrons per A.D.U. The CCD is thermoelectrically cooled to at least 10° below ambient temperature. The camera has a filter wheel with four colours; B,V,R and I in the Johnson-Cousins system. It is operated with the CCDSOFT software which can be programmed to capture an image through each of the filters in turn. The Infrared filter was the most sensitive leading to shorter exposure times. The exposure times for each filter were varied from night to night depending on the atmospheric seeing.

Dark, bias, and flat field frames were taken once or twice during each run of observations. The flat field images, in each filter, were obtained using a light mounted to the wall of the telescope building shining onto a white screen.

2.2 Spectroscopy

The High Efficiency and Resolution Canterbury University Echelle Spectrograph, (HERCULES), on the 1m McLellan telescope was used to observe V752 Centauri and V392 Carinae. BP Velorum, with a visual magnitude of 12.9, is too faint to observe with HERCULES.

The McLellan telescope is a reflecting telescope of diameter one metre. It was used with the configuration of a cassegrain focus of f/13.5, with the HERCULES system fed by an optical fibre with the 100μm diameter.

2.2.1 HERCULES

HERCULES is a fibre-fed echelle spectrograph which has been operational at MJUO since April 2001. The spectrograph consists of a large R2 echelle grating to provide primary dispersion. Cross-dispersion is achieved with a prism which gives higher efficiency at all wavelengths than conventional grating instruments. The whole instrument is situated inside a vacuum tank where the pressure is maintained at 1-5 torr. The tank resides in a thermally isolated and insulated room.

The light collected from the telescope is guided to HERCULES by optical fibre. There are three possible fibres for use as shown in table 2.1, the choice of which is controlled with a dial at the telescope. Fibre 1 is 100μm in diameter and provides a resolving power of 41000. Fibre 2 has a core diameter of 100μm superimposed by a 50μm micro slit and resolving power of 70000. Fibre 3 has a core diameter of 50μm with resolving power of 82000 (Hearnshaw et al., 2002).

Fibre Position	**Diameter**	**Resolution**
1	$100\mu m$	41000
2	$100\mu m$ *with* $50\mu m$ *slit*	70000
3	$50\mu m$	82000

Table 2.1: *The resolution of HERCULES fibre positions*

Optical fibre position one was used in the observations as the targets were appreciably faint. The exposure time for V752 Centauri varied from 1800 seconds to 2100 seconds depending on the quality of seeing each night. The short period of the system meant that with longer exposure times a significant portion of the orbital period would be observed

and thus the effect of blending would become important. Generally, an integration time less than 10% of the orbital period can avoid the effect of spectral line blending.

The exposure times for V392 Carinae varied from 1800 seconds to 3600 seconds and had a lower signal to noise. However, due to the longer period of V392 Car, the longer integration time was not comparable to the orbital period. The guiding camera on the telescope has difficulty at fainter magnitudes and 9^{th} magnitude appeared to be its limit.

The readout speed was chosen to be 200kHz, this has a slightly higher readout noise value than that corresponding to a readout speed of 100kHz, however it has a lesser value for the gain at 1.18, which, given the faint magnitude of the targets, was deemed a more important factor.

Each night radial velocity standards were observed and calibration images of white lamp and thorium lamp were taken. There were several spectra of poor quality which were not used in the radial velocity measurements.

Date	Target	Telescope	Instrument	Observations
14-19 February 2007	BP Velorum	O.C.	S BIG ST9 CCD BVRI photometry	1250
19-26 March 2007	V752 Centauri	O.C.	S BIG ST9 CCD BVRI photometry	3836
10-15 April 2007	V752 Centauri	O.C.	S BIG ST9 CCD BVRI photometry	1665
12-15 May 2007	V752 Centauri V392 Carinae	McLellen 1m	HERCULES Spectroscopy	21 8
23-27 June 2007	V722 Centauri V392 Carinae	McLellen 1m	HERCULES Spectroscopy	30 18
25-27 July 2007	V392 Carinae	McLellen 1m	HERCULES Spectroscopy	3

Table 2.2: *The dates of the observing runs completed for this research.*

Chapter 3

Reductions and Software

3.1 Photometry

The photometric images were all reduced using the MIRAMETRICS software MIRA AL.

3.1.1 MIRA AL

MIRA AL is a Microsoft Windows based photometric reduction software package. The software is widely used as a tool for differential photometry and uses equation 3.1 for the calculation of magnitudes.

$$m = K - 2.5\log(flux) \tag{3.1}$$

where K is the photometric zero point and $flux = Gain * Counts/Exptime$.

3.1.2 Reducing Photometric Images

The calibration frames were combined prior to the reduction of the data images. The bias frames were combined using the Mean method which calculates the arithmetic mean value at each pixel location and creates a master image. The pixels are combined with no weighting or rejection of bad values which is the preferred method for image sets which can be considered to contain well behaved statistical noise. The dark frames were combined by collecting the median values at each pixel location to create an image. This method, called the Median method, is effective for excluding extreme values. The flat field frames for each filter are combined using the Median method and the combined image is then normalised. Calibration of the images was completed following the steps below.

1. The set of bias images were combined using the Median method to create a Master Bias frame.

2. Each dark frame of a certain exposure length, had the Master Bias subtracted and then the bias subtracted darks were combined with the Mean method creating a Master Dark frame.

3. The flats from each filter were Master Bias and Master Dark subtracted. Each filter set was then combined using the Median method. The combined image was normalised creating the Master Flat.

4. Each data image had the Master Bias and the Master Dark (with the same exposure time) subtracted and then divided by the Master Flat. The processed data frame was then ready to be measured.

For all exposure times used for the data images, dark frames were taken. This saved the process of scaling the master dark images.

MIRA's aperture photometry tool was used to measure the differential magnitudes of the target with respect to three or more comparison stars within the same field. The comparison stars used were tested for variability by taking measurements of the comparison stars with respect to each other. With the comparison stars such a small distance from the target stars, each are equivalently affected by the atmospheric conditions.

The aperture photometry procedure allows the aperture sizes to be defined; the inner annulus encompasses the star while the outer annulus determines the background sky counts. The target can be calibrated against as many comparison stars as the field allows. In all measurements made for this research at least three comparison stars were used with each field. The more comparison stars used in the differential measurement the less biased the measurements of the target are. The output resulting from the aperture photometry is the relative magnitudes of both the target and the comparisons along with the signal to noise and error measurement. The Julian Dates are calculated in MIRA from the date and universal time given in the Fits header files.

The magnitudes presented in this thesis are not calibrated to the standard system. They are differential instrumental magnitudes in the different filters, with arbitrary zero points. The Wilson-Devinney code used to model the light curves does not require absolute calibration.

3.1.3 Heliocentric Correction

The finite velocity of light and the orbital motion of the Earth about the Sun introduces a shift in the dates of stellar measurements. To account for the possible differences in the timings of the observations, the point of reference for the observations is altered to the Sun which by comparison has negligible movement. The correction can be calculated and applied with equations 3.2 and 3.3.

$$HJD = JD(geo) + HelCorr \tag{3.2}$$

$$HelCorr = TR(\cos L \cos A \cos D) + TR(\sin L(\sin E \sin D + \cos E \cos D \sin A)) \tag{3.3}$$

T = time for light to travel 1 A.U. $\approx 499s$
R = Earth-Sun distance
L = Longitude of the Sun
A = Star's right ascension
D = Star's declination
E = obliquity of the ecliptic 23.45°

The heliocentric corrections were calculated for the photometric data in the EXCEL programme written by Dan Bruton, SFA Observatory.

The heliocentric corrected measurements were then imported into MATLAB where the period was converted into the phase. The corresponding data was converted into an ASCII file which is flexible and can be used in the PHOEBE software.

3.2 Reduction of the Spectroscopic Images

The images acquired with the HERCULES spectrograph were reduced with the Hercules Reduction Software Package (HRSP) (Skuljan, 2007).

HRSP prepares the two-dimensional images of the orders by flipping and rotating them for reducing. Then the transformation coefficients between the fixed spectrum and a thorium image are computed. HRSP reduces a given white lamp image to produce an order definition table, then reduces the stellar image producing a pair of spectra binned into logarithmic and linear wavelength scales. HRSP calculates the heliocentric date and radial velocity corrections during the reduction process. The heliocentric velocity

correction is not applied to the spectrum and is later applied using FIGARO's *vachel* command.

The spectra were intended to be reduced with the wavelength calibration in air rather than in vacuum. A new version of HRSP was used for the reduction process and unbeknown at the time, the dispersion solution configuration files within the new version HRSP were switched. This resulted in our spectra having wavelength calibrations in vacuum. It was later determined, (see equation 3.6), that this systematic error could be removed by applying a correction to the derived radial velocities.

3.3 Preparation of the Spectra

An important step in the cross-correlation preparation is fitting a continuum to the echelle orders. Applying a continuum normalises the spectrum to unity at each continuum point, ensuring the comparison with the template spectrum has been made with the same level of continuum (unity). The continuum fitting process employed in this research is a routine which fits a low order polynomial equation to the raw spectrum, this is repeated to minimise the residuals. For early type stars the absence of strong metallic lines means there is a strong presence of a reliable continuum throughout the spectrum. For later type stars where the metallic lines become stronger there is less continuum to work with. The automated routine was checked with the manual continuum fitting process *cfit* in FIGARO.

The low signal to noise, and long exposure times of these targets brought in more cosmic rays. The HRSP filtering of cosmic rays did not clean all of the spikes in the spectra. The continuum fitted spectra were run through a filtering procedure to further clean them of spikes.

3.4 Cross-correlation of the Spectra

The Doppler shift is used to measure the radial velocity of a star. This can be done by measuring the horizontal shift of a single line in the spectra with respect to a reference point. The shift can be translated into the Doppler shift and hence the velocity, if the horizontal axis has a logarithmic scale.

$$\frac{\Delta\lambda}{\lambda_0} = \frac{v}{c}. \tag{3.4}$$

However, the velocity from the Doppler shift determined from just one specific spectral line cannot be expected to be very accurate as different lines are created at different depths of the photosphere hence are subject to different temperatures and velocity gradients (Ramm, 2004).

Measuring the average velocity from a large number of lines provides a more accurate velocity. The technique of cross-correlation uses a convolution between the programme spectrum and a template spectrum. The convolution is made simpler when done in Fourier space. If the spectrum is in a logarithmic scale the velocity can be directly measured. The spectrum of an SB2 binary with its complicated splitting of spectral lines is a worthy candidate for the cross-correlation technique. Cross-correlation with a suitable template spectrum provides a single smoothed profile which can be easily and reliably measured giving the radial velocity.

The *cross-correlation function c(x)*, CCF, shown in equation 3.5 as the convolution of two functions $f(k)$ and $g(k)$, takes a value equal to the integral of the product of the two functions $f(k)$ and $g(k-x)$. The integral is evaluated for a range of values of x and $c(x)$ provides a numerical description of how well the functions $f(k)$ and $g(k)$ are matched (Hilditch, 2001).

$$c(x) = \int_{-\infty}^{+\infty} f(k)g(k-x)\,dk. \tag{3.5}$$

The CCF may then yield the shift in the program spectrum with respect to the template spectrum and, with the template's velocity well determined, the relative velocity of the program spectrum can be measured.

The cross-correlations performed in this thesis make use of the fast-Fourier-transform algorithm (FFT), and IFFT functions of MATLAB. The templates used are synthetic templates generated with temperatures corresponding to the spectral types of targets. The FFT requires a spectrum as free as possible of sharp discontinuities which exist at the ends of each echelle order. To remedy this, ten percent from the ends of the spectra are smoothed with a cosine bell function, causing the ends to gradually taper to zero (Brault and White, 1971).

The FFT's were performed in MATLAB using a script written by Dr. Michael Albrow (see Appendix A). For the target V752 Cen, with the unusual behaviour of its spectrum (see Chapter 6), the cross-correlation is performed with two templates. The program spectrum is first split into two by determining and applying high-pass frequency and low-pass frequency filters.

The resulting CCFs were gaussian-like profiles and thus fitted with gaussians using

the *gauss* command from the FIGARO software package. The error estimate on all radial velocities measured in this thesis is adopted as $2kms^{-1}$ which is approximately 1% of the average width of the CCF peaks.

As discussed in Section 3.2, the spectra were reduced with vacuum rather than air wavelengths. Images calibrated with air wavelengths is the international standard. Equation 3.6 can make the conversion from vacuum to air[1];

$$\lambda_{AIR} = \frac{\lambda_{VAC}}{1.0 + 2.7352 \times 10^{-4} + \frac{131.4182}{\lambda^2_{VAC}} + \frac{2.7625\times10^8}{\lambda^4_{VAC}}}. \tag{3.6}$$

The vacuum to air conversion was calculated for the radial velocities using a linearised version of equation 3.6 that neglected the final two terms in the denominator, with equation 3.4. The difference in ΔV using the full equation 3.6 or using the modified equation was well within the measurement uncertainty of the radial velocities, so the constant correction of $-82.0338kms^{-1}$ to the final velocities was used.

3.5 The Spectroscopic Orbital Solution

For spectroscopic binaries where both components' radial velocities are measurable, it is possible to determine the spectroscopic orbital solution.

For circular orbits, eccentricity $e = 0$, the radial velocity curves may be fitted with equation 3.7;

$$V_n = \gamma_n + K_n \sin\theta, \tag{3.7}$$

where $n = 1$ or 2 and γ is the systematic velocity, K is the semi-amplitude of the velocity curve and θ is the phase angle.

The mass-ratio q can be determined from the ratio of the semi-amplitudes $q = \frac{K_2}{K_1}$. The projected semi-major axis may also be determined by

$$a_n \sin i = (9.1920 \times 10^{-5}) K_n P \sqrt{1 - e^2}, (AU). \tag{3.8}$$

If the inclination is known, the components individual masses may be determined from equation 3.9;

$$M_{1,2} = (1.0361 \times 10^{-7}) \times P K_{2,1} (K_{1,2} + K_{2,1})^2 \left(\frac{\sqrt{1 - e^2}}{\sin i} \right)^3, (M_\odot). \tag{3.9}$$

[1] http://www.sdss.org/dr6/products/spectra/vacwavelength.html

3.6 PHysics Of Eclipsing BinariEs

The PHysics Of Eclipsing BinariEs software, PHOEBE, was released under the GNU public license. It is a modeling software for eclipsing binaries which uses the Wilson-Devinney code. The Wilson-Devinney code, WD code, computes a synthetic model of an eclipsing binary which is based on the Roche model. The inverse problem is solved using differential corrections. At PHOEBE's core, the modeling engine is running on WD-2003, the next layer consists of the incorporations of all scientific, numerical and technical extensions. At the outermost layer there is an user interface, serving as a bridge between the user and the model (Prša, 2006).

PHOEBE uses differential corrections, DC, to derive the χ^2 minimization. The differential corrections method was first proposed by Euler (1755). It is based on replacing partial derivatives with finite differences and is one of the most straight forward numerical methods to determine the best fit (Prša, 2006).

PHOEBE offers the user five options for the system's configuration: A general system with no constraints, a detached system, semi-detached system, double-contact, and two over-contact configurations: W UMa-type and one where the components are not in thermal contact. The model type selected adds constraints depending on the configuration.

The underlying WD code can be driven through either the *scripter* or the *PHOEBE Differential Corrections Minimization* window. After each iteration, the DC Minimization window displays the parameter name, the original value, the correction amount, the corrected value and the standard deviation of the corrected value.

The limb-darkening coefficients can be calculated within PHOEBE using either a linear cosine, quadratic or a square root limb-darkening law used with coefficients obtained by interpolating in the tables by van Hamme (1993) (Kaitchuck et al., 2006).

Chapter 4

BP Velorum

BP Velorum was discovered to be variable by de Koort in 1941 (Lapasset and Gomez, 1988), who obtained a photoelectric light curve and declared BP Vel to be a W UMa-type eclipsing binary system. Lapasset and Gomez (1988) observed BP Vel photoelectrically at Complejo Astronomico El Leoncito in Argentina with the 215cm telescope using the Vatican Observatory polarimeter as a photometer. From a total of 930 observations twelve times of minima were calculated. They deduced the depth of the primary and secondary minima to be 0.8 and 0.6 magnitudes.

Lapasset and Gómez revisited BP Vel along with Fariñas in 1996 in their collective work on three W UMa-type systems (Lapasset et al., 1996). Using the observations from Lapasset and Gómez (1988), Lapasset et al. (1996) analysed the light curve of BP Vel, which they found to belong to the W subclass of W Uma-type systems with asymmetries in the light curves modeled with cool spots on the more massive secondary component.

4.1 Previous Model

Using the Wilson-Devinney routine to model the light curves, Lapasset et al. (1996) derived the parameters listed in table 4.1. They used the WD code with a range of 18 fixed mass ratio values between 0.3 and 3.0, to obtain the best initial estimate of q. Their models for each given q had the following adjustable parameters: the inclination (i), the potential ($\Omega_1 = \Omega_2$), the polar temperature of the secondary component (T_2), and the relative monochromatic luminosities (L_{1V}, L_{1B}). They held fixed the polar temperature of the primary component (T_1), the gravity-darkening coefficients ($g_1 = g_2$), the bolometric albedos ($A_1 = A_2$) and the limb-darkening coefficients ($X_{1V} = X_{2V}, X_{1B} = X_{2B}$) along with the mass ratio (q).

The mass ratio which determined the solution with the best value of the sum of the squared weighted residuals was found to be $q = 1.9$. The sum of the squared weighted residuals, $\Sigma(wr^2)$, is termed the goodness-of-fit parameter. Figure 4.1 is the plot made by Lapasset et al. (1996). They adopted the solution determined when $q = 1.900$ as the unspotted solution for BP Vel.

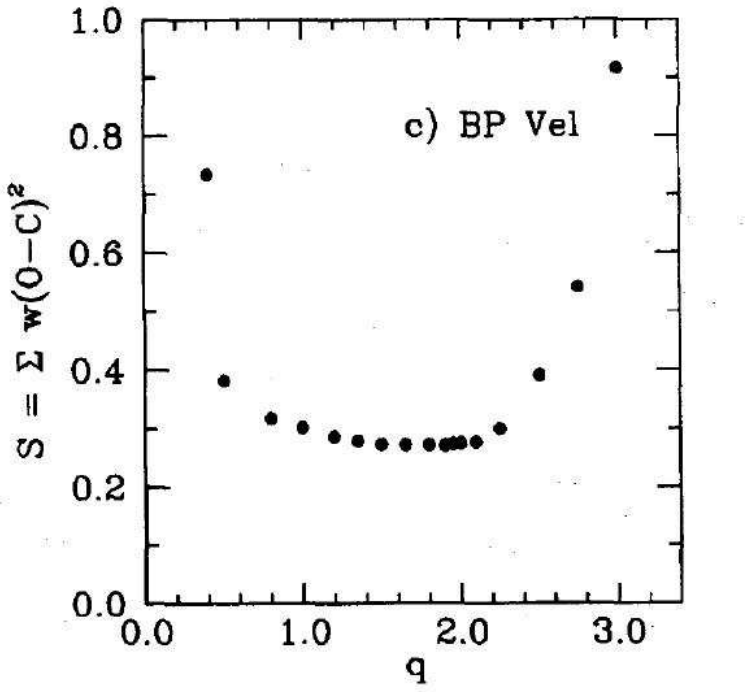

Figure 4.1: *Goodness of fit parameter,*$[S(q) = \sum \omega r^2 = \sum \omega (I_{obs} - Ith)^2]$ *vs. the mass ratio* $q = m_2/m_1$. *Figure taken from Lapasset et al. (1996).*

Since the theoretical light curve did not satisfactorily fit the observed points and there were systematic ambiguities in the residuals, a star spot with the parameters in table 4.1 was added to the solution. The spotted solution was found to yield a better fit between the theoretical and the observed light curves.

4.2 Preparation of the Light Curves

For this thesis, photometric observations of BP Vel were taken during February 2007 and were reduced with MIRA AL. The 311 images obtained in each filter were all processed in the way outlined in Chapter 3. The analysis of the period was conducted by producing an **O-C diagram** of the residuals, where the observed times of minimum magnitude are compared to calculated times. The predicted times of minimum light were calculated

	Unspotted Solution	Spotted Solution
q	1.900^*	1.8778 ± 0.0004
i	$81.60 \pm 0.24°$	$82.08 \pm 0.13°$
T_1	$5000° K^a$	$5000° K^a$
T_2	$4705 \pm 7° K$	$4717 \pm 4° K$
$\Omega_1 = \Omega_2$	5.047 ± 0.006	4.998 ± 0.007
$F = \frac{\Omega_{in} - \Omega}{\Omega_{in} - \Omega_{out}}$	$10.05 \pm 0.6\%$	$14.0 \pm 0.7\%$
$g_1 = g_2$	0.32^a	0.32^a
$A_1 = A_2$	0.50^a	0.50^a
$X_{1V} = X_{2V}$	0.712^a	0.712^a
$X_{1B} = X_{2B}$	0.866^a	0.866^a
$\frac{L_1}{L_1+L_2}(V)$	0.440	0.439
$\frac{L_1}{L_1+L_2}(B)$	0.449	0.448
$r_1(pole)$	0.309	0.312
$r_1(side)$	0.324	0.327
$r_1(back)$	0.360	0.364
$r_2(pole)$	0.415	0.416
$r_2(side)$	0.442	0.443
$r_2(back)$	0.472	0.474

Table 4.1: *Photometric Solutions for BP Velorum from Lapasset et al. (1996). Note: ^{a}Not altered.*

Location	Secondary
Colatitude	90° (adopted)
Longitude	$99.8 \pm 0.1°$
Spot Radius	$14.7 \pm 3.0°$
$\frac{T_{spot}}{T_{star}}$	0.76 ± 0.09

Table 4.2: *Star spot parameters from Lapasset et al. (1996).*

from equation 4.1, where P_{est} was the period taken from Viz, ($P_{est} = 0^d.26498597$), and E is the epoch.

$$C = HJD_0 + P_{est}E. \tag{4.1}$$

The residuals, O-C, were plotted and a straight line was fitted to them (see Figure 4.2), describing the nature of the period change. The new period was calculated from

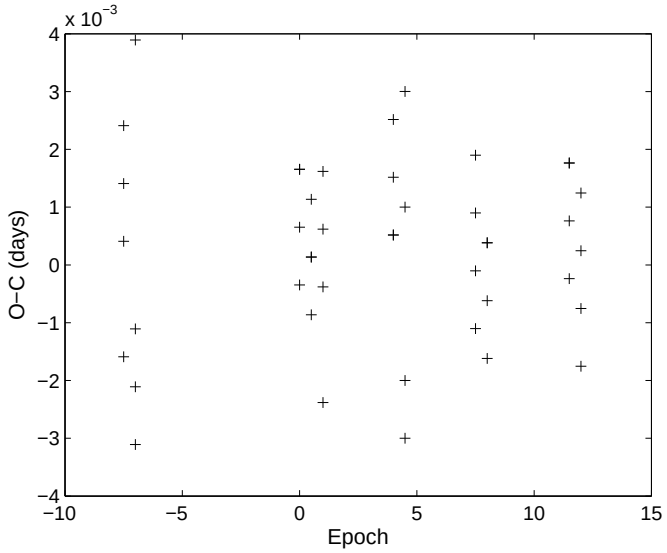

Figure 4.2: *BP Vel (O-C) residuals of minimun light showing the ten epochs in the four filters.*

$P = P_{est} + b$ where b is the slope in the line. The new period was found to be $P = 0^d.265034 \pm 0^d.000048$. From a linear least-squares fit of the ten times of observed minimum in our data, the ephemeris was found to be

$$HJD_0 = 2454147.934346(\pm 0.00002) + 0.265034(\pm 0.00005)$$

The reduced data was phased with the new period and then modeled with PHOEBE.

4.3 Modeling with PHOEBE

The PHOEBE configuration option of an over-contact system of the W UMa-type was attempted for the first fit. The results were not satisfactory however, the difference in the minimum depths was not sufficiently matched and the temperature of the primary diverged rather dramatically.

An over-contact system without thermal contact was found to be the best configuration option for BP Vel. This option, while complying with the contact configuration condition, that the potentials are equal $\Omega_1 = \Omega_2$, allowed the temperatures of the primary and the secondary to differ. The different temperatures drove the model to match BP Vel's observed minimum inequality. The primary minimum is around 0.15 mag deeper than the secondary eclipse in all filters.

A new analysis of the mass ratio corresponding to the best fit was undertaken. The

method would be employed for further light curve analysis. From Figure 4.1, a range of mass ratio values to test was decided upon. The values of q that we used, ranged from $1.2 \leq q \leq 2.4$.

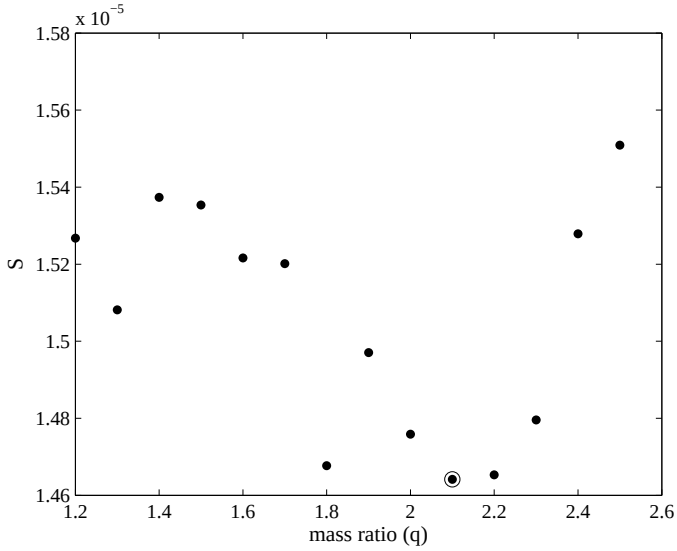

Figure 4.3: *Goodness of fit parameter,[$S(q) = \sum \omega r^2 = \sum \omega (O-C)^2$] vs. the mass ratio $q = m_2/m_1$, determined using models produced by PHOEBE for BP Vel. The circled value is the q used as a start point in the unspotted and spotted models.*

The WD code was implemented on fixed values of q within this range, leaving the relative monochromatic luminosities ($L_1(B,V,R,I)$), the primary and secondary temperatures (T_1, T_2), the potential ($\Omega_1 = \Omega_2$), the inclination (i) and the limb-darkening coefficients ($X_1(BVRI)$ and $X_2(BVRI)$) free to converge. The gravity-darkening coefficient and the bolometric albedo were fixed at $g_1 = g_2 = 0.32$ and $A = 0.5$. The values for q and A follow the convective envelope model for contact binaries taken from Lucy (1968a) and Ruciński (1969). The spectral type of BP Vel is KI so the initial value chosen for the temperatures of both components was $5000K$ (Lapasset et al., 1996). The limb-darkening coefficients were calculated using a square root limb-darkening law after each set of iterations.

The fit of the model was judged on the sum of the squared weighted residuals ($S = \Sigma(wr^2) = \Sigma(O-C)^2$). The values of S were plotted against q in Figure 4.3. The q that gives the best model is $q = 2.1$ compared with $q = 1.9$ found by Lapasset et al. (1996).

4.3.1 Unspotted Model

Our $BVRI$ light curves with the WD model are shown in Figure 4.4.

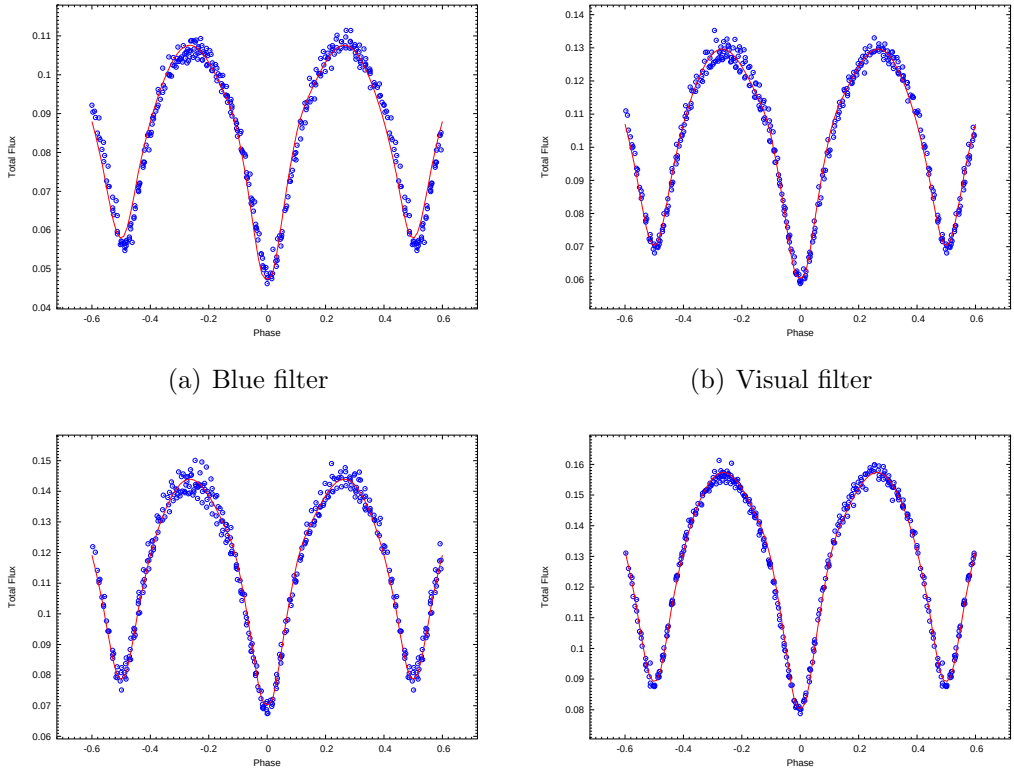

(a) Blue filter

(b) Visual filter

(c) Red filter

(d) Infrared filter

Figure 4.4: *The unspotted WD model in BVRI filters.*

The unspotted model was generated leaving the parameters described in the preceding section and the mass-ratio free. The goodness of fit for the unspotted model was $S = 1.41 \times 10^{-05}$. The observed light curves show unevenness at their maxima. This is more pronounced in the visual and red filters which rules out systematic errors from the instruments. If it were a case of a systematic error, one would expect it to be continued through the other filters and that there would be just as much scatter at minimum light. Lapasset et al. (1996) discovered a model with a star spot added to the secondary component produced the best fit. The placing of the star spot on the secondary component at the equator was repeated for this analysis.

4.3.2 Spotted Model

As shown in Figure 4.4 it is obvious there is some effect toying with the light curve near phase -0.25 in the Visual and Red filters. A star spot was placed on the secondary component at a colatitude of 90°. The other spot parameters (longitude, angular radius and temperature), were allowed to vary with the WD code through PHOEBE, until convergence. The system's other parameters which had previously converged, were adjusted

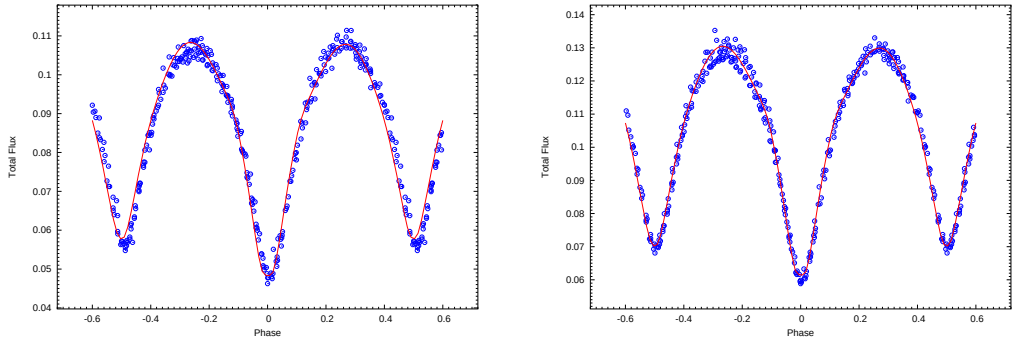

(a) Blue filter

(b) Visual filter

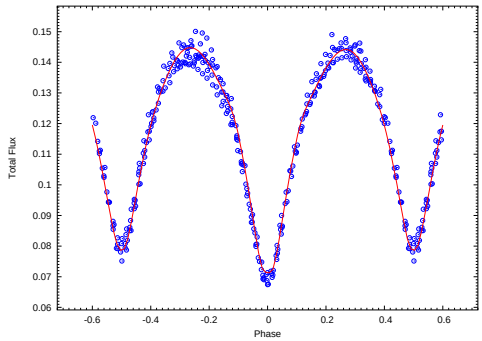

(c) Red filter

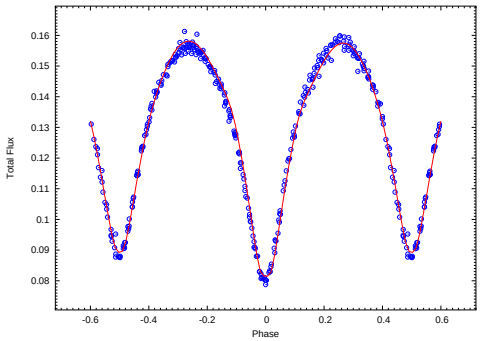

(d) Infrared filter

Figure 4.5: *The spotted WD model in BVRI filters.*

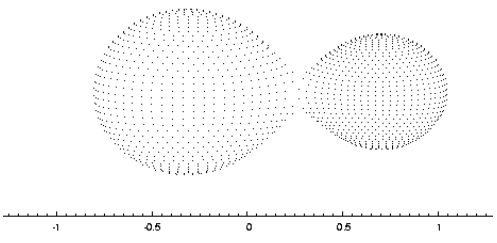

(a) phase = -0.25

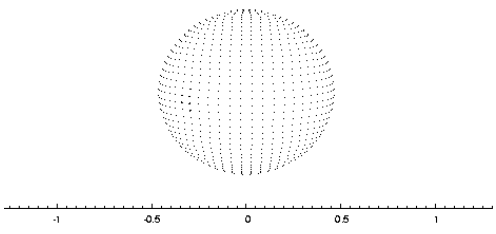

(b) phase = 0

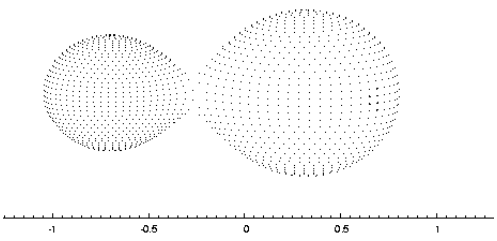

(c) phase = 0.25

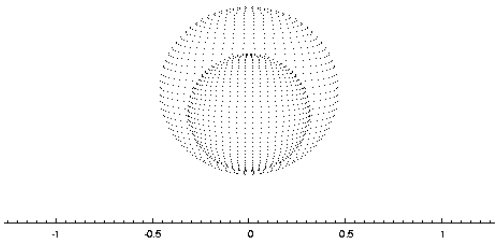

(d) phase = 0.5

Figure 4.6: *3-D plots of the surface of BP Velorum (with spot).*

again to account for the star spot. The resulting model is plotted with the observed light curve in Figure 4.5. The spotted solution has a goodness of fit $S = 1.35 \times 10^{-5}$ compared with $S = 1.41 \times 10^{-5}$ for the unspotted solution.

Location	Secondary
Colatitude	90° (adopted)
Longitude	$140.9 \pm 0.04°$
Spot Radius	$8.0 \pm 1.7°$
$\frac{T_{spot}}{T_{star}}$	0.79

Table 4.3: *Star spot parameters determined with PHOEBE.*

The light curves from each night of observation were investigated for evidence of fluctuation in intensity at the times of maximum light. The reason for this investigation is the idea that variability in star spots' location and/or strength would show up in the light curves. The times of maximum light may show variations from night to night as the spots travelled across the hemisphere facing us. Figures 4.7 and 4.8 show the V and R filters' observations of BP Velorum from five nights in February 2007. The maxima leading into the primary eclipse (phase=1.0 in Figures 4.7 and 4.8), show a dip in the intensity of light moving from the left to the right over three nights. These variations in the light curves are not thought to be due to random scatter since at the times where the least light is coming from the system, the light curves do not show scatter.

4.4 Solution

The photometric solution for BP Vel determined in this thesis produced slightly different values for the parameters than the solution Lapasset et al. (1996) found, the values for the parameters is shown in table 4.4. Figure 4.6 displays the surface of the spotted model of BP Vel at different phases.

The initial mass-ratio determination for this thesis, was conducted with a similar method to that which Lapasset et al. used in their 1996 analysis. The resulting mass-ratio value which produced the best fitting model was larger than the 1996 result. The main differences in the light curve synthesis method was the parameters which were allowed to vary. For this thesis, both the primary and the secondary temperatures were adjustable. The limb-darkening coefficients were calculated during the fit. In the Lapasset

	Unspotted Solution	Spotted Solution
q	2.1344 ± 0.0108	2.198 ± 0.0045
i	$83.81 \pm 0.25°$	$83.37 \pm 0.23°$
T_1	$5189 \pm 9.6K$	$5184 \pm 9.3K$
T_2	$4846 \pm 8.4K$	$4859 \pm 8.1K$
$\Omega_1 = \Omega_2$	5.305 ± 0.02	5.402 ± 0.007
$F = \frac{\Omega_{L_1} - \Omega}{\Omega_{L_1} - \Omega_{L_2}} + 1$	1.246	1.253
$g_1 = g_2$	0.32	0.32
$A_1 = A_2$	0.5	0.5
$X1B$	0.233 ± 0.095	0.004 ± 0.09
$X1V$	0.024 ± 0.095	-0.213 ± 0.092
$X1R$	0.109 ± 0.084	-0.166 ± 0.084
$X1I$	-0.141 ± 0.094	-0.318 ± 0.093
$X2B$	0.929 ± 0.43	0.678 ± 0.041
$X2V$	0.890 ± 0.036	0.639 ± 0.034
$X2R$	0.790 ± 0.034	0.552 ± 0.031
$X2I$	0.584 ± 0.037	0.353 ± 0.034
$\frac{L_1}{L_1+L_2}(B)$	0.443	0.430
$\frac{L_1}{L_1+L_2}(V)$	0.422	0.410
$\frac{L_1}{L_1+L_2}(R)$	0.406	0.395
$\frac{L_1}{L_1+L_2}(I)$	0.392	0.383
$r_1(pole)$	0.306	0.303
$r_1(side)$	0.321	0.318
$r_1(back)$	0.362	0.358
$r_2(pole)$	0.431	0.432
$r_2(side)$	0.461	0.463
$r_2(back)$	0.493	0.494
$\Sigma(wr^2)$	1.41×10^{-05}	1.35×10^{-05}

Table 4.4: *Photometric Solution for BP Velorum determined from our model generated using PHOEBE.*

et al. (1996) model the primary temperature and the limb-darkening coefficients were held fixed.

BP Vel was determined to belong to the W-type subgroup of W UMa-type binaries by Lapasset et al. (1996). The photometric solution determined in this thesis, supports the

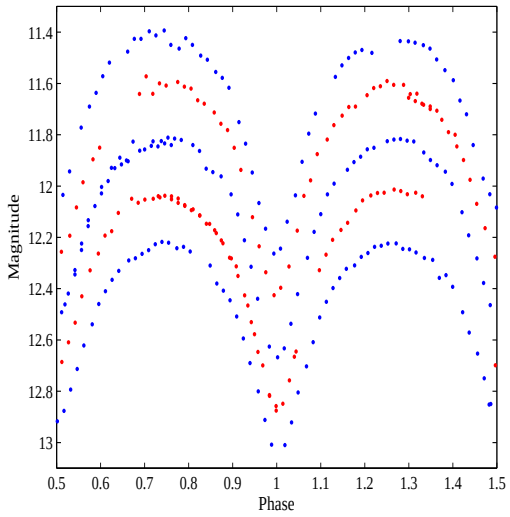

Figure 4.7: *The light curves of BP Vel in the Visual filter.*

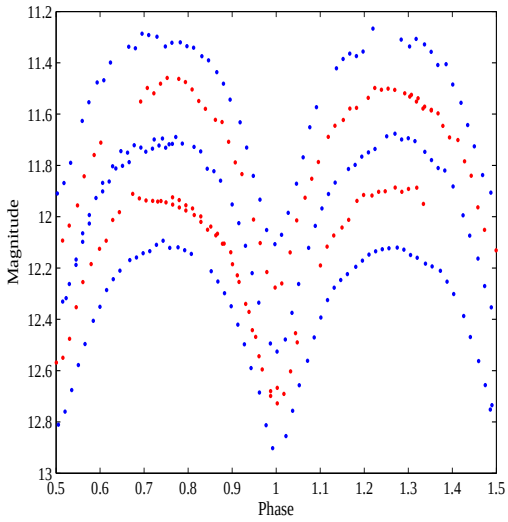

Figure 4.8: *The light curves of BP Vel in the Red filter.*

Light curves from five nights observing BP Vel in the Visual and Red filters. The dates of observations start from the bottom and move upwards. The variation in the intensity of light received from BP Vel at the time of maximum leading into the primary eclipse is further evidence for star spot activity on at least one component of BP Vel.

association with the W-type configuration in terms of the value for q. The dispersion for values of q for W-type systems is quite large; the statistical mean is around 2. W-type W UMa systems generally have higher values for q than A-type systems which generally have $q \leq 0.4$. The mass-ratio determined in this thesis, $q \approx 2.1$ is beyond the range of q values corresponding to A-type systems but, is close to the mean value for W-type systems.

The fill-out factor calculated in this analysis ($F = 1.25 = 25\%$), is somewhat larger than than the fill-out factor determined previously by Lapasset et al. (1996) ($F = 14.0\% \pm 0.007\%$). The indication that W-type systems have a lower degree of contact than A-type systems was thought to be a factor in deciding which category a system belonged to. However, this condition is not as reliable as classification by the mass-ratio (Pringle and Wade, 1985).

Therefore, from the value of mass-ratio determined from the analysis conducted during this thesis, the classification of BP Vel belonging to the W-type category for W UMa-type binaries stands. The shape of the light curve supports this claim. The deeper minimum corresponding to an occultation of the less massive component satisfies the condition for W-type systems of Binnendijk (Mochnacki, 1981).

The asymmetry of the light curve indicated the presence of a star spot on one of the components. The model benefited from the introduction of a cool spot on the secondary, more massive component. The variability near maximum may indicate one or more variable star spots on the surface. The nature of these variations may be revealed by further studies that employ high-time resolution spectroscopy or very high-time resolution photometry, perhaps using the Southern African Large Telescope.

Chapter 5

V392 Carinae

V392 Carinae, also nominated Cox 38, is a member of the open cluster NGC 2516. P. North discovered it to be an eclipsing system in 1982 (Debernardi and North, 2001). Hartoog classified Cox 38 as an Ap SrCrEu type star before its recognition as a binary system. North's discovery of V392 Car being a binary system was made during a systematic search for photometric variability in Ap stars. Debernardi and North (2001) analysed photometric and spectroscopic observations taken at the European Southern Observatory at La Silla, Chile.

The radial velocities were determined using two methods, with the main focus at the Sr II line at 4215$\mathring{A}$. Andersen and Nordström (1983) specified that radial velocity measurements made with the Sr II spectral line gives no bias for SB2 binaries from spectral types earlier than A5, after which there is large rotation dependence. The two methods of Debernardi and North (2001) consisted of measuring the shift of the Sr II line in V392 Car's spectrum with respect to both the lab wavelength value and also the position from Cox 98, a single star and member of NGC 2516 located in the same photometric 'box' as V392 Car, that is its six GENEVA colours are the same as V392 Car's within 0.02mag.

The radial velocities measured with respect to Cox 98 agreed very well with the ones measured against the lab value. The radial velocity of Cox 98 was implicitly assumed in the correlation to be representative of the radial velocity of the cluster NGC 2516, equal to the systematic velocity of V392 Car (Debernardi and North, 2001). The spectroscopic observations were taken over two nights and cover only the eclipse phases. However, the well determined photometric period is the same as the orbital one and with the eccentricity considered as zero due to synchronisation and circulisation effects, it was possible for Debernardi and North (2001) to determine the spectroscopic orbit.

The photometric observations analysed in Debernardi and North (2001) were observed

in the GENEVA photometric system between January 1978 and January 1991. The period of the system was determined from the photometry to be $3^d.174990 \pm 0^d.000001$. The effective temperature was derived to be $8746K$.

5.1 Photometry

5.1.1 Photometric Data Preparation

The photometric images were taken by Michael Snowden during 1997 at Mt John University Observatory principally with the 0.6m Bollens and Chivens telescope, with supplementary observations taken with the O.C. telescope. The observations were taken during January, February, March and April of 1997 in the Stromgren B and Y filters.

These observations were reduced by the author and M. Snowden using MIRA. The comparison stars used in these reductions were checked against each other to be sure of no variability. The systematic error from the night to night was negligible, the magnitudes of the comparison stars aligned well from night to night. The nights where the atmospheric conditions were not favourable were looked at carefully, and in some cases ignored as the quality of the reduced magnitudes was poor. The quality of the images deteriorated as each night progressed, evident in the increased scatter in the light curves. The resulting light curve was pieced together from the nights of better quality. The eclipses are well covered in the light curve. Unfortunately the times between the eclipses were not observed as often and only one full night provided coverage in these phases.

The poor phase coverage of the light curve observed in 1997 is supplemented with observations published in Debernardi and North's 2001 paper. The observations were taken at the European Southern Observatory, La Silla, Chile, from 1978 through to 1991. The photometric observations were made in the V filter in the GENEVA system and are available at the CDS[1] (Debernardi and North, 2001). The Debernardi observations have good overall phase coverage.

The observations from the three filters were phased with the period from the Vizie R catalogue. The phased light curves were then put into PHOEBE to undergo solution seeking with the differential corrections method.

[1] http://cdsweb.u-strasbg.fr/cgi-bin/qcat?J/A+A/374/204

5.1.2 Photometric Model

PHOEBE was used to generate a model to fit the light curves from V392 Car. The initial parameters which were input into PHOEBE were the HJD_0, the time of primary eclipse and the period. An initial estimate of the temperatures from Debernardi and North (2001) and the mass ratio determined from the radial velocity measurements were given to the model. The selection of a detached binary model constrained PHOEBE accordingly.

The light curve from Debernardi and North (2001) was taken as the most likely to give a good fit, due to the large phase coverage. Figures 5.1 and 5.2 show the 1997 Stromgren B and Y filter light curves with the model.

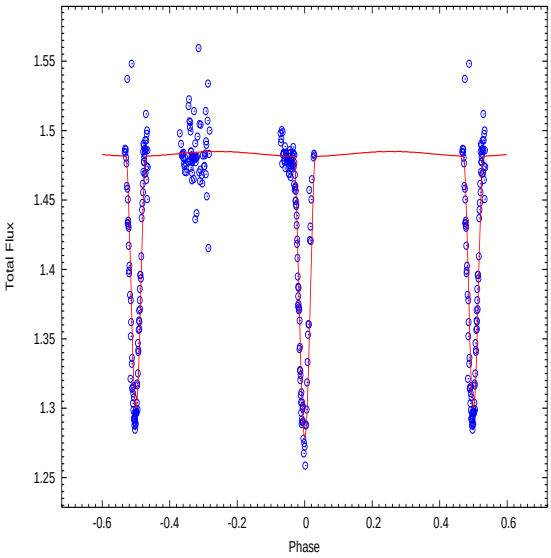

Figure 5.1: *The light curve of V392 Car in Stromgren B filter.*

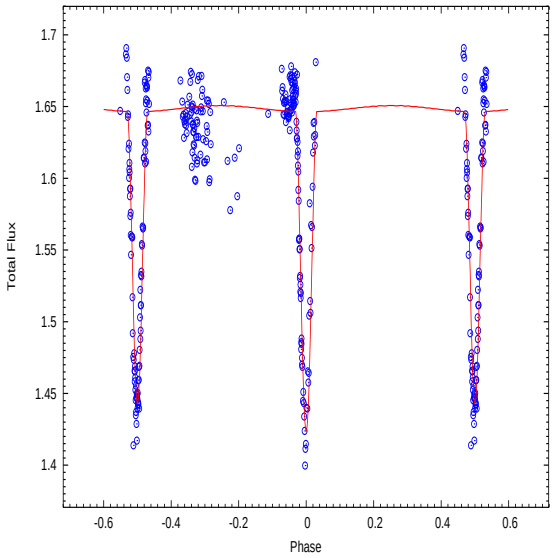

Figure 5.2: *The light curve of V392 car in Stromgren Y filter.*

The more complete light curve in the GENEVA V filter ,shown in figure 5.3, was the light curve which the model fit was based on. The model had a weighted σ of $\sigma_\omega = 0.014435$ in total flux units.

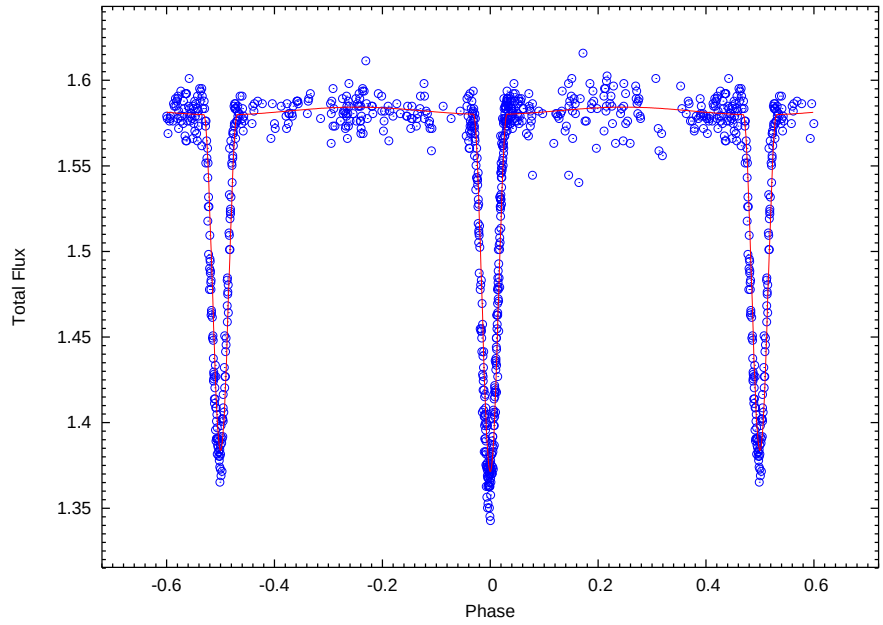

Figure 5.3: *The V-light curve in GENEVA filter of V392 Car.*

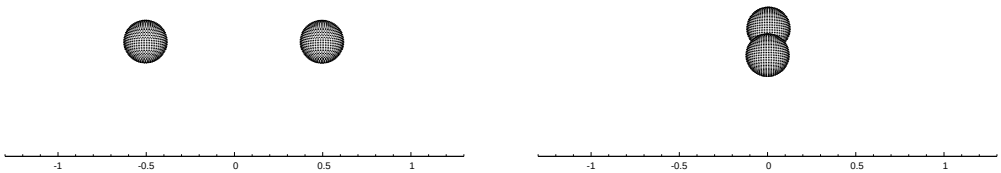

(a) phase = -0.25

(b) phase = 0

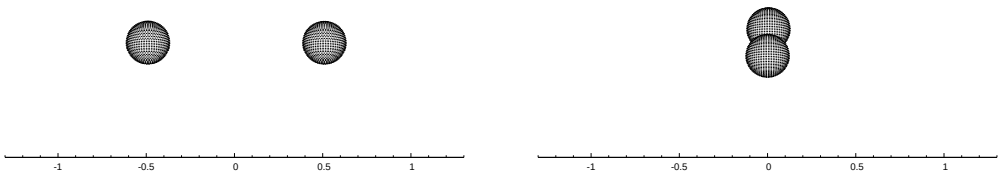

(c) phase = 0.25

(d) phase = 0.5

Figure 5.4: *3-D plots of the surface of V392 Car.*

5.2 Spectroscopy

5.2.1 Spectroscopic Data Preparation

The observed spectra of V392 Car were taken over three months. The orders were extracted by HRSP and the spectra were continuum fitted using a MATLAB script written by Duncan Wright (see appendix A). The continuum fitted orders were combined into one long spectrum using another MATLAB script from Duncan Wright (see appendix A). The process of combining the orders used non flat-fielded reduced images to get the mean at the cross-over regions and used these values to weight the flat-fielded reduced images which were then combined. Combining echelle orders gives a more informed cross correlation result as over the 2000$\mathring{A}$ wavelength range there is a lot more information than with individual orders typically of the 50$\mathring{A}$ range. Figure 5.5 shows an example of a combined spectrum of V392 Car. The strong absorption line around 4860$\mathring{A}$ is shown in Figure 5.6, it is the strong $H\beta$ line.

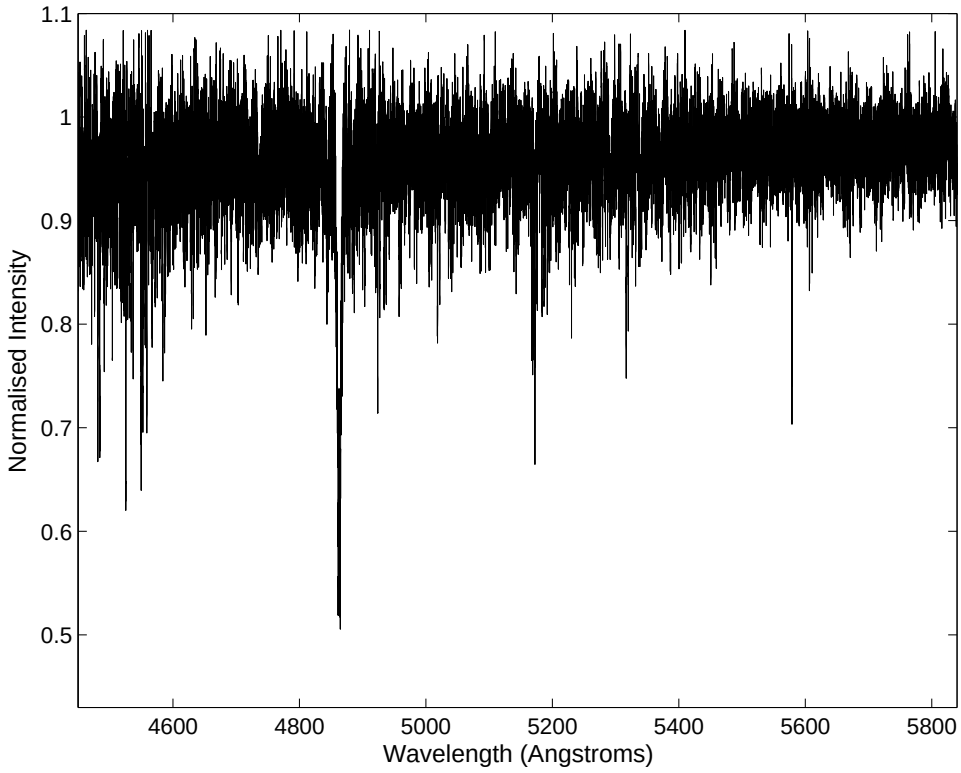

Figure 5.5: *The combined spectrum of V392 Car.*

These combined spectra were then run through a cosmic ray cleaning process to cor-

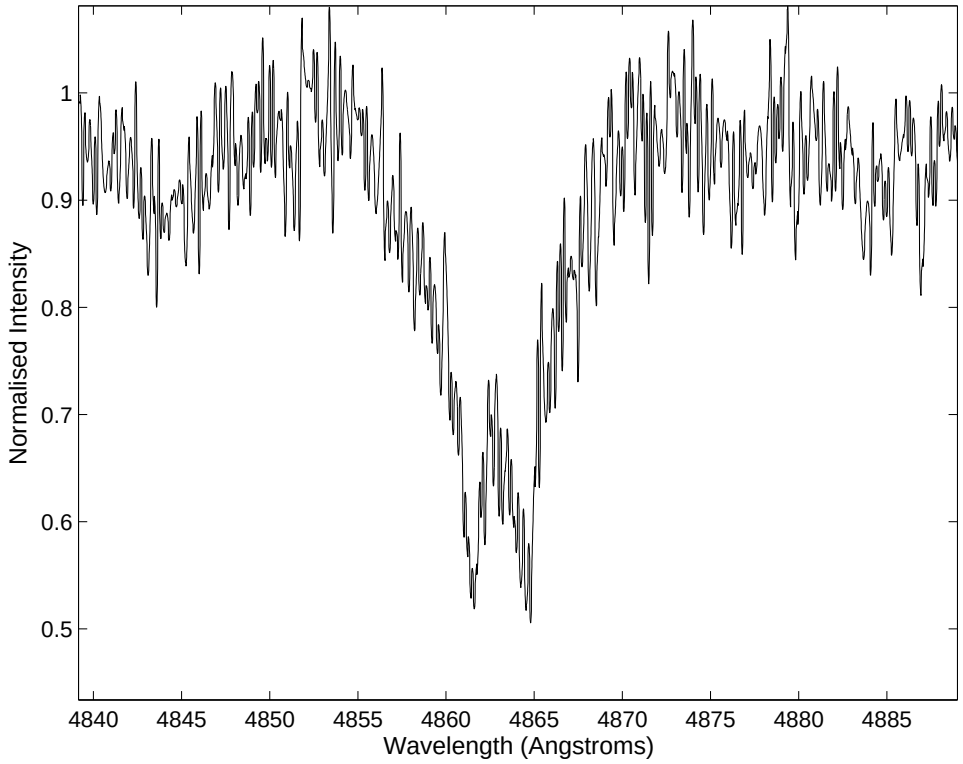

Figure 5.6: *The strong $H\beta$ absorption line from fig 5.5.*

rect for cosmic rays that were missed in the HRSP reduction. The long exposure times and poor signal to noise made the inbuilt HRSP cosmic ray extraction procedure less successful.

These spectra were then cross-correlated against a synthetic template spectrum ($T_{eff} = 8750K$, $\log g = 4.0$), which was computed from ATLAS9 model atmospheres. The cross-correlation is performed using the FFT technique in MATLAB. To prepare for the cross-correlation the combined spectra were scrunched to a constant logarithmic wavelength interval. The cross-correlation profiles produced defined peaks which were fitted with gaussians using FIGARO's *gauss* program.

5.2.2 Radial Velocity Measurements

The CCFs calculated with the cross-correlation performed in MATLAB showed well defined peaks in most images. Figures 5.7 and 5.8 display the CCFs at two times of V392 Car's orbit. The two peaks relate to the two components of the system. The CCF

peaks were of gaussian form and were fitted with gaussians to determine the centroid of the peaks. FIGARO's gaussian fitting package *gauss*, provides an interactive fitting tool where the limits and position of the gaussian profile are specified. The resulting profile can then be modified in width, height and peak position, *gauss* then optimizes the gaussian given optional constraints.

The output measurement consists of the peak position, height and flux, along with the standard deviation of the gaussian profile (sigma) and the r.m.s. error on the fit. The CCFs were all plotted in velocity space and thus the measure of the peak gave direct radial velocities. The error estimate for all our measured radial velocities is $2kms^{-1}$ as explained in Section 3.4. The measured radial velocities were then corrected to air wavelengths using equation 3.6, and phased and separated into components in MATLAB.

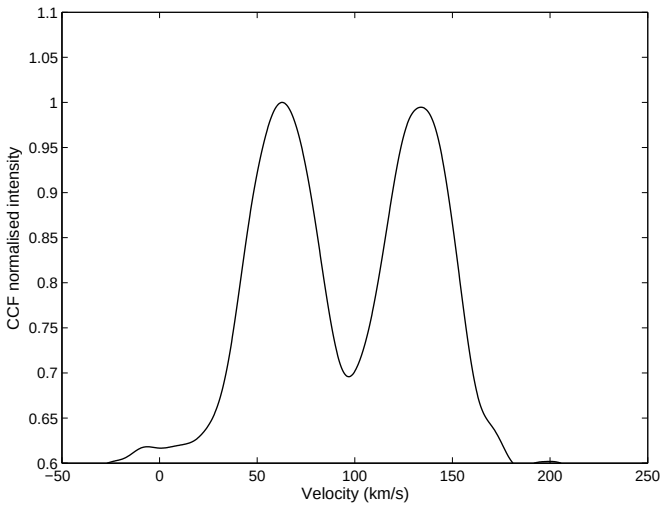

Figure 5.7: *The cross-correlation function for V392 Car coming into an eclipse.*

The radial velocities measured in this thesis were combined with the published radial velocities from Debernardi and North (2001). Debernardi and North's extensive coverage around the phases of maximum separation provided, when combined, a much greater coverage of the phases. Figure 5.9 shows the radial velocity curves for both components.

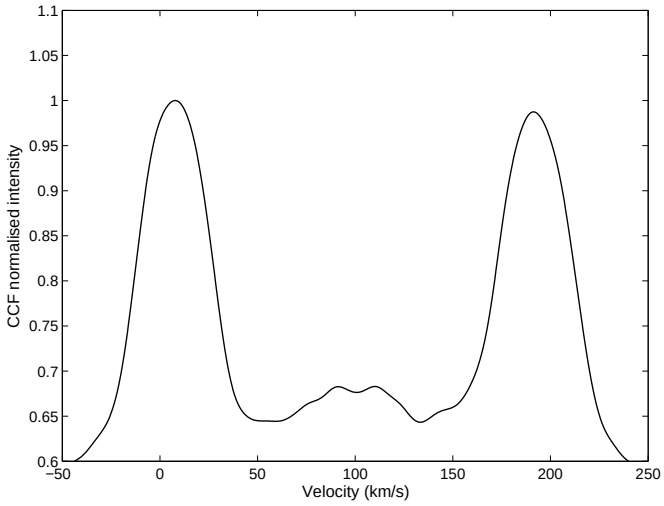

Figure 5.8: *The cross-correlation function of V392 Car near a time of maximum separation.*

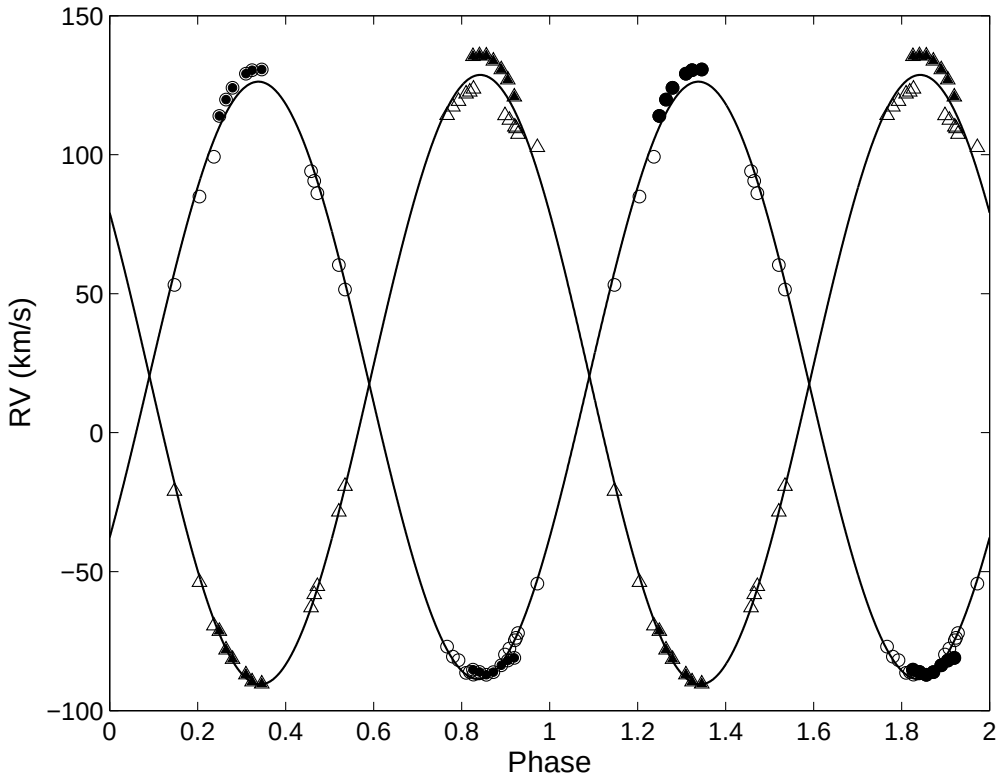

Figure 5.9: *The Radial Velocity curves from both components of V392 Car including the measurements from Debernardi and North (2001). Component one's velocities are the triangles, circles are the velocities from component two, filled symbols are the radial velocities from Debernardi and North (2001).*

5.3 Orbital Analysis

V392 Car is a SB2 type binary with eccentricity of zero. Therefore an orbital analysis from the measured radial velocities may be carried out using equation 3.7. The period of V392 Car was investigated with our measured radial velocities combined with the radial velocities from Debernardi and North (2001). The period used in Debernardi and North (2001) was not the best period for the velocity measurements. The best period was determined to be $q = 3^d.1749749 \pm 0.0000001$. This period was used in PHOEBE to produce the model of best fit.

The spectroscopic orbital parameters γ, K_n, $a_n \sin i$ were calculated from the fit of sine curves to the radial velocity curves. The fit was done in MATLAB using least-squares minimisation.

P	$3^d.149749 \pm 0^d.0000001$
e	0
$\gamma_1(kms^{-1})$	19.057 ± 0.130
$\gamma_2(kms^{-1})$	18.787 ± 0.129
$\gamma(kms^{-1})$	18.922 ± 0.092
$K_1(kms^{-1})$	109.635 ± 0.173
$K_2(kms^{-1})$	107.478 ± 0.174
$q = \frac{K_2}{K_1}$	0.980 ± 0.003
$a_1 \sin i(R_\odot)$	6.882 ± 0.011
$a_2 \sin i(R_\odot)$	6.747 ± 0.011
$M_1 \sin^3 i(M_\odot)$	1.667 ± 0.005
$M_2 \sin^3 i(M_\odot)$	1.700 ± 0.005

Table 5.1: *The orbital elements of V392 Car.*

5.4 Modeling with PHOEBE

V392 Car is a detached eclipsing binary. It's light curve displays partial eclipses of similar depth. The HJD_0, period and initial start points for the mass-ratio and temperatures were given to PHOEBE. The semi-major axis value could not be varied as it diverged with the first iteration, a value for this was adopted from Debernardi and North's model and then adjusted manually until the best fit was found.

	Primary	Secondary
$mass(M_\odot)$	1.915	1.862
$radius(R_\odot)$	1.74	1.74
$log(g)$	4.24	4.23
$a(R_\odot)$	7.103	6.825

Table 5.2: *The absolute parameters of V392 Car.*

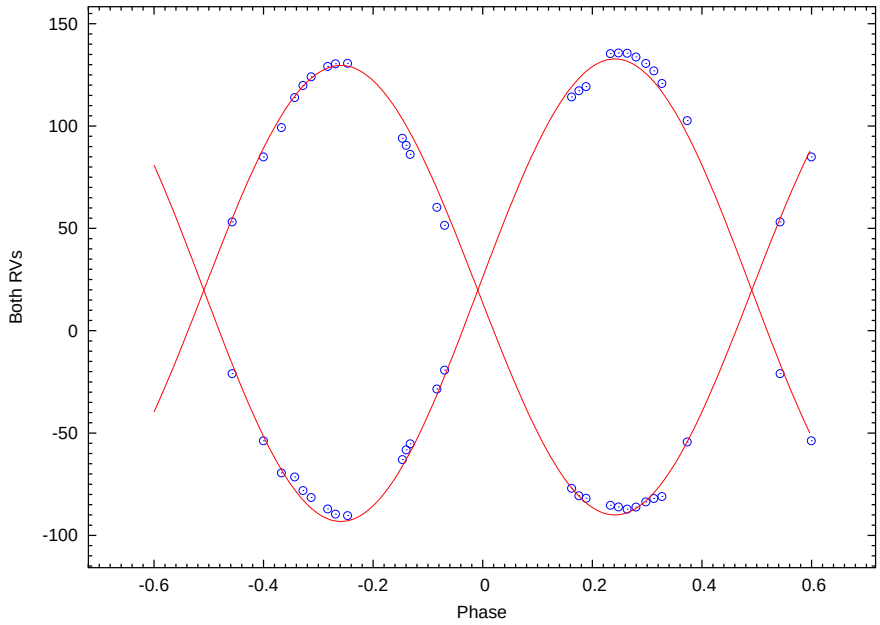

Figure 5.10: *The Radial Velocity curves from both components of V392 Car fitted with the model generated in PHOEBE.*

Figure 5.10 shows the radial velocities with the model determined in PHOEBE. The solution for V392 Car determined using PHOEBE is shown in table 5.3. The physical parameters of V392 Car given by the model are shown in table 5.2.

Parameter	Solution
HJD_0	2448000.55625
P	$3^d.1749749 \pm 0.0000001$
q	0.951 ± 0.021
i	$81.398 \pm 0.195^\circ$
$V_\gamma(kms^{-1})$	19.792 ± 5.118
$Semi - majorAxis(R_\odot)$	14.000
$T_1(^\circ K)$	8807 ± 100
$T_2(^\circ K)$	8646 ± 97
Ω_1	9.196 ± 0.132
Ω_2	8.856 ± 0.156
$g_1 = g_2$	0.3
A_1	0.909 ± 0.733
A_2	0.785 ± 0.716
$X1B$	0.451 ± 1.25
$X1Y$	0.588 ± 1.07
$X1V$	1.018 ± 0.302
$X2B$	1.235 ± 0.184
$X2Y$	1.127 ± 0.375
$X2V$	1.064 ± 0.318
$r1_{pole}$	0.121
$r1_{point}$	0.122
$r1_{side}$	0.121
$r1_{back}$	0.122
$r2_{pole}$	0.121
$r2_{point}$	0.122
$r2_{side}$	0.122
$r2_{back}$	0.122
$\Sigma(wr^2)$	9.15×10^{-4}
$\sigma_{RV1}(kms^{-1})$	3.841
$\sigma_{RV2}(kms^{-1})$	4.933

Table 5.3: *Solution of V392 Car determined from PHOEBE.*

$i[^\circ]$	81.89 ± 0.05
$a_1[R_\odot]$	7.160 ± 0.023
$a_2[R_\odot]$	6.982 ± 0.022
$a[R_\odot]$	14.142 ± 0.051
$M_1[M_\odot]$	1.900 ± 0.024
$M_2[M_\odot]$	1.853 ± 0.024
$R_1[R_\odot]$	1.625 ± 0.030
$R_2[R_\odot]$	1.601 ± 0.031
$log(g)_1$	4.286 ± 0.017
$log(g)_2$	4.310 ± 0.024
$T_{eff1}[K]$	8850 ± 200
$T_{eff2}[K]$	8650 ± 200

Table 5.4: *The physical parameters of V392 Car determined by Debernardi and North (2001)*

5.5 Comparison with Previous Model

V392 Car has been recently studied by Debernardi and North (2001), with observations taken a decade prior. The results from their photometric and orbital solution are given in table 5.4 and 5.5 respectively.

The radial velocity measurements made by Debernardi and North (2001), were combined with the measurements made for this thesis. The pooling of velocity measurements supplemented the recent measurements in the important phases corresponding to maximum separation of the components. The fits to the radial velocity curves show a considerable amount of scatter of the residuals. Unfortunately the radial velocities from the spectroscopic images observed in this thesis did not include velocities from times where the amplitude of the velocity curves can be determined.

The systematic velocity we have found ($\gamma = 19.8 \pm 5 kms^{-1}$, agrees within uncertainty of V392 Car's membership of the open cluster NGC 2516, where the average systematic velocity of the system is taken to be $22.7 \pm 0.4 kms^{-1}$ (the average velocity was found by taking the mean value from six stars from the WEB catalogue) (Robichon et al., 1999).

$P(J)$	3.174990 ± 0.000001
$T[HJD - 2400000]$	47999.7625 ± 0.0041
e	0
$\gamma[kms^{-1}]$	22.09 ± 0.77
$K_1[kms^{-1}]$	110.04 ± 0.49
$K_2[kms^{-1}]$	112.84 ± 0.49
$q = \frac{K_2}{K_1}$	0.975 ± 0.008
$a_1 \sin i[R_\odot]$	7.088 ± 0.0023
$a_2 \sin i[R_\odot]$	6.913 ± 0.021
$M_1 \sin^3 i[M_\odot]$	1.798 ± 0.018
$M_2 \sin^3 i[M_\odot]$	1.844 ± 0.018

Table 5.5: *The orbital parameters of V392 Car taken from Debernardi and North (2001).*

Chapter 6

V752 Centauri

The SB2, W UMa-type binary V752 Centauri was discovered in 1970 by H.E. Bond (Sisteró and Castore de Sisteró, 1973; Leung, 1976). Sisteró and Castore de Sisteró observed the system photometrically during April of 1971, and spectroscopically in May 1972 at Cerro Tololo Inter-American Observatory. Sisteró and Castore de Sisteró (1973) deduced a photometric solution for V752 Cen using the Russell model. Their solution suggested that the system was of a semi-detached configuration, where the larger and more massive component almost filled its Roche surface while the smaller component was smaller than its Roche surface.

Leung (1976) reanalysed Sisteró and Castore de Sisteró's observations with the better suited Wilson and Devinney code. Leung's solution indicated a contact system which is 6.3% overcontact.

Barone et al. (1993) reanalysed the observations made by Sisteró and Castore de Sisteró. They used the Wilson method to determine a synthetic model to fit the observations. Not all of the light curves were solved simultaneously and the temperature of the primary was fixed. The procedure they followed was one in which the constraints on the critical parameters were minimal, allowing the differential corrections procedure to converge on a solution with less bias toward the starting points. Their solution was completely different to that found by either Sisteró and Castore de Sisteró(1974) or Leung (1976).

Barone et al. (1993) found V752 Cen to be of 9% overcontact configuration. The primary minimum was due to an occultation which confirms the system as a W-type W UMa binary. The derived parameters from Barone et al. are shown in table 6.1.

	Solution
q	3.15 ± 0.07
$i(^\circ)$	81.66 ± 1.01
V_γ	29.15
Semi-major Axis	2.59 ± 0.04
T_1	6221 ± 81
T_2	5955 ± 77
$\Omega_1 = \Omega_2$	6.858 ± 0.084
$g_1 = g_2$	0.32
$A_1 = A_2$	0.5
$r1_{pole}$	0.269
$r1_{side}$	0.28
$r1_{back}$	0.318
$r2_{pole}$	0.459
$r2_{side}$	0.494
$r2_{back}$	0.522
$Fill - outfactor$	$8.7\% \pm 2.8\%$
l_3	0
$S = \left(\frac{1}{n}\right) \Sigma (l_{obs} - l_{comp})^2$	0.00253

Table 6.1: *The derived parameters of V752 Cen taken from Barone et al. (1993).*

6.1 Photometry

6.1.1 Photometric Data Preparation

The $BVRI$ photometric observations of V752 Cen were made by the author in March and April 2007. The observations were reduced in MIRA. A period study of the light curve was completed. A linear least-squares fit from the times of minimum observed yielded the following ephemeris;

$$HJD_0 = 2454183.128324 \pm 0.000027. \tag{6.1}$$

The period of the system was investigated with both the photometric observations and the spectroscopic measurements. The new period of this system was found to be $P = 0^d.370248$.

The reduced photometric measurements were phased using this period and entered into PHOEBE to determine the solution of V752 Cen.

6.1.2 Photometric Model

The photometric observations were fit simultaneously with the radial velocity curves in PHOEBE. The difference in the eclipse depths leads to a decision that the initial constraint of the PHOEBE model used was an over-contact system without thermal contact. This configuration allows a temperature difference between the components.

To fit the photometric data, first an unspotted model was attempted. The asymmetries in the maximum magnitudes of the light curves are often called the 'O'Connell effect'. The reason behind the effect is not well understood and is often modeled with star spots added to at least one of the binary's components. The addition of star spots to the photometric model increases the indeterminacy of the solution. Liu and Yang (2003) have attempted to explain the O'Connell effect with a theoretical model based on the hypothesis that the circumstellar material of a binary system is captured by its components. The O'Connell effect in our light curves were modeled with a solution containing a spot on the secondary component. The solutions to both attempts are shown in table 6.4. Figure 6.1 shows the light curves with the unspotted model. The introduction of a cool spot on the larger secondary component improved the model. Figure 6.2 shows the light curves from V752 Cen fitted with the spotted model.

The limb-darkening coefficients were calculated throughout the fitting process. The temperatures of both components were allowed to vary, the initial values of $6000K$ were made corresponding to the spectral types of the components. The gravity-darkening coefficient and the bolometric albedo were fixed at the values $g_1 = g_2 = 0.32$ and $A_1 = A_2 = 0.5$. The adjustable parameters were the mass-ratio q, the relative monochromatic luminosities ($L_1(B, V, R, I)$), the primary and secondary temperatures (T_1, T_2), the potential ($\Omega_1 = \Omega_2$), the inclination (i) and the limb-darkening coefficients ($X_1(BVRI)$ and $X_2(BVRI)$). The radial velocity curves were fitted simultaneously with the systematic velocity parameter free.

The unspotted model of the photometric data had a goodness of fit parameter $S = \Sigma(wr^2) = 2.38 \times 10^{-4}$ in flux units squared. The goodness of fit parameter was calculated using the total flux units as PHOEBE conducts most of its calculations in these units. The spotted model achieved a goodness of fit of $S = 1.77 \times 10^{-4}$. The value of the of the mass-ratio $q = 3.375 \pm 0.015$, and the primary, deeper eclipse being an occultation confirmed that V752 Cen is a W-type W UMa binary. Figure 6.3 illustrates the surfaces of the system in phase positions -0.25, 0, 0.25 and 0.5.

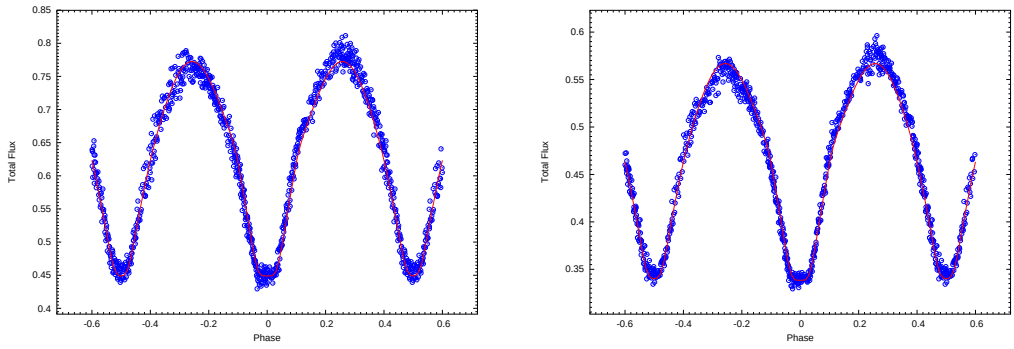

(a) Blue filter

(b) Visual filter

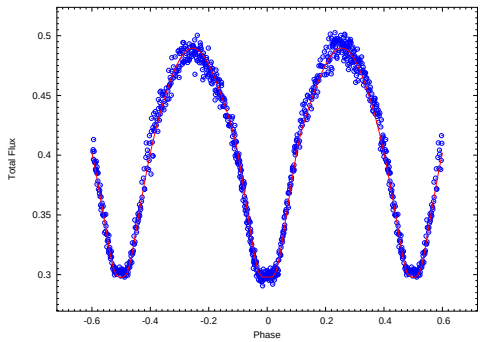

(c) Red filter

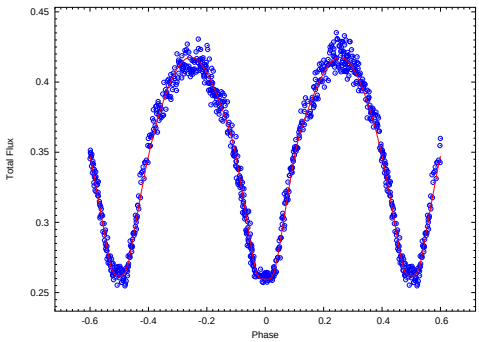

(d) Infrared filter

Figure 6.1: *The unspotted WD model in BVRI filters.*

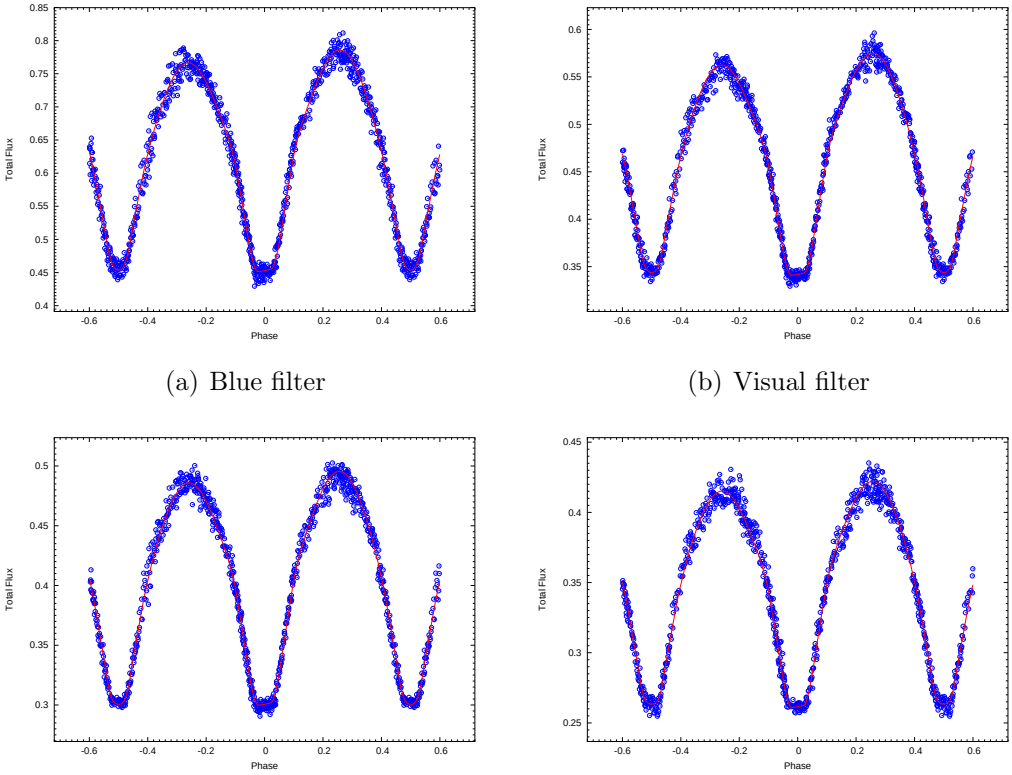

(a) Blue filter

(b) Visual filter

(c) Red filter

(d) Infrared filter

Figure 6.2: *The spotted WD model in BVRI filters.*

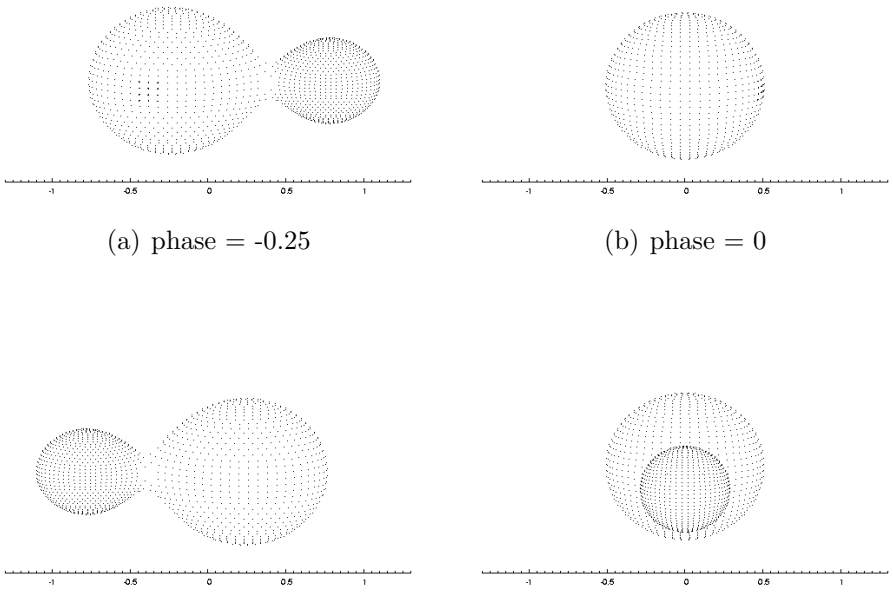

(a) phase = -0.25

(b) phase = 0

(c) phase = 0.25

(d) phase = 0.5

Figure 6.3: *3-D plots of the surface of V752 Cen (with spot).*

6.2 Spectroscopy

6.2.1 Radial Velocity Measurements

The spectroscopic images were all reduced in HRSP, then their echelle orders were extracted. Each order was scrunched onto a logarithmic scale with the same bin size. The spectra for V752 Cen were left in their echelle orders. The complexity of the spectrum for this target meant that we desired the added control of being able to cut out a certain wavelength range by dropping a specific order. This was judged of to be of more importance than combining the orders to maximise the information content with each cross-correlation.

A range of wavelengths was selected accounting for the atmospheric interference in the lower orders (higher wavelengths) and the deteriorating strength in the signal due to the white lamp flat image used in the reduction at the bluer end of the spectrum. The range of orders used was from order 101 to 130 corresponding to wavelengths $5500 - 4300\mathring{A}$. The strength of Hydrogen lines decrease steadily with spectral types F through G. Due to the great number of atoms contributing to these lines and the susceptibility of the atomic transitions of H-atoms to pressure broadening and the Stark effect, the Hydrogen lines are deeper and broader than the Fe lines. The great difference in their intrinsic shape from the sharp plentiful metallic lines means they should be avoided in the cross-correlation (Hilditch, 2001). The order 117 containing the strong $H\beta$ line at $4861\mathring{A}$ was neglected.

Each utilised order was re binned using FIGARO's *scrunch* technique and continuum fitted with the same routine as was applied to the combined spectra of V392 Car. The fitting of a continuum to spectra of an F8 type binary is not entirely precise as there is little continuum. This considered, the method of fitting a continuum by hand to each order would not have produced better results than the automated routine used. The automated routine treats each order equally and there is little or no bias which can arise when manual fitting is employed. The continuum fitted spectra were then run through the same filtering process as described previously in chapter 5.

Smoothing was applied to reduce the excessive noise using the *ixsmooth* command in FIGARO which smooths the data by reducing any perturbations on a scale smaller than the width of the specified gaussian. The spectra were smoothed with $\sigma = 6$ pixels. After smoothing the spectra were ready to be cross-correlated against a template.

The high resolution spectroscopy of this target revealed a previously unseen characteristic in its spectrum. The spectrum was dominated by the broad features expected from

such a short period binary, however there appeared to be weak sharp lines superimposed over the strong broad lines which are not expected from a synchronously rotating binary of a period of $0^d.370248$. This suggests that there is a third object contributing light to the spectrum, either within the system or perhaps in the line of sight of the target. The cross-correlation technique employed for this target therefore consisted of filtering out the sharp lined features from the broad in the hope of measuring velocities of this mysterious entity. Figure 6.4 shows one order of the spectrum of V752 Cen with the broad and sharp lined features separated.

Each order of the spectra was cross-correlated to a synthetic template which had a temperature of $7500K$ initially chosen from the spectral type Sisteró and Castore de Sisteró (1974) published, and validated from comparison of the two spectra. Another synthetic template with a temperature of $4000K$ was used to compare with the sharp lines featured in the spectra. The synthetic template spectra were computed from ATLAS9 model atmospheres and were not rotationally broadened to the same extent as the binary. The wavelength range for the template matched that of the order being cross-correlated.

The orders which were selected were all used in the cross-correlation routine. The CCFs were combined to produce a single CCF for each image. The orders do not produce CCFs of equivalent strengths and combining each order's CCF enhances the true profile. Figures 6.5 and 6.6 show the CCFs of the contact binary near times of eclipse and maximum separation of the components.

The combined CCF peaks were fitted with gaussians using FIGARO's *gauss* technique. The fitting of gaussians to these particular profiles was made difficult when measuring the binary's primary component as the CCF did not show a single peak. The secondary component's CCF peak profiles were well defined and therefore easier to measure. The error estimate for all our measured radial velocities is $2kms^{-1}$ as explained in Section 3.4. The method of cross-correlation as explained in Chapter 3, is a much more accurate way of determining velocities for late-type stars than the measurements from individual spectral lines. The measured velocities were corrected for the vacuum to air wavelength shift using a linearised version of equation 3.6.

Sisteró and Castore de Sisteró measured the shift of five individual lines from their 1972 spectra. A weighted mean of the five curves was calculated giving the final velocity curve. γ_1 and γ_2 were calculated and weighted giving the combined mean $\gamma = 29.3 \pm 6.6kms^{-1}$.

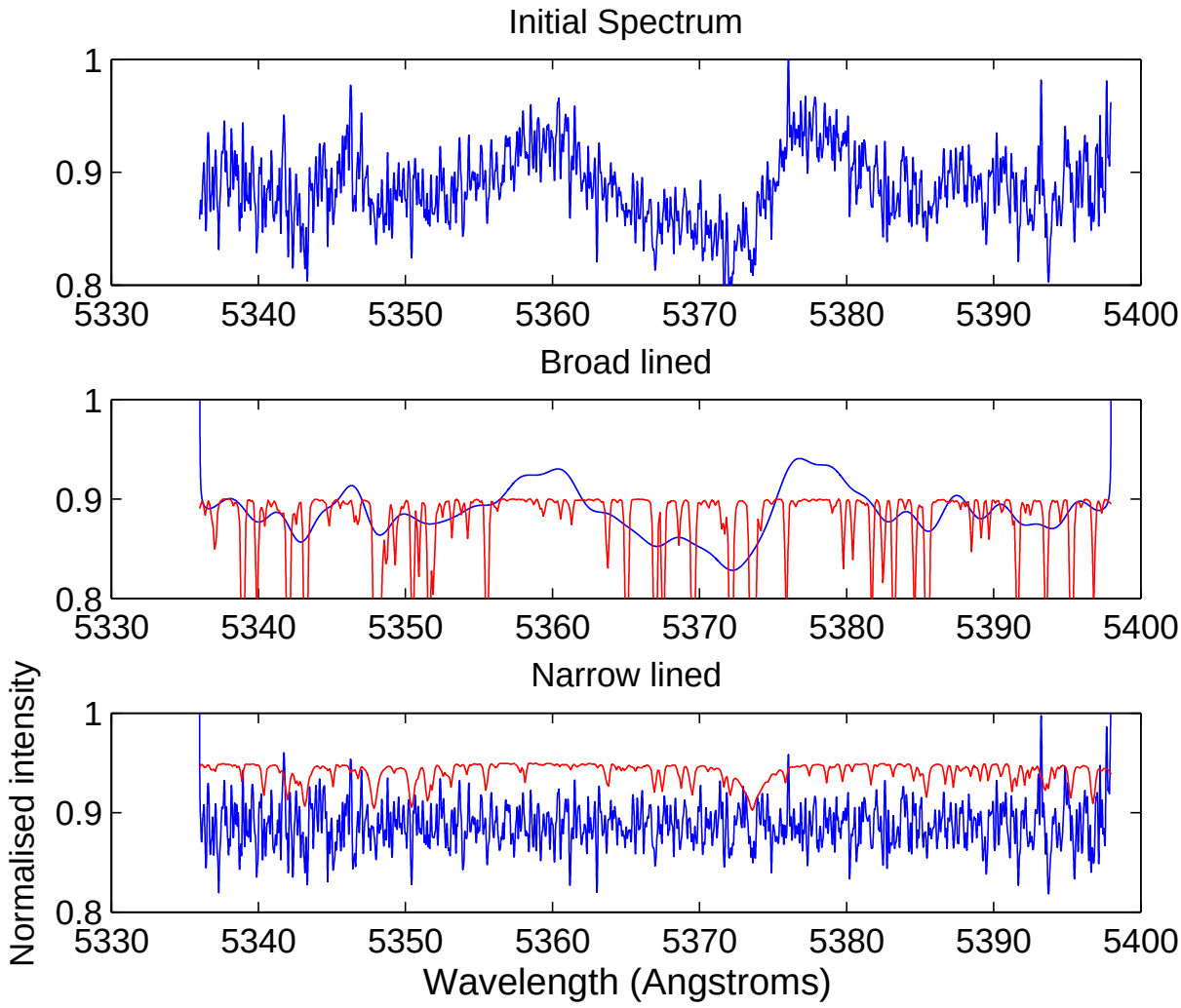

Figure 6.4: *Spectrum of V752 Cen near a time of eclipse. The uppermost plot shows one order of the observed spectrum after scrunching. smoothing, and continuum fitting. The middle plot shows the broad lined spectrum from the contact binary, in blue with the* $7500K$ *synthetic template in red. The bottom plot shows the narrow lined spectrum from the third component in blue with the* $5000K$ *synthetic template in red.*

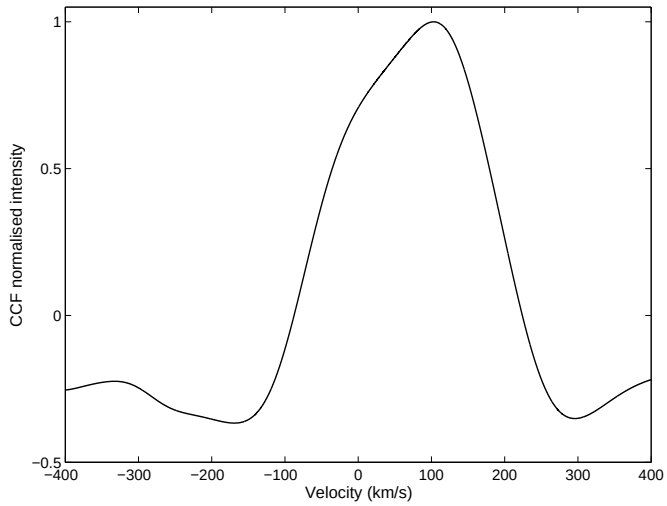

Figure 6.5: *A CCF profile of V752 Cen: the contact binary near a time of eclipse.*

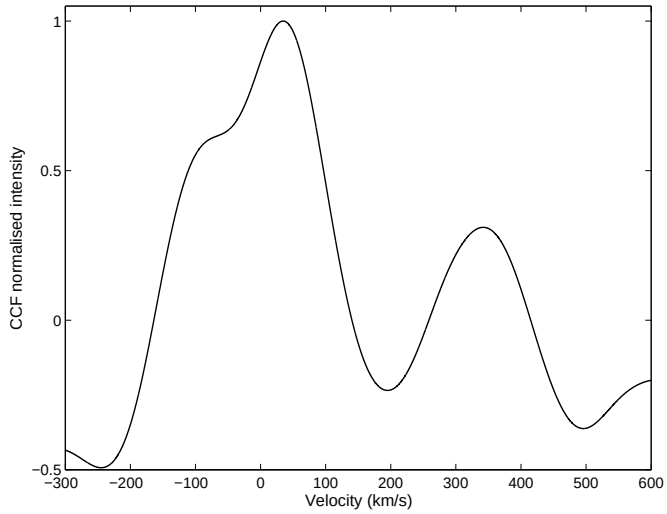

Figure 6.6: *A CCF profile of V752 Cen: the contact binary near a time of maximum separation.*

6.3 Orbital Analysis

The radial velocity curves for the two components of the W UMa-type system were independently fitted with sine curves. From equation 3.7, the semi-amplitudes and the systematic velocity of the system can be determined. Figure 6.7 show the best sinusoidal fit to the radial velocity measurements of the contact binary V752 Cen.

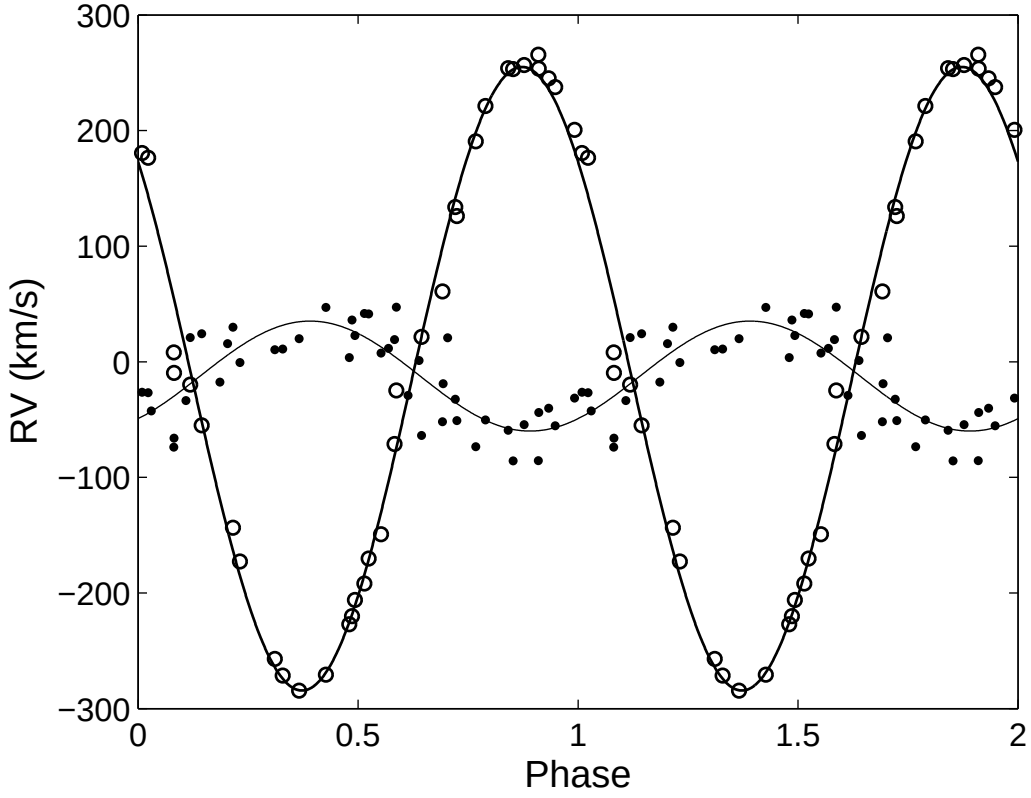

Figure 6.7: *The sine fit using least squares optimization for V752 Cen. Primary component's velocities are the filled circles. Secondary's are the hollow circles.*

A ratio of the semi-amplitudes gives a value for the mass-ratio $q = K_2/K_1$, which can be used as a starting point for the mass-ratio value in PHOEBE. As with BP Vel and V392 Car, the mass-ratio is set as an adjustable parameter when determining the solutions of the systems in PHOEBE.

The sinusoidal fits were performed using least-squares minimization. The scatter of the residuals from the fit are $24.1337 kms^{-1}$ for component one and $14.2637 kms^{-1}$ for component two.

$$V_1 = -12.398 + 47.563 \sin\theta,$$

and

$$V_2 = -14.593 + 269.678 \sin\theta. \tag{6.2}$$

The mass-ratio determined from the ratio of the semi-amplitudes was $q = 5.671 \pm 0.030$. This value is higher than the published result from Barone et. al (1993) $q = 3.15 \pm 0.07$. The radial velocity curves in Barone et. al are from Sisteró and Castore de Sisteró's spectroscopic observations made in 1972.

The previously published $q = 3.15 \pm 0.07$ determined by Barone et al. (1993), was adopted for use in PHOEBE. The parameter was allowed to vary and converged to its best value during the light and velocity curve modeling in PHOEBE. The value for q determined in our analysis was also attempted as a starting mass-ratio value for a model in PHOEBE. Table 6.2 shows the results from our spectroscopic orbital analysis.

P	0.370248
e	0
$\gamma_1(kms^{-1})$	-12.387 ± 0.094
$\gamma_2(kms^{-1})$	-14.695 ± 0.120
$\gamma(kms^{-1})$	-13.265 ± 0.1528
$K_1(kms^{-1})$	47.563 ± 0.213
$K_2(kms^{-1})$	269.679 ± 0.235
$q = \frac{K_2}{K_1}$	5.671 ± 0.030
$a_1 \sin i(R_\odot)$	0.348 ± 0.0003
$a_2 \sin i(R_\odot)$	1.974 ± 0.002
$M_1 \sin^3 i(M_\odot)$	1.042 ± 0.002
$M_2 \sin^3 i(M_\odot)$	0.184 ± 0.001

Table 6.2: *The orbital elements of V752 Cen*

6.4 PHOEBE

The light and radial velocity curves were simultaneously fitted in PHOEBE. There were two models with different starting points for the mass-ratio. The first adopted the mass-ratio $q = 3.15$, of Lapasset et al.ś model, while the second value for the mass-ratio $q = 5.67$, had been determined from our spectroscopic orbital analysis. The model in PHOEBE with the high mass-ratio value that we found would not converge to a fit with the light curves.

6.4.1 Model with initial mass-ratio $q = 3.15$

Initially the observations were fit with a model not including star spots. The light curves display the O'Connell effect which meant that the addition of a star spot to the model improved the fit. The residuals of the unspotted model with the observations showed an overestimation of flux in the maximum at phase -0.25 and it underestimated the flux at the maximum at phase 0.25. A cool spot was placed on the equator of the larger secondary component. The position, size and temperature differential of the cool spot are shown in table 6.3.

Location	Secondary
Colatitude	90° (adopted)
Longitude	$253.8 \pm 0.1°$
Spot Radius	$12.02 \pm 3.0°$
$\frac{T_{spot}}{T_{star}}$	0.8

Table 6.3: *Star spot parameters for V752 Cen.*

The radial velocity curves fitted with the spotted model determined by PHOEBE are shown in Figure 6.8.

The routine performed in PHOEBE was repeated with contribution to the luminosity from a third light source. The evidence of a third component in the spectrum means there would be some contribution to the total light of the system from this body. The initial parameters used in the previous models were used in the model with the third light. The third light was added as a percentage of the total light with the initial value 0.05, or 5% of the total light. The third light parameter was then left free to adjust during iterations. It converged to negative values in all but the infrared filter. This does not seem to be a physical explanation for what is truly happening with the system. A fit was also attempted by holding the third light parameter fixed at 0.05, but this did not improve the fit to the observations. Kaitchuck et al. (2006), encountered similar problems when they attempted to improve their fit to the contact binary FU Dra with the addition of third light.

The model generated with PHOEBE gave a systematic velocity of $\gamma = -13.3 \pm 4.4 kms^{-1}$. The systematic velocity determined from the sine curve fit in MATLAB was $\gamma = -13.778 kms^{-1}$ which agrees well within the uncertainty of the model's value. The systematic velocity of V752 Cen has changed significantly since the value determined from the 1972 observations $\gamma = 29.15 kms^{-1}$. The large shift in systematic velocity over the

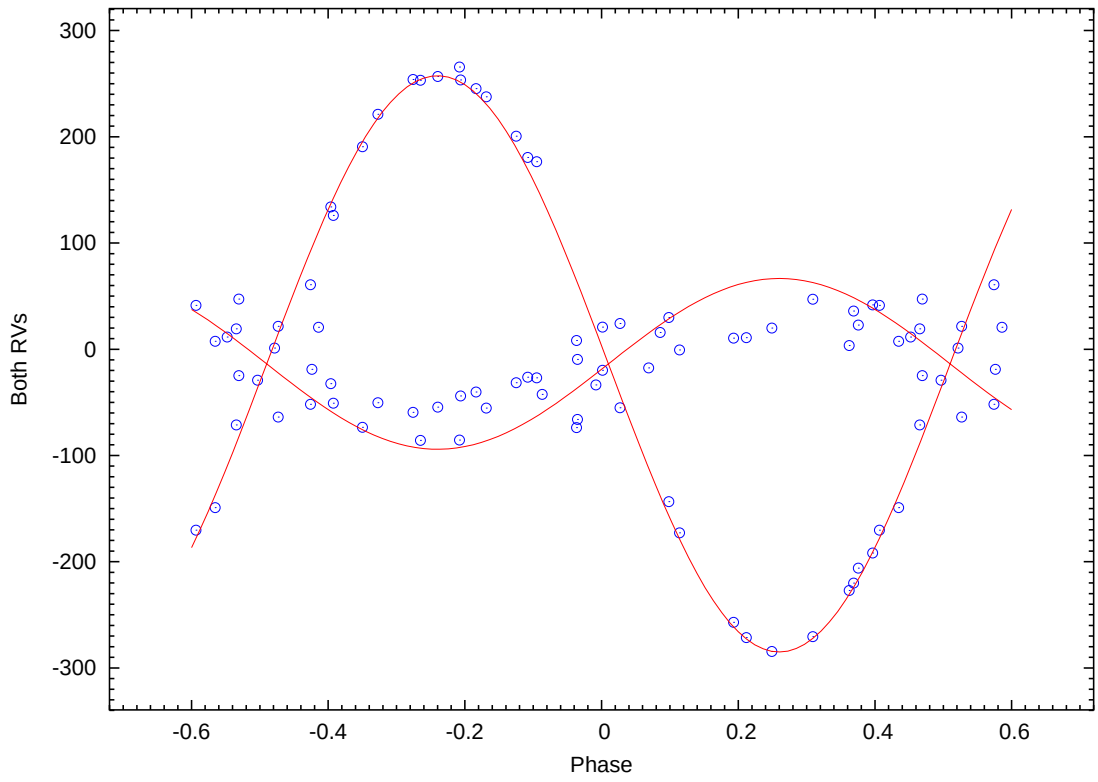

Figure 6.8: *PHOEBE's model radial velocity curves with the measured velocities from V752 Cen.*

≈ 30 year period indicates there may be some other gravitational effect acting on the system, causing V752 Cen the contact binary, to alter its motion with respect to the Sun. The added evidence of the sharp lined spectral features in the spectra of V752 Cen discovered with the use of the high resolution spectrograph HERCULES, enabled an insight as to what was causing the shift in systematic velocity of the W UMa-type binary.

	Unspotted Solution	Spotted Solution
q	3.19547 ± 0.0066	3.37507 ± 0.015
i	81.8748 ± 0.28	81.6269 ± 0.51
V_γ	-13.2979 ± 4.4	-13.7717 ± 4.3
Semi-major Axis	2.6	2.6
T_1	6083 ± 11	6187 ± 12
T_2	5905 ± 11	5965 ± 12
$\Omega_1 = \Omega_2$	6.63956 ± 0.0039	6.88613 ± 0.024
$g_1 = g_2$	0.32	0.32
$A_1 = A_2$	0.5	0.5
$X1B$	0.4123 ± 0.074	0.56006 ± 0.06
$X1V$	0.2513 ± 0.0127	0.4233 ± 0.105
$X1R$	0.2651 ± 0.154	0.3999 ± 0.133
$X1I$	-0.02577 ± 0.299	0.1388 ± 0.255
$X2B$	0.4208 ± 0.029	0.4848 ± 0.027
$X2V$	0.29098 ± 0.048	0.3512 ± 0.044
$X2R$	0.2182 ± 0.062	0.2827 ± 0.057
$X2I$	0.09847 ± 0.1	0.1749 ± 0.091
$r1_{pole}$	0.281	0.275
$r1_{side}$	0.295	0.289
$r1_{back}$	0.343	0.336
$r2_{pole}$	0.468	0.471
$r2_{side}$	0.507	0.51
$r2_{back}$	0.538	0.54
$\Sigma(wr^2)$	2.38×10^{-4}	1.77×10^{-4}

Table 6.4: *The solution to the spotted and unspotted models from PHOEBE.*

6.5 Third Component

Observed with the high resolution spectrograph HERCULES, the spectrum of V752 Cen displayed an interesting addition. Superimposed over the broad lines expected from a SB2 binary of such a short period with large rotational broadening, were sharp lined spectral features. The sharp lined component of the spectrum was isolated through a Fourier-filtering process during the cross-correlation. The isolated sharp lined spectrum was cross-correlated with a synthetic spectrum corresponding to a K solar type star.

The CCF from the cross-correlation was fitted with a gaussian profile as the other stars were. The radial velocity was measured from the centroid position of the gaussians. The error estimate on the velocities was adopted as $2kms^{-1}$ as explained in Chapter 3. Figure 6.9 shows an example of a CCF profile from the third component. The radial velocity measured from the CCFs were then corrected for the wavelength shift from vacuum to air wavelength calibration.

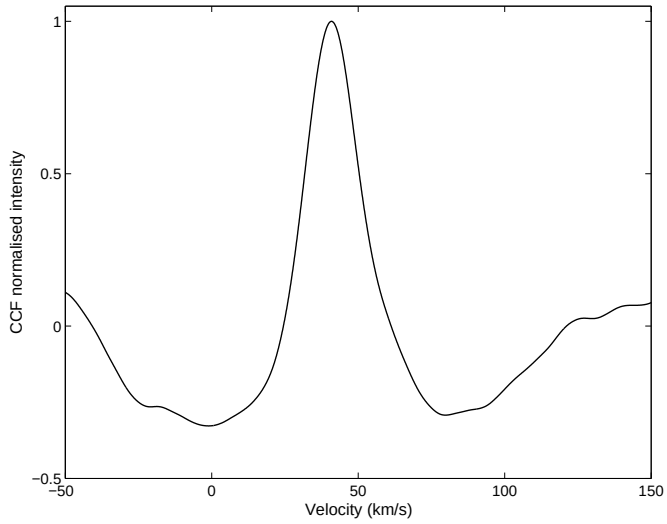

Figure 6.9: *An example of the CCF of the third component of V752 Cen.*

6.5.1 Determining the Period

The period of the potential third component was determined using a routine performed in MATLAB that fitted a sine curve to the radial velocity curve with least squares optimization. The parameters of the radial velocity curve were found to be $K = 43.359 \pm 0.203 kms^{-1}$, $\gamma = -7.253 \pm 0.096 kms^{-1}$ and the period of the additional component was

determined as $5^d.147$. The fit along with the radial velocity measurements is shown in Figure 6.10.

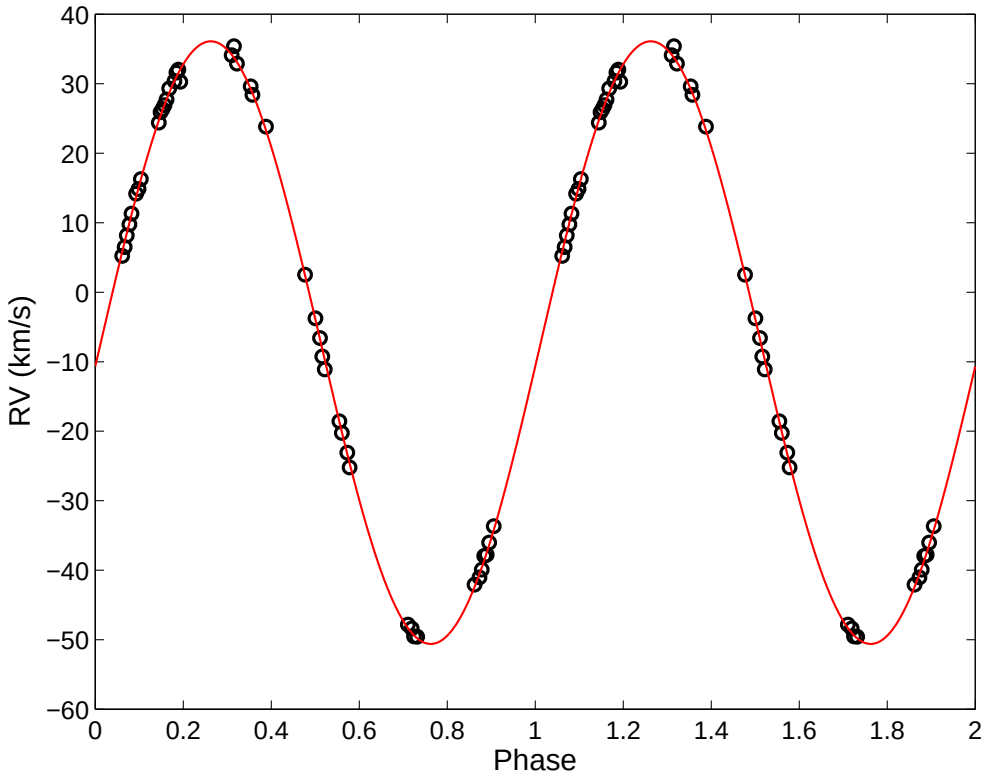

Figure 6.10: *The sine fit using least squares optimization for the third component's total velocities in MATLAB.*

6.5.2 V752 Centauri: A triple system?

The discovery of this third component in the spectrum of V752 Cen and the large change in systematic velocity of the system, raises some questions on the configuration of the system of V752 Cen.

There are two possible configurations; either the third component is orbiting about the contact binary, or the velocities that have been measured from the third component belong to a SB1 binary with a $5^d.147$ period, where the secondary was not detected with the spectroscopic observations. The system of V752 Cen could then be a quadruple system where the binary systems are orbiting each other with a much longer period, i.e. a triple-lined spectroscopic quadruple.

If the first scenario is true, the orbiting third body would affect the radial velocities

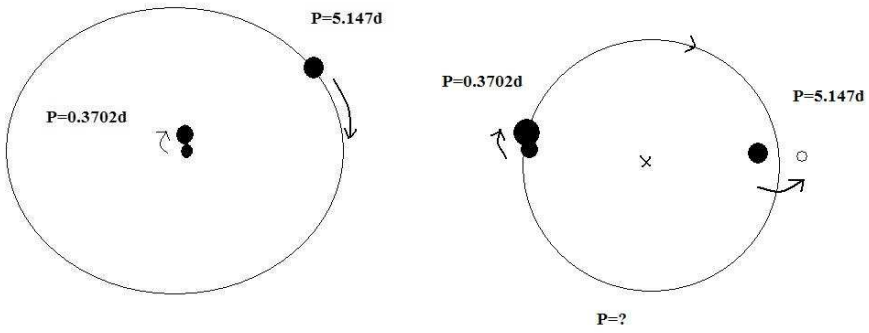

(a) *Third body orbiting about the contact binary with a period of* $5^d.147$

(b) *The* 5^d147 *period component is part of a separate SB1 system. Both contact binary and the longer period binary are orbiting each other at an unknown period.*

Figure 6.11: *Schematic diagrams showing the possible geometric configurations of the complete V752 system.*

of the contact binary. This has been tested by analysing the velocity curve of the second component of the contact binary. The residuals from the sine curve fit of component two were phased to the same period as the third component. If the third body were orbiting the contact binary with a period of $\approx 5^d$, the residuals of the second component's velocities may be expected show periodic variations at that period. There was no evidence of periodic variation in the velocity residuals of the contact binary.

The ratio of the intensity of the sharp lined spectrum to that of the binary was extremely difficult to measure. The spectral features from the sharp lined spectrum were at the level of the noise though they gave strong CCFs.

A comparison of Figures 6.4 and 6.12 suggest there is a slight increase in the strength of the sharp lined spectrum where the contact binary is at minimum light. An attempt was made to measure the difference in the equivalent widths of spectral lines from the sharp lined spectrum during times near eclipse and at maximum separation. It was very difficult to set a continuum around the spectral features as there was a high incidence of noise throughout the spectrum. The equivalent width measurements produced a difference of $\approx 5\%$ between the times of maximum and minimum light from the contact binary.

The sharp lined spectrum suggests the third component is a main sequence star with an early K spectral type. Had a body such as this been orbiting the contact binary with a 5 day period, the gravitational effect would have weakened the stability of the W UMa-type binary.

The likely configuration appears to be a quadruple system: two binary systems or-

biting about each other - the known W UMa-type binary V752 Cen with a period of $0^d.370248$ and the $5^d.147$ period SB1 binary discovered in this thesis. The inferred secondary component in the $5^d.147$ period system did not appear in the cross-correlation functions of the sharp lined spectrum, so is probably much less massive, perhaps an M dwarf.

The systematic velocity of V752 Cen has changed significantly from velocities found by Barone et al. (1993), $\gamma = 29.15 kms^{-1}$. The observations taken in 2007, provided velocities which gave a systematic velocity $\gamma = -13.77 \pm 4.3 kms^{-1}$. This gives added support to our model of two spectroscopic binaries in a long period orbit about each other. With only two measurements of the systematic velocity the orbital period of the whole system cannot be calculated.

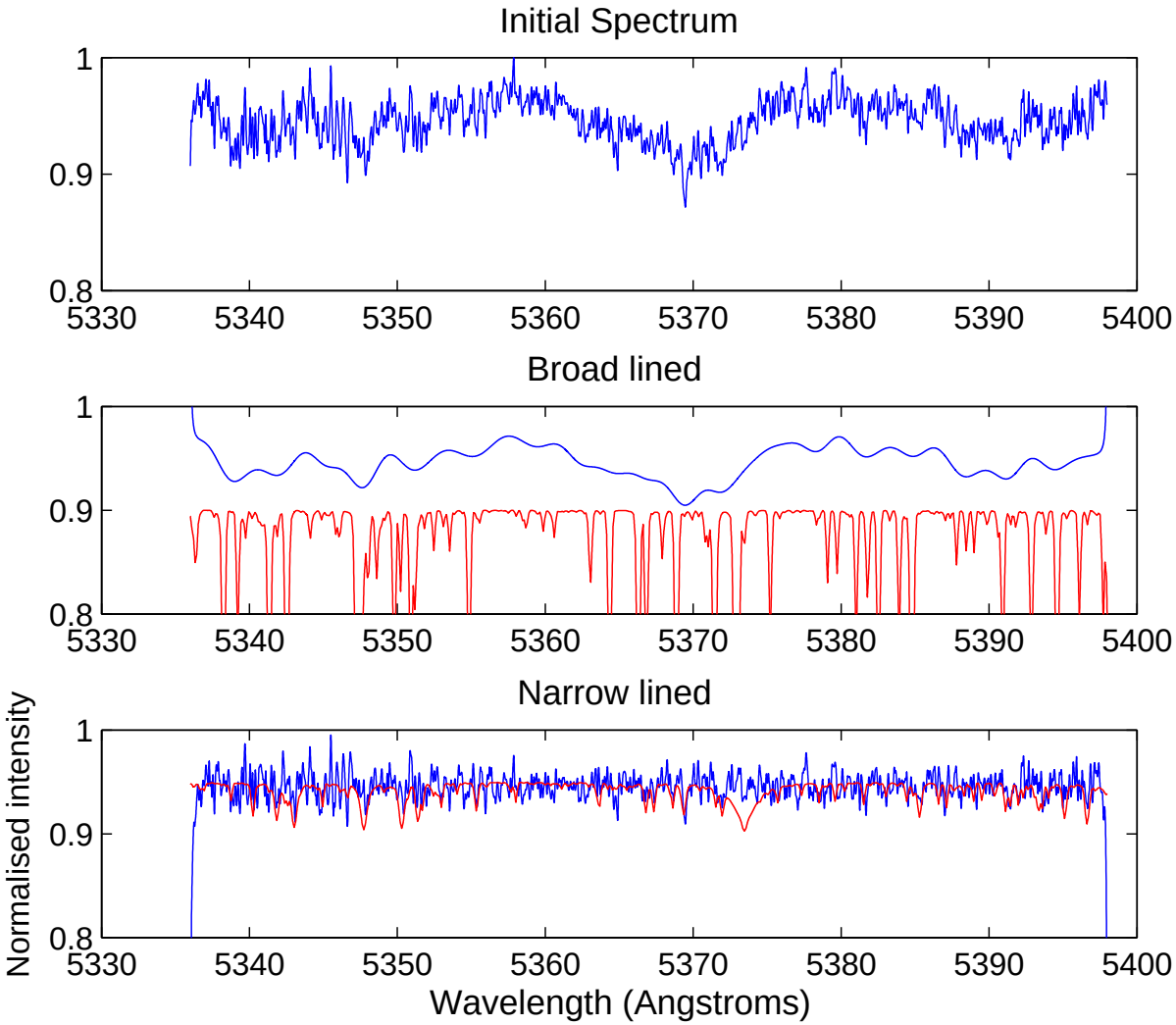

Figure 6.12: *Spectrum of V752 Cen near a time of maximum light from the contact binary. The uppermost plot shows one order of the observed spectrum after scrunching, smoothing, and continuum fitting. The middle plot shows the broad lined spectrum from the contact binary, in blue with the* $7500K$ *synthetic template in red. The bottom plot shows the narrow lined spectrum from the third component in blue with the* $5000K$ *synthetic template in red.*

Chapter 7

Summary

7.1 BP Velorum

A total of 1244 photometric observations were obtained through four filters. The photometric solution determine in this thesis used the software package PHOEBE. With no spectroscopic observations available for BP Vel, the determination of the mass-ratio was completed by holding the mass-ratio parameter fixed while the WD code fitted a model to the observations. The mass-ratio that provided the best fit by means of the sum of the squared weighted residuals was $q = 2.1$. This value was used as an initial starting point for the mass-ratio from which the WD code converged on the value $q = 2.1344 \pm 0.0108$. The light curves displayed an inequality in the depth minima, which was modeled by leaving both components' temperatures free to vary. There were asymmetries in the light curves about the maxima which suggested star spot activity on the surface of one of the components. The model was improved with the addition of a cool spot located near the equator on the secondary component, although it also appeared that there are residual cycle-to-cycle variations. The spotted model gave a larger value for the mass-ratio $q = 2.1980 \pm 0.0045$. The geometric configuration of the system was confirmed as being a W-type W UMa binary, with the deeper primary minimum resulting from an occultation of the smaller component.

7.2 V392 Carinae

The photometric observations taken by Michael Snowden of V392 Car were supplemented with the published V light curve from Debernardi and North (2001). The spectroscopic data obtained for this thesis failed to cover the areas corresponding to the maximum

separation of the components giving the maximum velocities. Fortunately the published velocities were from these times and when combined with our measurements, gave a more complete radial velocity curve. The spectroscopic orbital parameters were calculated after independent sinusoidal fitting of the velocity curves. The mass-ratio was determined from the ratio of the semi-amplitudes and found to be $q = 0.961$. The systematic velocity of the system determined from the sine fit was $\gamma = 20.011 kms^{-1}$. The light and velocity curves were simultaneously modeled using PHOEBE. An initial value for the mass-ratio which had been determined from the orbital parameters was used along with estimates of the temperatures of the stars. We determined a model for V392 Car with $q = 0.971966 \pm 0.0029$ and $\gamma = 19.7921 \pm 5.5 kms^{-1}$. The results from the fit made in PHOEBE agree within uncertainty with the results form the most recent publication of a solution for V392 Car; Debernardi and North (2001).

7.3 V752 Centauri

The previous studies of this contact binary all used observations made by Sisteró and Castore de Sisteró in 1972. The observations used in this new analysis were all taken during 2007. The new photometric images were taken with a CCD camera which allows the reduction of the images to be completed using comparison stars in the same field of view. The spectroscopic images were taken with the high resolution echelle spectrograph HERCULES, where the previous spectroscopic study was made with low resolution spectrograms. The high resolution spectra uncovered an interesting feature in the V752 Cen system. A third body was discovered to be contributing sharp lined features to the expected broad lined spectra of the contact binary. The method of cross-correlating the target spectra with synthetic templates extracted the velocity information from the three contributers to the spectrum. The W UMa contact binary components' velocities were measured and fitted simultaneously with the photometric light curves in PHOEBE. An orbital analysis using a sinusoidal fit to the velocities was conducted on the binary first. This gave a mass-ratio of $q = 5.7$ which is a lot higher than the previously published values $q = 3.15$ (Barone et al., 1993). The systematic velocity of the system was determined to be $\gamma = -13.778 kms^{-1}$ from the observations taken for this thesis. The systematic velocity from the latest publication was $\gamma = 29.15 kms^{-1}$. The PHOEBE model determined the mass-ratio of the system to be $q = 3.375 \pm 0.015$ and a systematic velocity of $\gamma = -13.772 \pm 4.3 kms^{-1}$.

The third component's velocities were measured and a sinusoidal fit was applied to the

measurements to determine a period. The fit produced a period of $5^d.147$, semi-amplitude $K = 43.381 kms^{-1}$ and a systematic velocity of $\gamma = -7.2825 kms^{-1}$. The configuration of the total system was deduced to be that of a quadruple system with two binary systems orbiting a common center of mass. Unfortunately, with only two measurements of the systematic velocity of V752 Cen, an orbital period of this quadruple system could not be determined.

7.4 Future work

To further the research of BP Velorum measurements of the radial velocities would provide an accurate value for the mass-ratio of the system. The photometric light curves published are well determined. The analysis of BP Vel conducted in this thesis produced the solutions sown in table 4.4. The spotted solution produced the best fit because of variations in the light curves in all filters at maximum light. The nature of the cycle-to-cycle photometric variations that we have found near maximum light could perhaps be revealed by spectroscopy, or very high-time resolution photometry. Either of these options would require the use of a large telescope.

V392 Carinae had been recently analysed by Debernardi and North (2001) using both light and radial velocity curves. The phase coverage of the radial velocity curves would benefit from more observations made particularly around the times of eclipse.

The discovery of a third component, possibly belonging to a SB1 binary, in the V752 Centauri system should be investigated further. More spectroscopic observations to further constrain the period determination of the third component and establish a more complete velocity curve would be the next step in determining the configuration of the whole system of V752 Cen. The period of the whole system of V752 Cen needs to be determined when there are further measurements of the systematic velocities made. Better quality radial velocity measurements for component one of the contact binary need to be made to determine the true mass-ratio of the contact system.

References

URL `http://vizier.u-strasbg.fr/viz-bin/VizieR`.

R. F. Sisteró and M. E. Castore de Sisteró. Radial Velocity Curves of HD 101799. *The Astronomical Journal*, 79:391–425, 1974.

J. Andersen and B. Nordström. Standardization of stellar radial velocities in the presence of stellar rotation. *Astronomy and Astrophysics*, 122:23–32, 1983.

F. Barone, L. di Fiore, L. Milano, and G. Russo. Analysis of contact binary systems-AA Ursae Majoris, V 752 Centauri, AO Camelopardalis, and V 677 Centauri. *The Astrophysical Journal*, 407:237, 1993.

D. H. Bradstreet and E. F. Guinan. Stellar Mergers and Acquisitions: The Formation and Evolution of W Ursae Majoris Binaries. In A. W. Shafter, editor, *Interacting Binary Stars*, volume 56 of *Astronomical Society of the Pacific Conference Series*, pages 228–+, 1994.

J. W. Brault and O. R. White. The Analysis and Restoration of Astronomical Data via the Fast Fourier Transform. *Astronomy and Astrophysics*, 13:169–189, July 1971.

B.A. Carroll and D.A. Ostlie. *An Introduction to Modern Astrophysics*. Aidon-Wesley Publishing Company Inc., 1996.

Sz. Csizmadia and P. Klagyivik. *Research Note* on the properties of contact binary stars. *Astronomy and Astrophysics*, 426:1001–1005, 2004.

Y. Debernardi and P. North. Eclipsing binaries with candidate CP stars II. Parameters of the system V392 Carinae. *Astronomy and Astrophysics*, 374:204–212, 2001.

J.B. Hearnshaw, S.I. Barnes, G.M. Kershaw, N. Frost, G. Graham, R. Ritchie, and G.R. Nankivell. The Hercules Échelle Spectrograph at Mt. John. *Experimental Astronomy*, 13(2):59–76, 2002.

R. W. Hilditch. *An Introduction tro Close Binary Stars*. Cambridge University Press, 2001.

R. H. Kaitchuck, R. L.Hill, A. P. Corn, J. Gevirtz, K. L.Levell, and T.L. Valenti. A Photometric Study of the Contact Binary System FU Dra. *Journal of the American Association of Variable Star Observers*, 34:1–7, 2006.

Zdeněk Kopal. *Close Binary Systems*, volume 5 of *The International Astrophysics Series*. Chapman & Hall Ltd., London, 1959.

E. Lapasset and M. Gomez. Photoelectric Minima Observations of the Short Period Eclipsing Binary BP Velorum. *Informational Bulletin on Variable Stars*, 3185:1–+, May 1988.

E. Lapasset, M. Gomez, and R. Farinas. Photometric Analyses of the Short-Period Contact Binaries HY Pavonis, AW Virginis, and BP Velorum. *Publications of the Astronomical Society of the Pacific*, 108:332–+, April 1996.

Kam-Ching Leung. The Contact Binary HD 101799. *Publications of the Astronomical Society of the Pacific*, 88:936–939, 1976.

Q.-Y. Liu and Y.-L. Yang. A Possible Explanation of the O'Connell Effect in Close Binary Stars. *Chinese Journal of Astronomy and Astrophysics*, 3:142–150, April 2003.

L.B. Lucy. The Light Curves of W Ursae Majoris Stars. *The Astrophysical Journal*, 153:877–884, 1968a.

L.B. Lucy. The Structure of Contact Binaries. *The Astrophysical Journal*, 151: 1123–1135, 1968b.

S. W. Mochnacki and N. A. Doughty. A model for the totally eclipsing W Ursae Majoris system AW UMa. *Monthly Notices of the Royal Astronomical Society*, 156: 51–56, 1972.

S.W. Mochnacki. Contact binary stars. *The Astrophysical Journal*, 245:650, 1981.

J.E. Pringle and R.A. Wade, editors. *Interacting Binary Stars*. Cambridge University Press, 1985.

Andrej Prša. *PHOEBE Scientific Reference*
Phoebe Version 3.0. University of Ljubljana, January 2006.

Claudius Ptolemaeus. *The Almagest*. William Benton, Encyclopaedia Britanniac Inc., 1952.

David J. Ramm. *A spectroscopic study of detached binary systems using precise radial velocities*. PhD thesis, University of Canterbury, 2004.

N. Robichon, F. Arenou, J.-C. Mermilliod, and C. Turon. Open clusters with Hipparcos. I. Mean astrometric parameters. *Astronomy and Astrophysics*, 345:471–484, May 1999.

S. M. Ruciński. The Proximity Effects in Close Binary Systems. II. The Bolometric Reflection Effect for Stars with Deep Convective Envelopes. *Acta Astronomica*, 19: 245–+, 1969.

Jorge Sahade and Frank Bradshaw Wood. *Interacting Binary Stars*, volume 95 of *International Series in Natural Philosophy*. Pergamon Press Ltd., 1978.

R. F. Sisteró and M. E. Castore de Sisteró. UBV light variation and orbital elements of HD101799. *The Astrophysical Journal*, 78;5:413–420, 1973.

Jovan Skuljan. *HRSP Hercules Reduction Software Package*. University of Canterbury, 3.0 edition, March 2007. Alterations by Duncan Wright.

Robert C. Smith. *Observational Astrophysics*. Cambridge University Press, 1995.

O. Vilhu. Detached to contact scenario for the origin of W UMa stars. *Astronomy and Astrophysics*, 109:17–22, May 1982.

Acknowledgements

First and foremost I would like to thank my supervisor, Dr. Michael Albrow. Without his help in every aspect, this thesis would not have been completed. Thank you for all the hours you have spent working on codes and reading through what I have written.

To my co-supervisor Prof. John Hearnshaw, thank you for your insight into the physical meaning of my observations in particular with the configuration of the quadruple system of V752 Cen.

To Michael Snowden, thank you for the use of your photometric observations and your wealth of knowledge in reducing photometric images. Thanks for the many hours you came in and assisted with the reductions.

I would like to thank Duncan Wright for all his help with HRSP and finding a way to combine the echelle orders of the spectra. Thank you for taking much valuable time away from your own thesis at such a critical stage of your PhD.

Observing at Mt John would be extremely difficult without the invaluable assistance from Alan Gilmore and Pam Kilmartin. For all the early morning calls of help to which you came swiftly to the rescue and for picking me up from Fairlee when the snow prevented me from making it further to Tekapo (even though the road up the mountain was still needing work), I am deeply grateful.

My time spent in room 801 was made all the more enjoyable with the company of my lovely office mates who have helped in various ways. In particular Robyn and Veronica for all their help and company throughout the year.

Thank you to Steph and Mum and Dad who proof read my thesis in its various stages of completion. Finally to Sam, for all his help and support and the many times he proof read this work even though he had his own thesis to work on, thank you so much.

Appendix A

MATLAB code

Cross Correlation

This MATLAB script was written by Dr. Michael Albrow. It uses the MATLAB functions FFT and IFFT to perform fast-Fourier algorithms and inverse discrete Fourier transforms. The high and low frequency components of the input spectrum are separated and are cross-correlated individually with the appropriate template spectrum.

Listing A.1: Cross Correlation Routine

```
files = {'w4279028s100csetsmt.asc' 'w4279028s104csetsmt.asc' '
    w4279028s105smt.asc' 'w4279028s106smt.asc' 'w4279028s108smt.asc' '
    w4279028s109csetsmt.asc'};

xz = -1000:0.1:1000;
yz1 = zeros(size(xz));
yz3 = zeros(size(xz));

for k = 1:numel(files)

% Read templates and data

  s1 = load('ap00T7500G40k2odfnew.asc');
  twave1 = s1(:,1);
  l1 = s1(:,4);
  tflux1 = convolve(twave1,l1,30000);

  s2 = load('ap00T4000G40k2odfnew.asc');
  twave3 = s2(:,1);
  l3 = s2(:,4);
```

```
  tflux3 = convolve(twave3,l3,30000);

  s3 = load(files{k});
  lambda = s3(:,1);
  flux = s3(:,2);
  flux = flux/max(flux);

%  Interpolate templates to same wavelengths as data

  tflux1a = interp1(twave1,tflux1,lambda);
  tflux3a = interp1(twave3,tflux3,lambda);

%  Mean flux levels

  mflux = mean(flux);
  mflux1 = mean(tflux1a);
  mflux3 = mean(tflux3a);

%  Compute 10% cosine bell

  nl = numel(lambda);
  cosbell = ones(nl,1);
  pp = 1:0.1*nl;
  cosbell(pp) = sin(pp*pi/(2*max(pp)));
  cosbell(nl+1-pp) = cosbell(pp);

%  Subtract mean flux and apply cosine bell

  cflux = (flux-mflux).*cosbell;
  cflux1 = (tflux1a-mflux1).*cosbell;
  cflux3 = (tflux3a-mflux3).*cosbell;

%  Take fourier transforms and compute power spectra

  fflux = fft(cflux);
  pflux = real(fflux).^2 + imag(fflux).^2;
  fflux3 = fft(cflux3);
  pflux3 = real(fflux3).^2 + imag(fflux3).^2;
  fflux1 = fft(cflux1);
  pflux1 = real(fflux1).^2 + imag(fflux1).^2;

%  Compute velocity shift per pixel

  xn = 1:nl;
```

```
  xnf = xn - 0.5*nl;
  vnf = xnf.*(lambda(2)-lambda(1))*3e5/lambda(1);

%  Centre fourier transforms

  dpflux = [pflux pflux];
  dflux = dpflux(xn+0.5*nl);
  dpflux1 = [pflux1 pflux1];
  dflux1 = dpflux1(xn+0.5*nl);
  dpflux3 = [pflux3 pflux3];
  dflux3 = dpflux3(xn+0.5*nl);

% Plot log of power spectra

  figure(1)
  clf
  subplot(3,1,1)
  plot(vnf,log10(dflux),'b')
  subplot(3,1,2)
  plot(vnf,log10(dflux1),'r')
  subplot(3,1,3)
  plot(vnf,log10(dflux3),'m')

%  Do cross correlation

  cm1 = fflux.*conj(fflux1);
  cm3 = fflux.*conj(fflux3);

%  Do reverse fourier transforms

  cc1 = ifft(cm1);
  cc3 = ifft(cm3);

%  Centre cross correlation functions

  dc1 = [cc1 cc1];
  dd1 = dc1(xn+0.5*nl);
  dc3 = [cc3 cc3];
  dd3 = dc3(xn+0.5*nl);

%  Plot cross correlation functions

  figure(2)
  clf
```

```
  plot(vnf,dd1,'r--')
  hold on
  plot(vnf,dd3,'m--')
  grid on

%  Construct low and high pass filters

  filter1 = zeros(nl,1);
  pp = 1:15;
  filter1(pp) = 1;
  filter1(nl+1-pp) = filter1(pp);
  pp = 15:30;
  filter1(pp) = cos((pp-min(pp))*pi/(2*(max(pp)-min(pp))));
  filter1(nl+1-pp) = filter1(pp);

  filter3 = ones(nl,1);
  pp = 1:15;
  filter3(pp) = 0;
  filter3(nl+1-pp) = filter3(pp);
  pp = 15:30;
  filter3(pp) = sin((pp-min(pp))*pi/(2*(max(pp)-min(pp))));
  filter3(nl+1-pp) = filter3(pp);

%  Plot filters

  figure(5)
  clf
  plot(xn,filter1,'r')
  hold on
  plot(xn,filter3,'m')

%  Apply filters

  ffluxc1 = fflux.*filter1;
  ffluxc3 = fflux.*filter3;

%  Do cross correlations

  cm1 = ffluxc1.*conj(fflux1);
  cm3 = ffluxc3.*conj(fflux3);

% Do reverse FFTs

  cc1 = ifft(cm1);
```

```
cc3 = ifft(cm3);

% Centre CCF's

dc1 = [cc1 cc1];
dd1 = (dc1(xn+0.5*nl));
dc3 = [cc3 cc3];
dd3 = (dc3(xn+0.5*nl));

% Plot CCFs

figure(2)
plot(vnf,dd1,'r-')
hold on
plot(vnf,dd3,'m-')

% Find maxima of CCFs

vmax1 = vnf(find(dd1==max(dd1)));
vmax3 = vnf(find(dd3==max(dd3)));

% Do reverse FFTs

ifluxc1 = ifft(ffluxc1);
ifluxc3 = ifft(ffluxc3);
iflux1 = ifft(fflux1);
iflux3 = ifft(fflux3);

figure(3)
clf

subplot(3,1,1)
plot(lambda,flux,'b')
set(gca,'YLim',[0.8 1.0])

subplot(3,1,2)
plot(lambda,ifluxc1./cosbell+mflux,'b')
hold on
tflux1v = interp1(twave1*(1+vmax1/3e5),tflux1,lambda);
plot(lambda,tflux1v*0.5+0.4,'r')
set(gca,'YLim',[0.8 1.0])

subplot(3,1,3)
plot(lambda,ifluxc3./cosbell+mflux,'b')
```

```
  hold on
  tflux3v = interp1(twave3*(1+vmax3/3e5),tflux3,lambda);
  plot(lambda,tflux3v*0.05+0.9,'r')
  set(gca,'YLim',[0.8  1.0])

  xx{k} = vnf;
  yy1{k} = dd1;
  yy3{k} = dd3;
  yz1 = yz1 + interp1(vnf,dd1,xz);
  yz3 = yz3 + interp1(vnf,dd3,xz);

  pause

end

figure(5)
clf
hold on
for k = 1:numel(files)
  plot(xx{k},yy1{k}+2*(k-1),'r')
  [numel(xx{k}) min(xx{k}) max(xx{k})]
end

figure(6)
clf
hold on
for k = 1:numel(files)
  plot(xx{k},yy3{k}+2*(k-1),'m')
  [numel(xx{k}) min(xx{k}) max(xx{k})]
end

figure(7)
clf
plot(xz,yz1,'r')
hold on
plot(xz,yz3,'m')
grid on
xlabel('V_km.s^{-1}')
ylabel('CCF')
```

Sine Fit

The sine fitting by least-squares optimization was performed using a MATLAB script written by Dr. Michael Albrow.

Listing A.2: Sine Fitting routine

```
clear all
format long g

hdata1=load('V752RVcomp1.txt');
t1 = hdata1(:,1)-2450000;
y1 = hdata1(:,2);
hdata2=load('V752RVcomp2.txt');
t = hdata2(:,1)-2450000;
y = hdata2(:,2);
sigma = 2.0;



per = 0.37:0.00001:0.3704;
%per = 0.369:0.00001:0.371;
phstart = 0:0.0001:0.9999;

per2 = 5.147;
cycle2 = t/per2;
phase2 = cycle2 - floor(cycle2);

chi2min = 1e9;

for i = 1:length(per)
  cycle = t/per(i);
  for j = 1:length(phstart)
    phase = cycle - floor(cycle);
    S = sum(sin(2*pi*(phase-phstart(j))));;
    S2 = sum(sin(2*pi*(phase-phstart(j))).^2);
    T = [length(y) S; S S2]./(sigma*sigma);
    b = ([sum(y) sum(y.*sin(2*pi*(phase-phstart(j))))]')./(sigma*sigma);
    Tinv = inv(T);
    a = Tinv*b;
    chi2 = sum((y - a(1) - a(2)*sin(2*pi*(phase-phstart(j)))).^2);
    if chi2 < chi2min
      [per(i) chi2 a(1) a(2)]
      chi2min = chi2;
      bestph = phstart(j);
```

```
      bestp = per(i);
      besta1 = a(1);
      besta2 = a(2);
      besta1err = Tinv(1,1);
      besta2err = Tinv(2,2);
    end
  end
end

cycle = t/bestp;
phase = cycle - floor(cycle);

chi2min = 1e9;
for j = 1:length(phstart)
  cycle1 = t1/bestp;
  phase1 = cycle1 - floor(cycle1);
  S = sum(sin(2*pi*(phase1-phstart(j))));;
  S2 = sum(sin(2*pi*(phase1-phstart(j))).^2);
  T = [length(y1) S; S S2]./(sigma*sigma);
  b = ([sum(y1) sum(y1.*sin(2*pi*(phase1-phstart(j))))]')./(sigma*sigma);
  Tinv = inv(T);
  a = Tinv*b;
    chi2 = sum((y1 - a(1) - a(2)*sin(2*pi*(phase1-phstart(j)))).^2);
    if chi2 < chi2min
      [chi2 a(1) a(2)]
      chi2min = chi2;
      bestph1 = phstart(j);
      besta11 = a(1);
      besta21 = a(2);
      besta11err = Tinv(1,1);
      besta21err = Tinv(2,2);
    end
end

cycle1 = t1/bestp;
phase1 = cycle1 - floor(cycle1);

xphase = 0:0.001:2;
model = besta1 + besta2*sin(2*pi*(xphase-bestph));
model1 = besta11 + besta21*sin(2*pi*(xphase-bestph1));



figure(1)
clf
```

```
plot([phase phase+1],[y y],'r.')
hold on
plot(xphase,model,'b-')
plot([phase1 phase1+1],[y1 y1],'g.')
plot(xphase,model1,'k-')

bestp

[besta1 besta1err]
[besta2 besta2err]

[besta11 besta11err]
[besta21 besta21err]
```

Continuum Fitting

The continuum fitting script was written by Duncan Wright. It applies a polynomial fit to the continuum regions of the spectrum.

Listing A.3: Continuum Fitting routine

```
function [newwave,newint]=contbyresid(wave,int)

if nargin ~= 2
    disp('[wave,int]=smoothandcontbyresid(wave,int)')
    disp('two inputs required')
end
warning off
newwave = wave; % no smoothing
newint = int; % no smoothing
tempwave=newwave;
tempint=newint;
[fresult,gof,residuals]=fit(newwave,newint,'poly5');
inds=find(abs(residuals.residuals)>2*std(residuals.residuals));
tempwave(inds)=[];
tempint(inds)=[];
[fresult,gof,residuals]=fit(tempwave,tempint,'poly5');
inds=find(abs(residuals.residuals)>2*std(residuals.residuals));
tempwave(inds)=[];
tempint(inds)=[];
[fresult,gof,residuals]=fit(tempwave,tempint,'poly5');
inds=find(residuals.residuals<-1*std(residuals.residuals));
tempwave(inds)=[];
tempint(inds)=[];
[fresult,gof,residuals]=fit(tempwave,tempint,'poly5');
inds=find(residuals.residuals<-1*std(residuals.residuals));
tempwave(inds)=[];
tempint(inds)=[];
[fresult,gof,residuals]=fit(tempwave,tempint,'poly5');
inds=find(residuals.residuals<-1*std(residuals.residuals));
tempwave(inds)=[];
tempint(inds)=[];
continfit=fresult.p1*newwave.^5+fresult.p2*newwave.^4+fresult.p3*newwave
    .^3+fresult.p4*newwave.^2+fresult.p5*newwave+fresult.p6+std(residuals.
    residuals);
newint=newint./continfit;
```

Combining Orders

Combining the echelle orders was performed using a script written by Duncan Wright.

Listing A.4: Routine for Combining Orders

```
function [xax,currentspec]=combineorderschangedbyme(cutoff,winsize)

if nargin ~= 2
    disp('[xax,currentspec]=combineorders(cutoff,winsize)')
    disp('requires cutoff and winsize inputs')
    disp('This program produces a single combined spectrum from every *v.
        asc file')
    disp('in the order range 60:160 in the current directory. File need to
        be named')
    disp('according to HRSP convention (format w****###s%%%.asc where ***
        is the')
    disp('whole number Julian date, ### is the observation number and %%%
        is the ')
    disp('order number. ''cutoff'' is the ratio of signal at which the
        lower signla is ')
    disp('not considered in the ''combination'' of the orders. ''winsize''
        is the size')
    disp('of the window considered for the median smoothing of the data.
        The simple')
    disp('median smoothing chops winsize/2 pixels off each end of each
        order. Values of')
    disp('cutoff=10 and windsize=20 should be reasonable. The function
        returns xax and')
    disp('currentspec which are the wavelength and intensity vectors for
        the combined data.')
    disp('')
    disp('Now also load and uses ascii spectrum named the same as the
        normalised and')
    disp('continuum fitted spectrum except it has ''noff'' before the .asc
        extension.')
    disp('this noff spectrum is used only for the weighting and the
        normalised and')
    disp('continuum fitted spectrum is combined (hopefully nicely) with the
        minimum')
    disp('of discontinuities (I hope).')
    return
end
warning off
```

```
% Setup standard axis (using 0.1 as it is an easy axis to project on to for
    any given spectrum)

xax=3500:0.1:9500;

% Make empy spectrum to add on to

currentspec(1:numel(xax))=0;

% winsize is used as hwinsize which is half the winsize given rounded to a
   whole number

hwinsize=round(winsize/2);

% use waitbar to indicate progress

h = waitbar(0,'Combining spectral orders, please wait...');
for t=60:160

    % Make filenames

    if t<100
        nam=['*0' num2str(t) '.asc'];
        namnoff=['*0' num2str(t) 'noff.asc'];
    else
        nam=['*' num2str(t) '.asc'];
        namnoff=['*' num2str(t) 'noff.asc'];
    end

    % s=t-59;
    % find files corresponding to names and if their is only one that
       corresponds then use it (only one order in directory)

    list=dir(nam);
    list2=dir(namnoff);
    if isempty(list)
        disp('Cannot find list files satisfying *###.asc where ### is the
            order number.')
        disp('Try changing the nam variable above to *v.asc')
        return
    end
    if isempty(list2)
        disp('Cannot find list files satisfying *###noff.asc where ### is
            the order number.')
```

```
    disp('Try changing the nam variable above to *noffv.asc')
    return
end
if (isempty(list) ~= 1 && numel(list) == 1)
    [wave,int]=textread(list(1).name,'%f %f\n','headerlines',10);
    [wave2,int2]=textread(list2(1).name,'%f %f\n','headerlines',10);
    szint=size(int);
    szwave=size(wave);
    % is int a column? if not make it one, same for wave
    if szint(2) > 1
        int=int';
    end
    if szwave(2) > 1
        wave=wave';
    end
    szint2=size(int2);
    szwave2=size(wave2);
    % is int2 a column? if not make it one, same for wave2
    if szint2(2) > 1
        int2=int2';
    end
    if szwave2(2) > 1
        wave2=wave2';
    end
    % project this on to part of the standard axis (as tempxax and
       newint) ->here's where the 0.1 wavelength step comes in ...
    tempxax=ceil(min(wave)):0.1:floor(max(wave));
    newint=spline(wave,int,tempxax);
    newint2=spline(wave2,int2,tempxax);

    % get same part of current added spectrum (as tempcurr)

    % disp('cutting out spectrum')
    % if you don't like linearfindnearest (it is much slower) use this
    % indcurr1=find(roundn(xax,-1)==roundn(min(tempxax),-1));
    % indcurr2=find(roundn(xax,-1)==roundn(max(tempxax),-1));

     indcurr1=linearfindnearest(xax,min(tempxax));
     indcurr2=linearfindnearest(xax,max(tempxax));

    % check we got indices right

    if (isempty(indcurr1) || isempty(indcurr2) || indcurr1 < 0 ||
       indcurr1 > numel(currentspec) || indcurr2 < 0 || indcurr2 >
```

```
    numel(currentspec) || indcurr1 > indcurr2)
     fprintf('cannot find entire order within standard x-axis, ...
         therefore order %f is skipped \n',t)
     continue
end

indcurr=indcurr1:1:indcurr2;
tempcurr=currentspec(indcurr);

% check we found it all

if (numel(newint)~=numel(tempcurr))
     fprintf('cannot find entire order within standard x-axis, ...
         therefore order %f is skipped \n',t)
     continue
end
if (numel(newint2)~=numel(tempcurr))
     fprintf('cannot find entire order within standard x-axis for ...
         noff file, therefore order %f is skipped \n',t)
     continue
end

% combine spectra using weights based on the value of each pixel
    from a median filter using noff spectrum (this is why the orders
     should not be normalised or flat fielded). Put the combined
    value into tempempty

% median smooth data with a winsize pixel window

% disp('median filtering')
medtempcurr(1:numel(newint2))=0;
mednewint(1:numel(newint2))=0;

for pix=hwinsize+1:numel(newint2)-hwinsize
     medtempcurr(pix)=median(tempcurr(pix-hwinsize:pix+hwinsize));
     mednewint(pix)=median(newint2(pix-hwinsize:pix+hwinsize));
end

% chop off first and last hwinsize pixels from all spectra

medtempcurr=medtempcurr(hwinsize+1:end-hwinsize);
mednewint=mednewint(hwinsize+1:end-hwinsize);
tempxax=tempxax(hwinsize+1:end-hwinsize);
newint=newint(hwinsize+1:end-hwinsize);
```

```
newint2=newint2(hwinsize+1:end-hwinsize);
tempcurr=tempcurr(hwinsize+1:end-hwinsize);
indcurr=indcurr(hwinsize+1:end-hwinsize);

% combine spectral orders

% disp('combining')
tempempty(1:numel(newint))=0;
for pix=1:numel(newint)
    if (round(mednewint(pix)*100)/100==0 && round(medtempcurr(pix)
        *100)/100==0)

      % (roundn(mednewint(pix),-2)==0 && roundn(medtempcurr(pix)
        ,-2)==0) - case if both equal zero (rounded to 10^-2)

        continue % already equals zero
    elseif (round(mednewint(pix)*100)/100==0 && round(medtempcurr(
        pix)*100)/100~=0)

      % (roundn(mednewint(pix),-2)==0 && roundn(medtempcurr(pix)
        ,-2)~=0) - if mednewint equals zero (rounded to 10^-2)

        tempempty(pix)=tempcurr(pix);
        continue
    elseif (round(mednewint(pix)*100)/100~=0 && round(medtempcurr(
        pix)*100)/100==0)

      % (roundn(mednewint(pix),-2)~=0 && roundn(medtempcurr(pix)
        ,-2)==0) - if medtempcurr equals zero (rounded to 10^-2)

        tempempty(pix)=newint(pix);
        continue
    elseif (round(mednewint(pix)*100)/100~=0 && round(medtempcurr(
        pix)*100)/100~=0)

      % (roundn(mednewint(pix),-2)~=0 && roundn(medtempcurr(pix)
        ,-2)~=0)

      % if neither equal zero combine based on median filtered
        values unless one is greater than the cutoff times, in
        which case use the higher one only.

        if mednewint(pix) > medtempcurr(pix)*cutoff
            tempempty(pix)=newint(pix);
```

```
                    continue
                elseif medtempcurr(pix) > mednewint(pix)*cutoff
                    tempempty(pix)=tempcurr(pix);
                    continue
                else

                    % weighted combination from FIGARO's ECHMERGE

                    tempempty(pix)=(mednewint(pix)*newint(pix)+medtempcurr(
                        pix)*tempcurr(pix))/(mednewint(pix)+medtempcurr(pix)
                        );
                    continue
                end
            else
                disp('This shouldn''t have been able to happen!')
            end
        end

    else
        continue
    end

    % change the piece of the combined spectrum to be the tempempty part

    if numel(indcurr)==numel(tempempty)
        % for y=1:numel(indcurr)
            currentspec(indcurr)=tempempty;
        % end
    end
    waitbar((t-61)/(159-61))
    clear temp* newint ind* med* pix
end
close(h)
figure
plot(xax,currentspec,'k')
```

Appendix B

Photometry Measurements

Table B.1: *The photometric measurements of BP Velorum.*

HJD [-2454000]	B mag.	HJD [-2454000]	V mag.	HJD [-2454000]	R mag.	HJD [-2454000]	I mag.
145.940286	12.9252	145.9419179	12.8519	145.9428669	12.7518	145.9438278	12.6049
145.9452047	13.1203	145.9468476	12.9173	145.9477856	12.8105	145.9487345	12.6442
145.9493475	13.13	145.9509914	12.8762	145.9519403	12.7598	145.9528892	12.6067
145.9534912	13.0486	145.9551341	12.7935	145.956083	12.6756	145.957033	12.5239
145.9576339	12.9585	145.9592778	12.7128	145.9602148	12.5782	145.9611647	12.4236
145.9617657	12.8551	145.9634096	12.6213	145.9643585	12.4961	145.9653074	12.352
145.9659094	12.7342	145.9675523	12.539	145.9685012	12.4057	145.9694512	12.2703
145.9700521	12.6752	145.971696	12.4596	145.972633	12.3513	145.9735819	12.2124
145.9742069	12.6196	145.9758388	12.4097	145.9767887	12.2856	145.9777377	12.1687

Table B.1 cont.: *The photometric measurements of BP Velorum.*

HJD [-2454000]	B mag.	HJD [-2454000]	V mag.	HJD [-2454000]	R mag.	HJD [-2454000]	I mag.
145.9783386	12.5419	145.9799825	12.3653	145.9809315	12.2435	145.9818804	12.1263
145.9824824	12.4815	145.9841372	12.3308	145.9850752	12.2103	145.9860351	12.1027
145.988014	12.4512	145.9896459	12.29	145.9905948	12.1691	145.9915438	12.0833
145.9921457	12.4531	145.9937776	12.2813	145.9947266	12.1587	145.9956755	12.0478
145.9962895	12.4251	145.9979324	12.2645	145.9988813	12.1422	145.9998303	12.0386
146.0004322	12.4649	146.0020761	12.2496	146.0030251	12.1341	146.003974	12.0218
146.004576	12.4676	146.0062188	12.2266	146.0071678	12.1098	146.0081057	12.0302
146.0087077	12.4084	146.0103506	12.2179	146.0112995	12.0937	146.0122485	12.0142
146.0128504	12.4071	146.0144943	12.2207	146.0154433	12.1213	146.0163922	12.0215
146.0169942	12.4033	146.0186371	12.2423	146.019586	12.1194	146.0205239	12.0295
146.0211259	12.4455	146.0227688	12.2368	146.0237177	12.1304	146.0246667	12.0345
146.0252686	12.4347	146.0269125	12.2554	146.0278615	12.1451	146.0288104	12.0561
146.0369809	12.5017	146.0386358	12.3099	146.0395737	12.2125	146.0405227	12.1092
146.0411246	12.5634	146.0427675	12.3798	146.0437165	12.2527	146.0446654	12.151
146.0452674	12.5972	146.0469113	12.4076	146.0478602	12.2982	146.0487971	12.1844
146.0493991	12.6449	146.051043	12.4453	146.0519919	12.3492	146.0529409	12.2335
146.0535428	12.6711	146.0551857	12.5087	146.0561347	12.4209	146.0570726	12.2847
146.0576746	12.7552	146.0593175	12.5943	146.0602554	12.4975	146.0612044	12.3655
146.0618063	12.8205	146.0634382	12.69	146.0643872	12.5901	146.0653361	12.4609
146.0659261	12.9302	146.06757	12.8001	146.0685189	12.6853	146.0694558	12.5601
146.0700578	13.0713	146.0717007	12.9118	146.0726506	12.8127	146.0735876	12.6386

Table B.1 cont.: *The photometric measurements of BP Velorum.*

HJD [-2454000]	B mag.	HJD [-2454000]	V mag.	HJD [-2454000]	R mag.	HJD [-2454000]	I mag.
146.0741895	13.2564	146.0758324	13.008	146.0767704	12.9025	146.0777193	12.7279
146.082545	13.1473	146.0841889	13.0099	146.0851378	12.8554	146.0860868	12.6711
146.0866888	13.0955	146.0883316	12.9214	146.0892816	12.7567	146.0902305	12.5791
146.0908205	13.0616	146.0924634	12.8048	146.0934123	12.6571	146.0943623	12.4825
146.0949632	12.9479	146.0966071	12.703	146.0975561	12.5614	146.098505	12.3712
146.099107	12.8267	146.1007499	12.6086	146.1016988	12.4706	146.1026487	12.3033
146.1032497	12.7426	146.1048936	12.5124	146.1058425	12.3929	146.1067915	12.2365
146.1073934	12.6386	146.1090253	12.451	146.1099743	12.3248	146.1109352	12.1732
146.1115252	12.5823	146.1131681	12.3975	146.114117	12.2766	146.115067	12.132
146.1156679	12.51	146.1173118	12.3585	146.1182608	12.247	146.1191977	12.1167
146.1197997	12.5216	146.1214436	12.3228	146.1223925	12.2235	146.1233414	12.092
146.1241164	12.4966	146.1257603	12.3091	146.1266972	12.1951	146.1276472	12.0586
146.1282481	12.437	146.129892	12.2763	146.130841	12.171	146.1317899	12.0445
146.1323919	12.4412	146.1340348	12.2608	146.1349847	12.1477	146.1359336	12.0346
146.1365346	12.4215	146.1381785	12.2369	146.1391274	12.1349	146.1400764	12.0112
146.1406663	12.395	146.1423102	12.2328	146.1432592	12.1269	146.1442081	11.9971
146.1448101	12.4111	146.146453	12.224	146.1474139	12.1232	146.1483628	11.9911
146.1489648	12.3827	146.1506087	12.2237	146.1515576	12.1206	146.1525066	12.0143
146.1531085	12.3829	146.1547514	12.2452	146.1557124	12.1286	146.1566493	12.0109
146.1572513	12.4402	146.1588952	12.2466	146.1598441	12.1493	146.1607931	12.0249
146.161395	12.4796	146.1630379	12.259	146.1639869	12.1602	146.1649358	12.041

Table B.1 cont.:*The photometric measurements of BP Velorum.*

HJD [-2454000]	B mag.	HJD [-2454000]	V mag.	HJD [-2454000]	R mag.	HJD [-2454000]	I mag.
146.1667187	12.4559	146.1683846	12.2805	146.1693225	12.1828	146.1702715	12.0655
146.1708734	12.5368	146.1725283	12.2878	146.1734653	12.1936	146.1744142	12.0906
146.1791479	12.526	146.1766601	12.3582	146.177609	12.211	146.1785459	12.1108
146.1833026	12.5886	146.1807918	12.3473	146.1817517	12.2531	146.1827007	12.149
146.1897032	12.6279	146.1849345	12.3927	146.1858835	12.3016	146.1868324	12.1862
146.193835	12.7074	146.1913351	12.4919	146.1922841	12.3871	146.193233	12.2744
146.1979777	12.7913	146.1954899	12.5712	146.1964388	12.4689	146.1973758	12.3396
146.2021325	12.9109	146.1996216	12.653	146.2005706	12.5629	146.2015195	12.4488
146.2062872	12.9887	146.2037763	12.7496	146.2047253	12.6562	146.2056862	12.5361
147.8608837	12.4619	146.2079311	12.8496	146.20888	12.7346	146.209829	12.5531
147.8650045	12.4525	147.8625156	12.2396	147.8634646	12.1408	147.8644025	12.0161
147.8691362	12.4574	147.8666474	12.2378	147.8675853	12.1441	147.8685343	12.0307
147.873268	12.459	147.8707681	12.2514	147.8717171	12.1529	147.872666	12.0331
147.8773997	12.4748	147.8749109	12.2487	147.8758598	12.1641	147.8767978	12.0425
147.8824454	12.4887	147.8790426	12.2776	147.8799806	12.1757	147.8809295	12.0487
147.8866232	12.5167	147.8840773	12.2905	147.8850263	12.1936	147.8860332	12.0731
147.8907779	12.5481	147.8882671	12.3147	147.889216	12.2203	147.8901649	12.1015
147.8949097	12.5597	147.8924218	12.347	147.8933588	12.2506	147.8943077	12.1137
147.8990534	12.6107	147.8965536	12.3719	147.8975025	12.2726	147.8984514	12.1584
147.905222	12.687	147.9006963	12.4119	147.9016453	12.3052	147.9025832	12.1983
147.9093538	12.7376	147.9068539	12.4818	147.9078029	12.3849	147.9087518	12.2349

Table B.1 cont.: *The photometric measurements of BP Velorum.*

HJD [-2454000]	B mag.	HJD [-2454000]	V mag.	HJD [-2454000]	R mag.	HJD [-2454000]	I mag.
147.9134965	12.8324	147.9109967	12.5504	147.9119456	12.4541	147.9128946	12.3331
147.9176403	12.9358	147.9151404	12.6262	147.9160894	12.5398	147.9170383	12.4025
147.921772	13.0436	147.9192722	12.7305	147.9202211	12.6423	147.9211701	12.4916
147.9281486	13.2341	147.9234149	12.8466	147.9243639	12.7438	147.9253128	12.6033
147.9322804	13.3026	147.9297925	13.0182	147.9307415	12.8986	147.9316784	12.7323
147.9364121	13.3076	147.9339233	13.0756	147.9348732	12.9279	147.9358102	12.7594
147.9405549	13.2375	147.938055	13.0487	147.939004	12.8905	147.9399539	12.7029
147.9446986	13.1309	147.9421868	12.9577	147.9431357	12.8029	147.9440847	12.6249
147.9583898	12.7686	147.9463415	12.845	147.9472915	12.69	147.9482404	12.5101
147.9625336	12.6959	147.9600217	12.5282	147.9609707	12.3899	147.9619196	12.2418
147.9667343	12.6434	147.9641765	12.4677	147.9651254	12.3168	147.9660743	12.1781
147.971074	12.5785	147.9684242	12.4099	147.9694191	12.2731	147.9704381	12.1565
147.9752058	12.5698	147.9727059	12.3711	147.9736549	12.2423	147.9746038	12.1253
147.9807035	12.5031	147.9768497	12.343	147.9777986	12.2124	147.9787476	12.111
147.9848352	12.4516	147.9823354	12.2948	147.9832843	12.1381	147.9842332	12.0843
147.98899	12.4251	147.9864781	12.2557	147.9874271	12.115	147.988376	12.0298
147.9931217	12.444	147.9906219	12.2368	147.9915708	12.1175	147.9925197	12.0408
147.9972645	12.4355	147.9947646	12.2269	147.9957136	12.1031	147.9966635	12.0108
148.0035031	12.3993	147.9989084	12.226	147.9998573	12.1008	148.0008062	12.0034
148.0076228	12.4119	148.005135	12.2138	148.0060839	12.0861	148.0070329	12.0231
148.0117776	12.4189	148.0092667	12.2193	148.0102157	12.1031	148.0111646	12.0232

Table B.1 cont.:*The photometric measurements of BP Velorum.*

HJD [-2454000]	B mag.	HJD [-2454000]	V mag.	HJD [-2454000]	R mag.	HJD [-2454000]	I mag.
148.0159093	12.4201	148.0134095	12.2316	148.0143584	12.0915	148.0153074	12.0356
148.0200531	12.4301	148.0175532	12.2258	148.0185022	12.0871	148.0194511	12.0723
148.0639394	13.1237	148.021696	12.2401	148.0226449	12.1502	148.0236059	12.0549
148.0680712	13.1535	148.0655713	12.8985	148.0665203	12.7686	148.0674692	12.6416
148.0722019	13.0872	148.0697141	12.8858	148.070663	12.7501	148.071612	12.5973
148.0763577	13.0007	148.0738578	12.8092	148.0748068	12.6758	148.0757557	12.5426
148.0805004	12.8833	148.0780006	12.7328	148.0789495	12.5527	148.0798985	12.4565
148.0858471	12.777	148.0821443	12.6298	148.0830933	12.455	148.0840422	12.3533
148.0899908	12.7331	148.087491	12.5283	148.0884399	12.3847	148.0893889	12.2679
148.0941336	12.631	148.0916338	12.4634	148.0925827	12.3251	148.0935326	12.2066
148.0982653	12.5887	148.0957655	12.3933	148.0967144	12.2937	148.0976634	12.1517
148.1024091	12.5505	148.0999093	12.3761	148.1008582	12.2125	148.1018071	12.1199
148.1104526	12.5037	148.104052	12.3048	148.1050009	12.1822	148.1059499	12.1059
148.1145954	12.479	148.1120845	12.2494	148.1130335	12.1112	148.1139934	12.0519
148.1187391	12.4573	148.1162393	12.2651	148.1171882	12.1285	148.1181371	12.0501
148.1228819	12.4545	148.120382	12.2527	148.121343	12.1367	148.1222809	12.0291
148.1270256	12.4507	148.1245258	12.2493	148.1254747	12.1382	148.1264236	12.0173
148.1344212	12.4412	148.1286685	12.244	148.1296175	12.139	148.1305674	12.0251
148.1385639	12.4596	148.1360531	12.2397	148.137002	12.1245	148.137962	12.0144
148.1427077	12.4719	148.1402078	12.2655	148.1411568	12.1352	148.1421057	12.0292
148.1468504	12.4876	148.1443506	12.2743	148.1453115	12.1555	148.1462485	12.0409

Table B.1 cont.: *The photometric measurements of BP Velorum.*

HJD [-2454000]	B mag.	HJD [-2454000]	V mag.	HJD [-2454000]	R mag.	HJD [-2454000]	I mag.
148.1509942	12.5055	148.1484943	12.2938	148.1494433	12.1676	148.1503922	12.0607
148.1570008	12.5329	148.1526371	12.3143	148.153586	12.1988	148.154535	12.0705
148.1611326	12.5797	148.1586327	12.3477	148.1595817	12.2385	148.1605306	12.1033
148.1652753	12.6216	148.1627755	12.3835	148.1637244	12.266	148.1646733	12.1463
148.1694191	12.6612	148.1669192	12.4232	148.1678682	12.305	148.1688171	12.1885
148.1735618	12.7309	148.171062	12.4792	148.1720109	12.3388	148.1729598	12.2376
148.1805874	12.8596	148.1752057	12.5132	148.1761547	12.4283	148.1771036	12.2896
148.1847301	12.9693	148.1822303	12.6657	148.1831792	12.5712	148.1841282	12.4267
148.1888619	13.1009	148.186374	12.7776	148.187323	12.6685	148.1882719	12.5312
148.1930166	13.1934	148.1905058	12.8989	148.1914547	12.7952	148.1924037	12.639
148.1971714	13.3372	148.1946605	13.0149	148.1956095	12.88	148.1965584	12.7121
148.2084677	13.0807	148.1988033	13.0575	148.1997522	12.8669	148.2007012	12.7395
148.8650025	13.1133	148.2100996	12.8652	148.2110485	12.654	148.2120085	12.5499
148.8753719	12.8686	148.872872	12.7448	148.873821	12.5669	148.8747699	12.4567
148.8697012	13.113	148.8666454	12.8611	148.8675943	12.7172	148.8685433	12.5849
148.8795156	12.7877	148.8770158	12.6239	148.8779647	12.4649	148.8789137	12.3552
148.8836584	12.6838	148.8811585	12.533	148.8821075	12.3932	148.8830564	12.281
148.8877901	12.6475	148.8852903	12.4777	148.8862392	12.3268	148.8871882	12.2343
148.8938428	12.5522	148.889434	12.4032	148.890383	12.2682	148.8913319	12.1663
148.8979745	12.5295	148.8954747	12.3291	148.8964236	12.2032	148.8973726	12.1231
148.9021063	12.4984	148.8996184	12.2892	148.9005674	12.1445	148.9015163	12.0946

Table B.1 cont.: *The photometric measurements of BP Velorum.*

HJD [-2454000]	B mag.	HJD [-2454000]	V mag.	HJD [-2454000]	R mag.	HJD [-2454000]	I mag.
148.90625	12.4727	148.9037502	12.3003	148.9046991	12.1505	148.9056481	12.0808
148.9103928	12.4553	148.9078929	12.2266	148.9088419	12.1215	148.9097908	12.0492
148.9188643	12.4378	148.9120367	12.2622	148.9129856	12.1304	148.9139346	12.0392
148.9229961	12.4353	148.9204962	12.2256	148.9214451	12.0988	148.9223951	12.0185
148.9271398	12.4456	148.92464	12.2248	148.9255889	12.0949	148.9265378	12.0165
148.9312826	12.4393	148.9287827	12.2111	148.9297327	12.1176	148.9306816	12.0105
148.9354263	12.4412	148.9329265	12.2152	148.9338754	12.089	148.9348244	12.0266
148.9423699	12.4673	148.9370692	12.2205	148.9380192	12.1147	148.9389681	12.0235
148.9464907	12.4816	148.9440018	12.2402	148.9449508	12.1277	148.9458997	12.0639
148.9506224	12.5251	148.9481336	12.2634	148.9490825	12.1456	148.9500205	12.0812
148.9547542	12.5581	148.9522653	12.3321	148.9532033	12.2127	148.9541522	12.1056
148.9588739	12.5794	148.9563971	12.3454	148.957335	12.2224	148.958284	12.1303
148.9651586	12.6682	148.9605178	12.362	148.9614548	12.2594	148.9624037	12.1715
148.9693013	12.7365	148.9668015	12.4322	148.9677504	12.3522	148.9686993	12.2443
148.9734331	12.8153	148.9709332	12.5106	148.9718822	12.425	148.9728311	12.3163
148.9775768	12.9147	148.975077	12.611	148.9760259	12.5133	148.9769749	12.3888
148.9817086	13.0272	148.9792197	12.7145	148.9801687	12.6201	148.9811176	12.4825
148.9887562	13.2409	148.9833515	12.8395	148.9843004	12.7351	148.9852494	12.5819
148.9928769	13.3011	148.9903881	13.0257	148.991337	12.8941	148.992286	12.7277
148.9970197	13.278	148.9945198	13.0677	148.9954688	12.9259	148.9964177	12.7404
149.0011634	13.2051	148.9986636	13.0328	148.9996125	12.8788	149.0005615	12.6814

Table B.1 cont.: *The photometric measurements of BP Velorum.*

HJD [-2454000]	B mag.	HJD [-2454000]	V mag.	HJD [-2454000]	R mag.	HJD [-2454000]	I mag.
149.0053062	13.0791	149.0028063	12.9366	149.0037553	12.7745	149.0047042	12.5785
149.0109779	12.9093	149.0069501	12.821	149.007899	12.6624	149.008848	12.4699
149.0151206	12.8064	149.0126208	12.68	149.0135697	12.5212	149.0145186	12.3404
149.0192644	12.7173	149.0167645	12.5785	149.0177015	12.4355	149.0186624	12.2772
149.0234071	12.6439	149.0209073	12.5094	149.0218562	12.3677	149.0228052	12.2116
149.0275389	12.602	149.025039	12.4326	149.025988	12.3116	149.0269369	12.1789
149.0352124	12.5234	149.0291828	12.3906	149.0301317	12.2672	149.0311037	12.1359
149.0393442	12.4971	149.0368443	12.3366	149.0377933	12.214	149.0387422	12.0892
149.0434869	12.4727	149.0409871	12.3067	149.041936	12.198	149.042885	12.0636
149.0476877	12.4543	149.0451538	12.2857	149.0461258	12.1658	149.0470867	12.0471
149.0518314	12.4309	149.0493316	12.2566	149.0502805	12.1492	149.0512295	12.0241
149.058891	12.4289	149.0534753	12.251	149.0544243	12.1359	149.0553732	12.0465
149.0630348	12.4218	149.0605349	12.2253	149.0614839	12.0866	149.0624328	12.0059
149.0671775	12.4281	149.0646777	12.2187	149.0656266	12.0764	149.0665756	12.0026
149.0713093	12.4234	149.0688214	12.2165	149.0697704	12.099	149.0707193	12.0149
149.075464	12.4375	149.0729642	12.2229	149.0739021	12.0942	149.0748621	12.0231
149.0814707	12.4727	149.077096	12.2261	149.0780449	12.1054	149.0789938	12.0407
149.0856144	12.4965	149.0831256	12.2691	149.0840635	12.1473	149.0850125	12.0711
149.0897692	12.5292	149.0872574	12.2985	149.0882063	12.1793	149.0891552	12.0851
149.093901	12.5617	149.0914121	12.3191	149.0923611	12.2103	149.093299	12.1063
149.0980437	12.5872	149.0955439	12.344	149.0964928	12.22	149.0974418	12.1586

Table B.1 cont.: *The photometric measurements of BP Velorum.*

HJD [-2454000]	B mag.	HJD [-2454000]	V mag.	HJD [-2454000]	R mag.	HJD [-2454000]	I mag.
149.1046983	12.6922	149.0996876	12.3919	149.1006476	12.2821	149.1015975	12.1923
149.1088301	12.7749	149.1063302	12.5018	149.1072792	12.3945	149.1082281	12.2923
149.1129618	12.8679	149.110474	12.5921	149.1114229	12.4739	149.1123719	12.3752
149.1171056	12.9673	149.1146167	12.682	149.1155657	12.563	149.1165146	12.4643
149.1212483	13.0722	149.1187485	12.7778	149.1196974	12.6703	149.1206464	12.562
149.1280539	13.1379	149.1228923	12.8638	149.1238412	12.7535	149.1247901	12.6303
149.1321967	13.0971	149.1296969	12.8917	149.1306458	12.7309	149.1315957	12.6088
149.1363285	12.9944	149.1338406	12.8191	149.1347896	12.6623	149.1357265	12.5254
149.1404722	12.8883	149.1379724	12.7274	149.1389323	12.5878	149.1398823	12.4401
149.144615	12.7952	149.1421151	12.6493	149.1430641	12.498	149.144013	12.3543
149.1519755	12.6743	149.1462589	12.556	149.1472078	12.4268	149.1481568	12.2757
149.1561073	12.6066	149.1536074	12.4287	149.1545564	12.3013	149.1555063	12.1889
149.1602511	12.5707	149.1577512	12.3805	149.1587001	12.2625	149.1596491	12.1211
149.1644058	12.5379	149.161894	12.3299	149.1628439	12.2119	149.1638038	12.0989
149.1685496	12.5027	149.1660497	12.3157	149.1669987	12.2016	149.1679476	12.0804
149.17819	12.4553	149.1701925	12.3035	149.1711414	12.1875	149.1720904	12.0612
149.1823798	12.4425	149.1798329	12.257	149.1808288	12.1464	149.1817778	12.0192
149.1865225	12.4352	149.1840227	12.2435	149.1849716	12.1349	149.1859205	12.0159
149.1906663	12.4096	149.1881774	12.2456	149.1891264	12.1222	149.1900753	12.0081
149.194821	12.4244	149.1923092	12.2338	149.1932581	12.1312	149.1942071	12.0179
149.8675588	12.4573	149.1964529	12.24	149.1974019	12.1162	149.1983618	12.0195

Table B.1 cont.: *The photometric measurements of BP Velorum.*

HJD [-2454000]	B mag.	HJD [-2454000]	V mag.	HJD [-2454000]	R mag.	HJD [-2454000]	I mag.
149.8716906	12.4665	149.8691907	12.256	149.8742834	12.1509	149.8710896	12.0153
149.8758343	12.4866	149.8733345	12.2686	149.8701397	12.1319	149.8752324	12.0409
149.8799771	12.4916	149.8774893	12.2791	149.8784272	12.1783	149.8793761	12.061
149.8841209	12.5222	149.881621	12.2998	149.88257	12.1831	149.8835189	12.0875
149.8963192	12.6265	149.8857638	12.3062	149.8867247	12.197	149.8876627	12.1055
149.9004629	12.6984	149.8979631	12.4453	149.898912	12.301	149.899861	12.2484
149.9046057	12.7529	149.9021058	12.4985	149.9030548	12.3841	149.9040037	12.3304
149.9087494	12.8682	149.9062496	12.5758	149.9071985	12.4403	149.9081475	12.4074
149.9128922	12.9847	149.9103924	12.6691	149.9113413	12.5634	149.9122902	12.4919
149.9195928	13.1062	149.9145361	12.764	149.9154851	12.6512	149.916434	12.5799
149.9237366	13.111	149.9212487	12.8753	149.9221977	12.7311	149.9231346	12.6419
149.9278803	13.0316	149.9253805	12.8563	149.9263294	12.6928	149.9272784	12.6006
149.9320231	12.9463	149.9295232	12.7935	149.9304722	12.6344	149.9314211	12.5335
149.9361669	12.8558	149.933667	12.6832	149.934616	12.5561	149.9355649	12.4277
149.9423235	12.7171	149.9378098	12.585	149.9387587	12.4424	149.9397077	12.3414
149.9464553	12.6837	149.9439554	12.496	149.9449044	12.3595	149.9458533	12.2376
149.9702499	12.4637	149.9480872	12.4504	149.9490481	12.311	149.9499851	12.2002
149.9743937	12.4513	149.9718818	12.2411	149.9728308	12.1512	149.9737797	12.0322
149.9785364	12.4412	149.9760256	12.1722	149.9769855	12.098	149.9779345	12.0056
149.9826682	12.4094	149.9801683	12.2403	149.9811173	12.1188	149.9820662	11.981
149.9868229	12.4126	149.9843121	12.1997	149.985261	12.0814	149.986221	12.0083

Table B.1 cont.: *The photometric measurements of BP Velorum.*

HJD [-2454000]	B mag.	HJD [-2454000]	V mag.	HJD [-2454000]	R mag.	HJD [-2454000]	I mag.
149.9929106	12.4216	149.9884669	12.2082	149.9894158	12.0592	149.9903647	12.0115
149.9970424	12.4288	149.9945545	12.1941	149.9955034	12.0629	149.9964524	12.0251
150.0011971	12.4445	149.9986973	12.2126	149.9996462	12.0749	150.0005952	12.0416
150.0053409	12.4721	150.002841	12.2201	150.00379	12.1038	150.0047389	12.0615
150.0094726	12.5024	150.0069728	12.2657	150.0079217	12.1487	150.0088707	12.0752
150.0151433	12.5331	150.0111155	12.2791	150.0120645	12.1793	150.0130134	12.0911
150.0192751	12.5711	150.0167752	12.3133	150.0177242	12.2221	150.0186731	12.1249
150.0234188	12.6346	150.020919	12.3569	150.0218679	12.2306	150.0228169	12.1676
150.0275616	12.6782	150.0250617	12.3815	150.0260107	12.3081	150.0269596	12.2251
150.0317054	12.7476	150.0292055	12.4506	150.0301545	12.3885	150.0311034	12.2868
150.038568	12.9204	150.0333483	12.5368	150.0342972	12.434	150.0352462	12.3522
150.0427107	13.0548	150.0402109	12.7213	150.0411608	12.6111	150.0421098	12.5086
150.0468425	13.1724	150.0443546	12.8349	150.0453036	12.7026	150.0462525	12.6088
150.0509863	13.244	150.0484864	12.936	150.0494353	12.8157	150.0503843	12.7026
150.055129	13.2751	150.0526292	13.0253	150.0535791	12.8764	150.054528	12.7277
150.0607537	13.1872	150.0567729	12.9968	150.0577219	12.8599	150.0586828	12.707
150.0648855	13.0904	150.0623856	12.9136	150.0633345	12.7393	150.0642845	12.575
150.0690292	12.9582	150.0665294	12.7736	150.0674783	12.6145	150.0684273	12.48
150.073161	12.8481	150.0706721	12.6383	150.0716221	12.5261	150.072559	12.3846
150.0773037	12.7456	150.0748039	12.5779	150.0757528	12.4523	150.0767028	12.3041
150.0836924	12.6596	150.0789476	12.4755	150.0798966	12.3869	150.0808455	12.2276

Table B.1 cont.: *The photometric measurements of BP Velorum.*

HJD [-2454000]	B mag.	HJD [-2454000]	V mag.	HJD [-2454000]	R mag.	HJD [-2454000]	I mag.
150.0878361	12.5937	150.0853363	12.4186	150.0862852	12.2886	150.0872342	12.1483
150.0919789	12.5688	150.089479	12.3622	150.090428	12.2454	150.0913769	12.1107
150.0961227	12.5285	150.0936228	12.3254	150.0945717	12.2228	150.0955207	12.0932
150.1002544	12.4961	150.0977656	12.2915	150.0987145	12.1786	150.0996645	12.0773
150.106932	12.4562	150.1018973	12.2904	150.1028463	12.1756	150.1037952	12.0469
150.1110758	12.4344	150.1085759	12.2457	150.1095249	12.1366	150.1104738	12.0189
150.1152186	12.4267	150.1127187	12.2176	150.1136797	12.0978	150.1146166	12.0122
150.1193623	12.4111	150.1168625	12.2111	150.1178114	12.105	150.1187604	12.0049
150.1235051	12.4275	150.1210052	12.1903	150.1219662	12.1006	150.1229031	11.9906
150.1289218	12.4272	150.125149	12.2053	150.1260979	12.1053	150.1270469	11.9932
150.1330645	12.4315	150.1305647	12.2056	150.1315136	12.1188	150.1324626	12.0048
150.1371963	12.4513	150.1347084	12.2413	150.1356574	12.1248	150.1366063	12.0277
150.1413511	12.4704	150.1388512	12.2399	150.1398002	12.1381	150.1407491	12.0311
150.1454948	12.489	150.142995	12.283	150.1439439	12.1707	150.1448929	12.0485
150.1521264	12.5357	150.1471377	12.2896	150.1480867	12.1861	150.1490366	12.0715
150.1562692	12.5798	150.1537694	12.3413	150.1547183	12.2458	150.1556672	12.122
150.160413	12.607	150.1579131	12.3895	150.1588621	12.2907	150.159811	12.1528
150.8831839	12.5794	150.1620559	12.3998	150.8857648	12.2213	150.8867137	12.1238
150.8873047	12.5291	150.8889476	12.3296	150.8898966	12.1848	150.8908455	12.0819
150.8914475	12.4857	150.8930914	12.3003	150.8940403	12.1641	150.8949773	12.0644
150.8955792	12.4555	150.8972231	12.279	150.8981721	12.1738	150.899121	12.0358

Table B.1 cont.: *The photometric measurements of BP Velorum.*

HJD [-2454000]	B mag.	HJD [-2454000]	V mag.	HJD [-2454000]	R mag.	HJD [-2454000]	I mag.
150.899723	12.4909	150.9013549	12.2693	150.9023039	12.1562	150.9032528	12.0521
150.9053937	12.482	150.9070946	12.2805	150.9080785	12.0667	150.9260525	11.9946
150.9096874	12.4045	150.9241546	12.2346	150.9251036	12.1096	150.9311792	12.031
150.9225227	12.4105	150.9292813	12.2358	150.9302303	12.1363	150.935311	12.0418
150.9276374	12.4492	150.9334131	12.2412	150.9343621	12.1066	150.9394538	12.0597
150.9317692	12.462	150.9375559	12.2507	150.9385048	12.128	150.9435975	12.0852
150.935913	12.4742	150.9416876	12.2644	150.9426366	12.1573	150.9477293	12.116
150.9400447	12.4842	150.9458314	12.3066	150.9467804	12.2086	150.953284	12.1508
150.9441875	12.5318	150.9513861	12.3481	150.952335	12.2055	150.9574398	12.2062
150.9497432	12.5596	150.9555299	12.3871	150.9564908	12.2848	150.9615715	12.2688
150.953886	12.6098	150.9596846	12.4664	150.9606216	12.356	150.9657143	12.3602
150.9580407	12.6766	150.9638164	12.5203	150.9647653	12.4426	150.9698581	12.4416
150.9621725	12.7318	150.9679592	12.6401	150.9689081	12.5256	150.9754127	12.5577
150.9663163	12.8467	150.9735149	12.7706	150.9744638	12.6377	150.9795565	12.6421
150.9718829	12.9555	150.9776576	12.8319	150.9786076	12.7062	150.9836883	12.6389
150.9760147	13.0607	150.9817894	12.884	150.9827393	12.7095	150.9878311	12.5853
150.9801465	13.1095	150.9859332	12.8346	150.9868821	12.6688	150.9919628	12.4984
150.9842893	13.1034	150.9900649	12.7429	150.9910139	12.59	150.9992774	12.346
150.988421	13.0249	150.9973795	12.5723	150.9983285	12.4265	151.0034092	12.27
150.9957356	12.8625	151.0015113	12.4904	151.0024602	12.354	151.0075519	12.2213
150.9998674	12.7762	151.0056541	12.4367	151.006603	12.2764	151.0116837	12.1593

Table B.1 cont.: *The photometric measurements of BP Velorum.*

HJD [-2454000]	B mag.	HJD [-2454000]	V mag.	HJD [-2454000]	R mag.	HJD [-2454000]	I mag.
151.0040111	12.6836	151.0097858	12.3719	151.0107348	12.268	151.0158275	12.1354
151.0081429	12.6275	151.0139296	12.3188	151.0148785	12.1989	151.0270189	12.0558
151.0122857	12.5951	151.025121	12.2761	151.0260699	12.1376	151.0311616	12.0471
151.0234891	12.4994	151.0292637	12.2263	151.0302127	12.1432	151.0352934	12.0356
151.0276208	12.4749	151.0333955	12.2261	151.0343444	12.0866	151.0394372	12.0337
151.0317636	12.4633	151.0375503	12.1965	151.0384992	12.0916	151.0435799	12.0037
151.0359074	12.4214	151.041682	12.2129	151.042631	12.0984	151.0491936	12.0046
151.0400391	12.4309	151.0472957	12.1933	151.0482447	12.1361	151.0533364	11.9871
151.0456518	12.4305	151.0514385	12.2499	151.0523874	12.1219	151.0574801	12.0264
151.0497956	12.4276	151.0555703	12.264	151.0565312	12.1201	151.0616119	12.0421
151.0539383	12.4379	151.059714	12.2234	151.060663	12.1354	151.0657547	12.062
151.0580821	12.4478	151.0638568	12.2499	151.0648057	12.1412	151.0711714	12.0967
151.0622249	12.4756	151.0692735	12.2915	151.0702224	12.1744	151.0753152	12.1149
151.0676416	12.4974	151.0734163	12.3075	151.0743652	12.1903	151.0794459	12.1482
151.0717734	12.5297	151.07756	12.355	151.078509	12.2363	151.0835897	12.1832
151.0759161	12.5599	151.0816918	12.3781	151.0826407	12.2813	151.0877215	12.2293
151.0800479	12.591	151.0858236	12.4166	151.0867725	12.3433	151.0934501	12.3164
151.0841917	12.6455	151.0915522	12.5506	151.0925012	12.4317	151.0976049	12.4222
151.0899203	12.7436	151.095695	12.6345	151.096656	12.5305	151.1017367	12.5069
151.0940521	12.8362	151.0998508	12.747	151.1007997	12.6407	151.1058804	12.6033
151.0982069	12.9409	151.1039825	12.8659	151.1049315	12.7336	151.1100232	12.7029

Table B.1 cont.:*The photometric measurements of BP Velorum.*

HJD [-2454000]	B mag.	HJD [-2454000]	V mag.	HJD [-2454000]	R mag.	HJD [-2454000]	I mag.
151.1023386	13.0437	151.1081253	12.9663	151.1090743	12.8519	151.1150809	12.7393
151.1064824	13.1704	151.113183	13.0634	151.114132	12.9072	151.1192127	12.6992
151.1115511	13.2791	151.1173148	13.044	151.1182638	12.8708	151.1233565	12.607
151.1156829	13.296	151.1214576	12.9387	151.1224185	12.7851	151.1274992	12.5023
151.1198147	13.2098	151.1256013	12.836	151.1265503	12.6713	151.131631	12.403
151.1239574	13.0976	151.1297331	12.7054	151.1306821	12.5684	151.1358788	12.3108
151.1281012	12.9663	151.1339809	12.5956	151.1349298	12.451	151.1400105	12.2446

Table B.2: *The photometric measurements of V752 Centauri.*

HJD [-2454000]	B mag.	HJD [-2454000]	V mag.	HJD [-2454000]	R mag.	HJD [-2454000]	I mag.
HJD [-2454000]	B mag.	HJD [-2454000]	V mag.	HJD [-2454000]	R mag.	HJD [-2454000]	I mag.
182.989359	8.3976	182.989833	8.7744	182.990146	8.8753	182.990458	9.0422
182.990771	8.4144	182.991257	8.7444	182.991569	8.8814	182.991882	9.0378
182.992194	8.4006	182.9926689	8.7558	182.9929809	8.8904	182.9932939	9.0616
182.9936059	8.3939	182.9940919	8.7002	182.9944049	8.8947	182.9947169	9.064
182.9950299	8.3563	182.9955159	8.6912	182.9958278	8.8601	182.9961408	9.0659
182.9965688	8.3614	182.9970548	8.7009	182.9973678	8.8965	182.9976798	9.0182
182.9979928	8.3595	182.9984788	8.7521	182.9987908	8.8648	182.9990918	9.0607
182.9994047	8.3824	182.9998907	8.6986	183.0002147	8.8522	183.0005277	9.0241
183.0008397	8.3551	183.0013257	8.7194	183.0016387	8.8581	183.0019507	9.0487

Table B.2 cont.: *The photometric measurements of V752 Centauri.*

HJD [-2454000]	B mag.	HJD [-2454000]	V mag.	HJD [-2454000]	R mag.	HJD [-2454000]	I mag.
183.0022517	8.3774	183.0027496	8.6953	183.0030616	8.85	183.0033746	9.0176
183.0038486	8.3852	183.0043346	8.7048	183.0046476	8.8314	183.0049596	9.0014
183.0052836	8.3281	183.0057586	8.6971	183.0060715	8.8427	183.0063835	9.0237
183.0066965	8.3569	183.0071825	8.6921	183.0074945	8.7934	183.0077955	9.0234
183.0081085	8.3532	183.0085945	8.6814	183.0089065	8.8321	183.0092195	8.9907
183.0095314	8.3345	183.0100174	8.6769	183.0103304	8.825	183.0106424	8.9993
183.0109554	8.2911	183.0114414	8.6691	183.0117534	8.8286	183.0120774	8.9842
183.0123904	8.3098	183.0128643	8.6979	183.0131773	8.8202	183.0134893	8.9676
183.0138023	8.3292	183.0142883	8.6975	183.0146013	8.7812	183.0149133	8.9998
183.0152263	8.3025	183.0157123	8.6535	183.0160243	8.818	183.0163372	8.9949
183.0166492	8.3114	183.0171352	8.6696	183.0174482	8.8107	183.0177602	8.9532
183.0180732	8.3147	183.0185592	8.6481	183.0188602	8.7799	183.0191722	8.9628
183.0194851	8.3251	183.0199711	8.6503	183.0202831	8.7976	183.0205961	8.9568
183.0209081	8.3135	183.0213951	8.6828	183.0217071	8.8018	183.0220201	8.9868
183.0223321	8.2928	183.022818	8.6478	183.023131	8.801	183.023443	8.9602
183.023756	8.3024	183.024242	8.6781	183.024554	8.7852	183.024867	8.979
183.025179	8.2576	183.025665	8.6129	183.025978	8.7981	183.0262899	8.9746
183.0266029	8.2836	183.0270769	8.6327	183.0273899	8.8024	183.0277019	8.964
183.0280149	8.2823	183.0285009	8.6386	183.0288139	8.7981	183.0291259	8.9666
183.0294389	8.3127	183.0299248	8.6542	183.0302368	8.7902	183.0305498	8.9386
183.0308618	8.32	183.0313478	8.6227	183.0316608	8.7912	183.0319728	8.9695

Table B.2 cont.: *The photometric measurements of V752 Centauri.*

HJD [-2454000]	B mag.	HJD [-2454000]	V mag.	HJD [-2454000]	R mag.	HJD [-2454000]	I mag.
183.0322858	8.2995	183.0327718	8.6121	183.0330837	8.7716	183.0333967	8.9844
183.0337087	8.3236	183.0341957	8.6196	183.0345197	8.7841	183.0348207	8.971
183.0351327	8.2895	183.0356187	8.6401	183.0359317	8.7601	183.0362437	8.9797
183.0365566	8.2997	183.0370426	8.6505	183.0373546	8.7768	183.0376676	8.9572
183.0379796	8.3007	183.0384656	8.6419	183.0387786	8.7782	183.0390906	8.992
183.0421345	8.2879	183.0426095	8.6543	183.0429215	8.7658	183.0432344	8.9585
183.0435464	8.2745	183.0440324	8.672	183.0443454	8.7751	183.0446574	8.9723
183.0449704	8.3016	183.0454564	8.664	183.0457694	8.795	183.0460814	8.9334
183.0464054	8.28	183.0468803	8.6577	183.0471923	8.7914	183.0475053	8.9647
183.0478173	8.2877	183.0483033	8.6804	183.0486163	8.8055	183.0489283	8.9489
183.0492413	8.2967	183.0497273	8.6457	183.0500392	8.8095	183.0503522	8.981
183.0506642	8.3076	183.0511392	8.6214	183.0514512	8.7932	183.0517642	8.9732
183.0520762	8.2975	183.0525632	8.6674	183.0528752	8.7736	183.0531881	8.9694
183.0535001	8.3331	183.0539861	8.624	183.0542991	8.8171	183.0546111	8.9335
183.0549241	8.3111	183.0554101	8.6177	183.0557221	8.806	183.0560461	9.0292
183.0563471	8.3392	183.056833	8.6655	183.057146	8.8017	183.057458	8.9512
183.057771	8.3567	183.058257	8.696	183.05857	8.8272	183.058882	9.0398
183.059195	8.3322	183.059681	8.654	183.0599929	8.8403	183.0603059	8.9686
183.0606179	8.3433	183.0611039	8.6886	183.0614169	8.8269	183.0617289	8.9738
183.0620419	8.3715	183.0625159	8.7129	183.0628289	8.8168	183.0631409	9.0122
183.0634538	8.3653	183.0639398	8.6664	183.0642518	8.8258	183.0645648	9.0119

Table B.2 cont.: *The photometric measurements of V752 Centauri.*

HJD [-2454000]	B mag.	HJD [-2454000]	V mag.	HJD [-2454000]	R mag.	HJD [-2454000]	I mag.
183.0648768	8.373	183.0653518	8.7087	183.0656638	8.8388	183.0659648	9.0268
183.0662658	8.4089	183.0667517	8.712	183.0670527	8.8595	183.0673537	9.0223
183.0676667	8.3574	183.0681407	8.7071	183.0684537	8.8608	183.0687547	9.0184
183.0690557	8.4039	183.0695417	8.6883	183.0698537	8.8411	183.0701546	9.0426
183.0704676	8.4078	183.0709416	8.7186	183.0712426	8.8773	183.0715556	9.0137
183.0718566	8.384	183.0723306	8.735	183.0726436	8.8724	183.0729446	9.0342
183.0732566	8.3803	183.0737315	8.7197	183.0740315	8.8758	183.0743445	9.0163
183.0746455	8.4156	183.0751315	8.7338	183.0754325	8.8522	183.0757445	9.0212
183.0760455	8.425	183.0765315	8.7528	183.0768444	8.8932	183.0771564	9.0599
183.0775154	8.4215	183.0780014	8.7425	183.0783144	8.9185	183.0786264	9.0621
183.0789274	8.4157	183.0794134	8.7635	183.0797264	8.9109	183.0800384	9.0338
183.0803513	8.4035	183.0808373	8.7617	183.0811503	8.9305	183.0814743	9.0804
183.0817863	8.4321	183.0822723	8.8095	183.0825853	8.9159	183.0828973	9.0898
183.0832103	8.4621	183.0836962	8.8156	183.0840082	8.9109	183.0843212	9.1262
183.0846332	8.4805	183.0851192	8.7862	183.0854322	8.9385	183.0857442	9.0983
183.0860572	8.4706	183.0865432	8.8354	183.0868562	8.9293	183.0871561	9.1437
183.0874691	8.4918	183.0879551	8.8274	183.0882681	8.9634	183.0885801	9.1482
183.0888931	8.4829	183.0893791	8.8474	183.0897031	8.9942	183.0900151	9.137
183.0903281	8.5326	183.090814	8.8755	183.091126	8.9982	183.091439	9.1605
183.091751	8.5368	183.092237	8.868	183.09255	9.0084	183.092862	9.1486
183.093175	8.5378	183.093661	8.8601	183.0939739	9.0179	183.0942859	9.1792

Table B.2 cont.:*The photometric measurements of V752 Centauri.*

HJD [-2454000]	B mag.	HJD [-2454000]	V mag.	HJD [-2454000]	R mag.	HJD [-2454000]	I mag.
183.0945989	8.555	183.0950849	8.9015	183.0953969	9.0501	183.0957099	9.2207
183.0960219	8.5848	183.0965079	8.9404	183.0968209	9.0648	183.0971328	9.1761
183.0974458	8.6104	183.0979318	8.9349	183.0982438	9.0684	183.0985568	9.2087
183.0988688	8.6119	183.0993558	8.9416	183.0996798	9.109	183.0999808	9.2588
183.1002808	8.6297	183.1007677	8.9372	183.1010797	9.1088	183.1013927	9.2389
183.1017047	8.6749	183.1021907	9.0233	183.1025037	9.1257	183.1028277	9.2888
183.1031397	8.6761	183.1036257	9.0032	183.1039266	9.148	183.1042396	9.3297
183.1045516	8.6949	183.1050376	9.043	183.1053506	9.1551	183.1056626	9.2809
183.1059756	8.709	183.1064616	9.0115	183.1067746	9.1859	183.1070866	9.3575
183.1073995	8.7431	183.1078855	9.0323	183.1081975	9.2361	183.1085105	9.3376
183.1088225	8.744	183.1093085	9.0506	183.1096215	9.2357	183.1099335	9.3656
183.1102465	8.7755	183.1107324	9.1116	183.1110444	9.2717	183.1113574	9.3831
183.1116694	8.7809	183.1121554	9.1231	183.1124684	9.2725	183.1127804	9.4272
183.1226421	8.871	183.1231161	9.1808	183.1234291	9.2907	183.1237411	9.4124
183.1240541	8.8378	183.12454	9.1695	183.124852	9.3118	183.125165	9.4292
183.125477	8.8464	183.125963	9.2012	183.126276	9.2978	183.126588	9.4502
183.126901	8.9038	183.127387	9.1796	183.1276989	9.2952	183.1280119	9.4577
183.1283239	8.8945	183.1288109	9.1651	183.1291229	9.2973	183.1294359	9.4449
183.1297479	8.8699	183.1302339	9.1506	183.1305699	9.2995	183.1308709	9.4685
183.1311828	8.8374	183.1316688	9.1994	183.1319818	9.3141	183.1322938	9.4306
183.1326068	8.8777	183.1330928	9.1629	183.1334048	9.3173	183.1337178	9.4614

Table B.2 cont.: *The photometric measurements of V752 Centauri.*

HJD [-2454000]	B mag.	HJD [-2454000]	V mag.	HJD [-2454000]	R mag.	HJD [-2454000]	I mag.
183.1340298	8.8658	183.1345167	9.1979	183.1348287	9.2938	183.1351417	9.4133
183.1354537	8.8961	183.1359397	9.1716	183.1362527	9.3002	183.1365647	9.4537
183.1368777	8.8682	183.1373637	9.1788	183.1376757	9.2978	183.1379886	9.4431
183.1383006	8.8952	183.1387866	9.1597	183.1390996	9.2743	183.1394116	9.4332
183.1397246	8.8271	183.1402106	9.1318	183.1405236	9.307	183.1408356	9.3666
183.1411486	8.8516	183.1416345	9.1115	183.1419465	9.2635	183.1422595	9.4429
183.1425715	8.8479	183.1430575	9.1304	183.1433705	9.2436	183.1436825	9.3313
183.1439955	8.809	183.1444815	9.0944	183.1447934	9.2505	183.1451064	9.3787
183.1454074	8.7734	183.1458814	9.1014	183.1461824	9.2055	183.1464954	9.3722
183.1467964	8.7625	183.1472824	9.0781	183.1475834	9.1876	183.1478954	9.3472
183.1481963	8.7371	183.1486713	9.0256	183.1489833	9.1882	183.1492843	9.2959
183.1495853	8.6846	183.1500713	9.0137	183.1503843	9.1775	183.1506963	9.3993
183.1510093	8.696	183.1514952	8.9874	183.1518072	9.135	183.1521202	9.2989
183.1524322	8.6386	183.1529182	8.9902	183.1532422	9.1047	183.1535432	9.2304
183.1538562	8.6336	183.1543422	8.9906	183.1546542	9.0827	183.1549671	9.2507
183.1552791	8.6519	183.1557661	8.9453	183.1560781	9.0845	183.1563911	9.2413
183.1567031	8.6413	183.1571891	8.9138	183.1575021	9.064	183.1578141	9.2307
183.159492	8.5948	183.159967	8.915	183.160279	9.026	183.160592	9.1847
183.160904	8.5549	183.161391	8.8453	183.1617029	8.9853	183.1620159	9.1751
183.1623279	8.563	183.1642379	8.845	183.1631269	8.9774	183.1634389	9.1567
183.1637519	8.53	183.1656498	8.8138	183.1645499	8.9623	183.1648629	9.1331

Table B.2 cont.:*The photometric measurements of V752 Centauri.*

HJD [-2454000]	B mag.	HJD [-2454000]	V mag.	HJD [-2454000]	R mag.	HJD [-2454000]	I mag.
183.1651638	8.525	183.2100695	8.649	183.2061226	8.7581	183.1662748	9.134
183.1665868	8.4921	183.2114935	8.6269	183.2075346	8.7848	183.1677098	9.132
183.1680228	8.4461	183.2129164	8.5838	183.2089586	8.812	183.2135414	8.9594
183.2053017	8.2933	183.2143404	8.6576	183.2103935	8.8154	183.2149654	8.9535
183.2067366	8.2847	183.2157644	8.5923	183.2118055	8.7669	183.2163893	8.9466
183.2081596	8.3133	183.2171873	8.6084	183.2132404	8.767	183.2178123	8.9033
183.2095835	8.2648	183.2186113	8.6366	183.2146524	8.7812	183.2192363	8.9139
183.2110075	8.2813	183.2202202	8.6176	183.2160763	8.7917	183.2208562	8.9664
183.2124305	8.2671	183.2216552	8.5451	183.2175003	8.7621	183.2222802	8.928
183.2138654	8.2671	183.2230781	8.6308	183.2189233	8.7801	183.2237031	8.9189
183.2152774	8.3008	183.2245021	8.5614	183.2205442	8.752	183.2251391	8.9366
183.2167013	8.31	183.2259371	8.5948	183.2219672	8.775	183.226574	8.9368
183.2181253	8.2879	183.227928	8.6392	183.2233911	8.7704	183.228553	8.9601
183.2197452	8.241	183.229352	8.6284	183.2248151	8.7992	183.2299769	8.9744
183.2211692	8.2676	183.2307749	8.5851	183.226261	8.7499	183.2313999	8.945
183.2225922	8.2733	183.2321989	8.6369	183.22824	8.7845	183.2328349	8.9592
183.2240161	8.3025	183.2336338	8.6191	183.2296639	8.8065	183.2342468	8.9671
183.2254511	8.2813	183.2365847	8.6269	183.2310879	8.816	183.2414806	8.9563
183.227442	8.3316	183.2422796	8.7546	183.2325229	8.7647	183.2372097	8.947
183.228865	8.2807	183.2380087	8.6327	183.2339458	8.7978	183.2429156	8.9971
183.2302889	8.3397	183.2394327	8.6737	183.2368977	8.7826	183.2386337	8.968

Table B.2 cont.: *The photometric measurements of V752 Centauri.*

HJD [-2454000]	B mag.	HJD [-2454000]	V mag.	HJD [-2454000]	R mag.	HJD [-2454000]	I mag.
183.2317129	8.2887	183.2408556	8.6318	183.2425916	8.7978	183.2400456	8.9991
183.2331478	8.284	183.847621	9.0508	183.2383097	8.8007	183.848535	9.3678
183.2361108	8.2836	183.8507919	9.0915	183.2397326	8.841	183.8517059	9.4017
183.2417936	8.4013	183.8530839	9.1274	183.2411686	8.8276	183.8539978	9.3992
183.2375227	8.3102	183.8553748	9.1361	183.848107	9.2027	183.8562898	9.4445
183.2389457	8.3667	183.8576667	9.1714	183.8512779	9.2455	183.8585807	9.4604
183.2403696	8.3251	183.8599467	9.1638	183.8535698	9.2701	183.8608606	9.4522
183.846683	8.7351	183.8622386	9.1662	183.8558608	9.293	183.8631526	9.4561
183.849854	8.7668	183.8645295	9.1765	183.8581527	9.3026	183.8654445	9.4534
183.8521339	8.8115	183.8668215	9.1524	183.8604327	9.2962	183.8677354	9.4466
183.8544258	8.8334	183.8691134	9.165	183.8627246	9.3134	183.8700394	9.453
183.8567178	8.8649	183.8714043	9.1744	183.8650155	9.3213	183.8723193	9.4459
183.8589977	8.8538	183.8736843	9.168	183.8673075	9.314	183.8745992	9.4663
183.8612896	8.8635	183.8759762	9.1633	183.8695994	9.3118	183.8768902	9.4524
183.8635806	8.8575	183.8782681	9.1672	183.8718903	9.3059	183.8791821	9.4294
183.8658725	8.8853	183.8805481	9.1478	183.8741713	9.3128	183.881462	9.4477
183.8681644	8.8731	183.882839	9.1266	183.8764622	9.314	183.883754	9.4017
183.8704554	8.8668	183.8851309	9.0956	183.8787541	9.3087	183.8860459	9.3553
183.8727353	8.8596	183.8874109	9.0715	183.8810341	9.2974	183.8883259	9.3483
183.8750272	8.8644	183.8897138	9.0263	183.883326	9.2639	183.8906168	9.2929
183.8773192	8.8614	183.8919947	8.9951	183.8856169	9.2276	183.8929087	9.2586

Table B.2 cont.:*The photometric measurements of V752 Centauri.*

HJD [-2454000]	B mag.	HJD [-2454000]	V mag.	HJD [-2454000]	R mag.	HJD [-2454000]	I mag.
183.8795991	8.8425	183.8942857	8.9702	183.8879089	9.1969	183.8952007	9.2511
183.88189	8.8298	183.8965776	8.921	183.8902008	9.1731	183.8974806	9.2078
183.884182	8.7796	183.8988576	8.8953	183.8924807	9.1311	183.8997715	9.1766
183.8864619	8.7604	183.9011495	8.8731	183.8947717	9.0849	183.9020515	9.1742
183.8887538	8.7085	183.9034294	8.849	183.8970636	9.0631	183.9043434	9.1383
183.8910458	8.6882	183.9057204	8.8064	183.8993435	9.0468	183.9066233	9.1124
183.8933367	8.6456	183.9107202	8.7755	183.9016355	9.0315	183.9116352	9.0888
183.8956286	8.5961	183.916866	8.7316	183.9039154	8.9885	183.917781	9.0535
183.8979086	8.5659	183.9266698	8.6947	183.9062073	8.9588	183.9275837	9.0249
183.9002005	8.5462	183.9289727	8.6851	183.9112072	8.9336	183.9298757	9.004
183.9024804	8.5077	183.9312526	8.6711	183.917352	8.8993	183.9321666	9.0095
183.9047714	8.478	183.9335446	8.6557	183.9271557	8.8587	183.9344585	8.9754
183.9097712	8.4425	183.9358245	8.6413	183.9294467	8.8512	183.9367385	8.9609
183.9159061	8.4176	183.9381154	8.6452	183.9317386	8.8338	183.9390304	8.99
183.9257198	8.3693	183.9404194	8.6389	183.9340305	8.8088	183.9413213	8.9719
183.9280117	8.3579	183.9426993	8.6335	183.9363105	8.8085	183.9436133	8.9707
183.9303037	8.33	183.9450022	8.6318	183.9386014	8.7918	183.9459052	8.959
183.9325946	8.3374	183.9472822	8.6118	183.9409054	8.7824	183.9481961	8.952
183.9348755	8.3079	183.9495741	8.6048	183.9431853	8.7738	183.9504881	8.9398
183.9371665	8.3019	183.951865	8.5922	183.9454762	8.7916	183.95278	8.9289
183.9394584	8.2889	183.954169	8.6055	183.9477682	8.7733	183.9550829	8.9201

Table B.2 cont.: *The photometric measurements of V752 Centauri.*

HJD [-2454000]	B mag.	HJD [-2454000]	V mag.	HJD [-2454000]	R mag.	HJD [-2454000]	I mag.
183.9417503	8.2851	183.9573509	8.5965	183.9500711	8.7572	183.9581959	8.9486
183.9440413	8.2805	183.9591688	8.5863	183.952351	8.767	183.9600248	8.9155
183.9463332	8.2781	183.9609968	8.6029	183.954655	8.7621	183.9618418	8.9269
183.9486251	8.258	183.9628137	8.6057	183.9578259	8.7586	183.9636707	8.9448
183.9509161	8.2727	183.9646427	8.5918	183.9596548	8.7653	183.9655107	8.9195
183.953219	8.2467	183.9666446	8.5957	183.9614828	8.7628	183.9675016	8.9405
183.9567259	8.2543	183.9684616	8.6051	183.9632997	8.7652	183.9693185	8.9252
183.9585668	8.2598	183.9702905	8.5957	183.9651407	8.7663	183.9711475	8.9548
183.9603948	8.2719	183.9721195	8.6061	183.9671306	8.7633	183.9729754	8.9391
183.9622117	8.248	183.9739484	8.5967	183.9689486	8.7732	183.9748044	8.9622
183.9640407	8.254	183.9762623	8.6069	183.9707765	8.7773	183.9771193	8.9708
183.9660316	8.2885	183.9780913	8.6108	183.9726054	8.7685	183.9789483	8.9461
183.9678606	8.2744	183.9799082	8.6107	183.9744344	8.7596	183.9807762	8.9761
183.9696885	8.2639	183.9817492	8.6253	183.9767493	8.7738	183.9826052	8.9784
183.9715175	8.2634	183.9835771	8.6156	183.9785773	8.7805	183.9844221	8.994
183.9733464	8.257	183.9855801	8.644	183.9804062	8.7991	183.9864361	8.9689
183.9756724	8.2673	183.987408	8.6402	183.9822352	8.7962	183.988265	8.9814
183.9774893	8.2683	183.989237	8.6551	183.9840521	8.8089	183.9901049	8.9942
183.9793063	8.2604	183.9910659	8.6457	183.9860771	8.8019	183.9919219	9.0012
183.9811472	8.2575	183.9928939	8.6542	183.987894	8.7919	183.9937508	8.9981
183.9829752	8.2888	183.9967138	8.6724	183.989723	8.8114	183.9975697	9.032

Table B.2 cont.:*The photometric measurements of V752 Centauri.*

HJD [-2454000]	B mag.	HJD [-2454000]	V mag.	HJD [-2454000]	R mag.	HJD [-2454000]	I mag.
183.9849781	8.2965	183.9985427	8.6838	183.9915519	8.8216	183.9993867	9.0277
183.986806	8.31	184.0003827	8.6988	183.9933799	8.8226	184.0012276	9.0407
183.988635	8.3227	184.0021996	8.708	183.9971997	8.8564	184.0030556	9.0557
183.9904639	8.3446	184.0040286	8.7063	183.9990287	8.8506	184.0048845	9.0485
183.9922929	8.3087	184.0068175	8.7293	184.0008566	8.8641	184.0076734	9.0607
183.9961238	8.3428	184.0086464	8.7322	184.0026856	8.8769	184.0095144	9.077
183.9979407	8.3736	184.0104864	8.7507	184.0045145	8.8728	184.0113423	9.0829
183.9997687	8.342	184.0123153	8.7747	184.0073035	8.8902	184.0131713	9.0944
184.0015976	8.366	184.0141323	8.781	184.0091324	8.8968	184.0150002	9.122
184.0034266	8.4005	184.0160302	8.7968	184.0109724	8.9028	184.0167592	9.141
184.0062155	8.4064	184.0177312	8.8135	184.0128013	8.9174	184.0184721	9.1503
184.0080444	8.4131	184.0194441	8.8443	184.0146183	8.9503	184.0201851	9.1599
184.0098844	8.4511	184.0211571	8.8496	184.0164472	8.9693	184.021898	9.1787
184.0117133	8.4454	184.02287	8.8715	184.0181602	8.9823	184.023599	9.1953
184.0135303	8.4472	184.024595	8.8818	184.0198731	9.0107	184.0253349	9.2142
184.0154282	8.4623	184.0263079	8.9034	184.0215851	9.009	184.0270479	9.207
184.0171292	8.4899	184.0280209	8.9165	184.023287	9.022	184.0287609	9.2639
184.0188421	8.4631	184.0297338	8.9511	184.025023	9.0254	184.0304628	9.2676
184.0205551	8.5183	184.0314468	8.9759	184.0267359	9.0651	184.0321868	9.3103
184.022257	8.5486	184.0338417	9.0058	184.0284489	9.0943	184.0345827	9.333
184.024004	8.5441	184.0355547	9.0269	184.0301498	9.1395	184.0362956	9.3271

Table B.2 cont.: *The photometric measurements of V752 Centauri.*

HJD [-2454000]	B mag.	HJD [-2454000]	V mag.	HJD [-2454000]	R mag.	HJD [-2454000]	I mag.
184.0257059	8.5863	184.0372676	9.0523	184.0318748	9.1392	184.0380086	9.3705
184.0274189	8.6051	184.0389806	9.0731	184.0342707	9.1385	184.0397215	9.4005
184.0291318	8.6163	184.0406935	9.0894	184.0359836	9.1907	184.0414225	9.4073
184.0308448	8.6571	184.0439464	9.1339	184.0377076	9.1943	184.0446864	9.4205
184.0332517	8.669	184.0456474	9.133	184.0394095	9.2278	184.0463883	9.4529
184.0349537	8.7	184.0473723	9.1305	184.0411225	9.2387	184.0481123	9.4371
184.0366666	8.7326	184.0490733	9.1408	184.0443744	9.2839	184.0498253	9.4285
184.0383786	8.7427	184.0507972	9.1371	184.0460754	9.2865	184.0515382	9.4277
184.0400915	8.7997	184.0525102	9.1406	184.0477883	9.2696	184.0532512	9.4369
184.0433444	8.793	184.0542231	9.1514	184.0495013	9.2605	184.0549531	9.4184
184.0450574	8.8079	184.0559361	9.162	184.0512262	9.3195	184.0566771	9.4444
184.0467583	8.8158	184.057649	9.1442	184.0529272	9.3112	184.05839	9.444
184.0484713	8.8213	184.059362	9.1625	184.0546401	9.2905	184.060103	9.448
184.0501962	8.8392	184.0610639	9.1437	184.0563651	9.3082	184.0618039	9.438
184.0518972	8.8422	184.0627769	9.1433	184.058078	9.3146	184.0635169	9.4408
184.0536221	8.8326	184.0644898	9.1191	184.059791	9.2974	184.0652298	9.4281
184.0553231	8.8298	184.0662028	9.096	184.0614919	9.276	184.0669428	9.3999
184.057047	8.8463	184.0679037	9.0772	184.0632049	9.2874	184.0686447	9.3736
184.05876	8.8213	184.0696167	9.0711	184.0649178	9.2759	184.0703577	9.3725
184.0604619	8.8271	184.0713296	9.0423	184.0666308	9.2707	184.0720706	9.3334
184.0621749	8.8332	184.0730196	9.0296	184.0683317	9.2465	184.0737596	9.3175

Table B.2 cont.:*The photometric measurements of V752 Centauri.*

HJD [-2454000]	B mag.	HJD [-2454000]	V mag.	HJD [-2454000]	R mag.	HJD [-2454000]	I mag.
184.0638879	8.8255	184.0747085	9.005	184.0700447	9.2181	184.0754385	9.3067
184.0656008	8.806	184.0763985	8.9952	184.0717576	9.1735	184.0771275	9.2645
184.0673138	8.7906	184.09259	8.8088	184.0734476	9.1856	184.093331	9.1256
184.0690147	8.7478	184.094303	8.7907	184.0751375	9.1566	184.095044	9.1008
184.0707277	8.7381	184.0960049	8.7931	184.0768155	9.1423	184.0967459	9.0904
184.0724286	8.7402	184.0977179	8.7674	184.093019	8.9657	184.0984579	9.0953
184.0741186	8.7099	184.0994308	8.7632	184.094732	8.9398	184.1001708	9.0874
184.0758085	8.6826	184.1011318	8.75	184.0964329	8.9412	184.1018728	9.0963
184.0919891	8.4963	184.1028447	8.7374	184.0981459	8.9288	184.1035857	9.0715
184.093702	8.4659	184.1045577	8.7397	184.0998588	8.942	184.1052987	9.047
184.095403	8.4649	184.1062587	8.7443	184.1015598	8.9183	184.1069996	9.0481
184.0971159	8.4585	184.1079716	8.7282	184.1032727	8.905	184.1087126	9.0618
184.0988289	8.4592	184.1096846	8.7254	184.1049857	8.8922	184.1104375	8.9954
184.1005298	8.4161	184.1113975	8.7177	184.1066876	8.8653	184.1121385	9.0098
184.1022428	8.4193	184.1131225	8.7034	184.1084006	8.879	184.1138634	9.0226
184.1039557	8.4346	184.1148354	8.6923	184.1101245	8.8859	184.1155764	8.9896
184.1056577	8.403	184.1165594	8.7176	184.1118265	8.8745	184.1173003	8.9955
184.1073706	8.4109	184.1182723	8.6933	184.1135504	8.8742	184.1190013	9.029
184.1090826	8.404	184.1199853	8.6658	184.1152634	8.8449	184.1207142	9.0096
184.1107955	8.408	184.1216982	8.6779	184.1169883	8.8666	184.1224272	8.9777
184.1125205	8.3806	184.1234002	8.6789	184.1186893	8.8751	184.1241401	8.9881

Table B.2 cont.: *The photometric measurements of V752 Centauri.*

HJD [-2454000]	B mag.	HJD [-2454000]	V mag.	HJD [-2454000]	R mag.	HJD [-2454000]	I mag.
184.1142334	8.3902	184.1251131	8.6574	184.1204023	8.8582	184.1258531	9.0112
184.1159464	8.368	184.1268141	8.6556	184.1221152	8.7917	184.127566	8.9871
184.1176593	8.3733	184.128539	8.6407	184.1238282	8.8178	184.129279	8.978
184.1193723	8.3459	184.130251	8.6444	184.1255411	8.8098	184.130992	8.9572
184.1210962	8.3482	184.1319639	8.6303	184.1272541	8.8313	184.1327049	8.9689
184.1227982	8.3616	184.1336659	8.6469	184.128967	8.7851	184.1344069	8.972
184.1245111	8.3453	184.1447186	8.6155	184.13068	8.8055	184.1454595	8.9775
184.1262121	8.3065	184.1464195	8.6239	184.1323929	8.8019	184.1471605	8.9709
184.127948	8.3608	184.1481325	8.6282	184.1340939	8.8186	184.1488734	8.9537
184.12965	8.3212	184.1498454	8.6353	184.1451466	8.7749	184.1505864	8.9756
184.1313629	8.3288	184.1515704	8.6321	184.1468485	8.8251	184.1523343	8.9728
184.1330759	8.3285	184.1533063	8.6497	184.1485615	8.7942	184.1540473	8.9318
184.1441056	8.3251	184.1550193	8.6417	184.1502744	8.7519	184.1557603	8.9634
184.1458185	8.2823	184.1567442	8.6399	184.1520334	8.7854	184.1574732	8.9664
184.1475315	8.3223	184.1584332	8.635	184.1537343	8.7707	184.1591742	9.0089
184.1492444	8.3083	184.1601581	8.6709	184.1554473	8.7885	184.1608991	8.9827
184.1509564	8.2911	184.1618711	8.6685	184.1571602	8.8358	184.1626121	8.9647
184.1527043	8.2954	184.163595	8.6809	184.1588622	8.7986	184.164325	9.0593
184.1544173	8.3264	184.165297	8.664	184.1605861	8.8034	184.166038	8.9968
184.1561302	8.3354	184.1669979	8.6698	184.1622991	8.8227	184.1677389	8.9972
184.1578312	8.3105	184.1687109	8.6747	184.164012	8.7753	184.1694519	9.0115

Table B.2 cont.:*The photometric measurements of V752 Centauri.*

HJD [-2454000]	B mag.	HJD [-2454000]	V mag.	HJD [-2454000]	R mag.	HJD [-2454000]	I mag.
184.1595441	8.338	184.1704238	8.6875	184.165725	8.8137	184.1711648	8.9997
184.1612691	8.3283	184.1721368	8.6796	184.1674259	8.8172	184.1728778	9.0091
184.16297	8.3268	184.1738377	8.6839	184.1691389	8.8142	184.1745787	9.0217
184.164695	8.31	184.1755507	8.6985	184.1708518	8.8332	184.1762917	9.0399
184.166396	8.3471	184.1772636	8.7219	184.1725648	8.8649	184.1780046	9.0191
184.1681089	8.3521	184.1789766	8.7349	184.1742667	8.8875	184.1797176	9.0586
184.1698219	8.3413	184.1806785	8.7127	184.1759797	8.8356	184.1814185	9.0231
184.1715348	8.3649	184.1823915	8.7323	184.1776926	8.8357	184.1831315	9.0456
184.1732478	8.3642	184.1841045	8.7496	184.1794056	8.8665	184.1848444	9.0335
184.1749497	8.3748	184.1858284	8.7615	184.1811065	8.8668	184.1865574	9.0664
184.1766627	8.3869	184.1963371	8.8102	184.1828195	8.8891	184.1970671	9.1696
184.1783746	8.3802	184.1980501	8.8364	184.1845324	8.8825	184.19878	9.1323
184.1800876	8.3953	184.199763	8.839	184.1862454	8.9091	184.200504	9.1701
184.1817895	8.422	184.201476	8.8778	184.1967661	8.9804	184.2022169	9.1986
184.1835025	8.4313	184.2036749	8.8928	184.198467	8.9961	184.2044159	9.2133
184.1852154	8.4152	184.2053769	8.91	184.200192	8.9912	184.2061178	9.193
184.1957361	8.529	184.2071008	8.9244	184.2019049	9.0156	184.2078418	9.2477
184.1974371	8.4964	184.2088138	8.9417	184.2041039	9.0232	184.2095547	9.2665
184.19915	8.557	184.2114297	8.9967	184.2058048	9.0756	184.2121587	9.2881
184.200874	8.5024	184.2131306	8.9969	184.2075298	9.1027	184.2138716	9.3272
184.2030849	8.5277	184.2148436	9.0263	184.2092307	9.0565	184.2155846	9.3049

Table B.2 cont.: *The photometric measurements of V752 Centauri.*

HJD [-2454000]	B mag.	HJD [-2454000]	V mag.	HJD [-2454000]	R mag.	HJD [-2454000]	I mag.
184.2047869	8.5615	184.2165565	9.0175	184.2118467	9.1194	184.2172975	9.3561
184.2064878	8.6163	184.2190105	9.0733	184.2135596	9.1599	184.2197394	9.417
184.2082118	8.6022	184.2207114	9.1082	184.2152726	9.1927	184.2214524	9.3955
184.2108277	8.6813	184.2224244	9.1048	184.2169855	9.1588	184.2231653	9.4171
184.2125296	8.6999	184.2241373	9.1411	184.2194275	9.2197	184.2248783	9.4357
184.2142426	8.6999	184.2264173	9.159	184.2211404	9.2881	184.2271582	9.4467
184.2159546	8.7472	184.2281302	9.1962	184.2228644	9.2358	184.2288712	9.4758
184.2184085	8.7547	184.8944197	8.6462	184.2245663	9.2685	184.8952647	9.0294
184.2218234	8.8152	184.8966426	8.6334	184.2268462	9.3444	184.8974986	8.9565
184.2235363	8.8259	184.8988756	8.663	184.2285592	9.3377	184.8997326	9.0016
184.2258163	8.8735	184.9010985	8.686	184.8949057	8.7893	184.9019545	8.9963
184.2275292	8.8918	184.9033315	8.6959	184.8971286	8.8161	184.9041764	8.964
184.8934707	8.3125	184.9060864	8.6752	184.8993616	8.8005	184.9069424	8.9884
184.8956927	8.3099	184.9083203	8.663	184.9015845	8.8096	184.9091763	8.997
184.8979266	8.303	184.9105543	8.6779	184.9038174	8.8299	184.9113982	8.9843
184.9001605	8.3272	184.9127762	8.6795	184.9065724	8.8364	184.9136322	9.0131
184.9023825	8.3234	184.9149981	8.7099	184.9088063	8.8319	184.9158541	9.0221
184.9051484	8.3247	184.9361436	8.8114	184.9110283	8.8488	184.9368845	9.082
184.9073714	8.3161	184.9377985	8.7812	184.9132622	8.8761	184.9385395	9.1388
184.9096043	8.3385	184.9394535	8.8136	184.9154841	8.8365	184.9401945	9.1307
184.9118272	8.3466	184.9410974	8.8215	184.9365716	8.9446	184.9418374	9.106

Table B.2 cont.:*The photometric measurements of V752 Centauri.*

HJD [-2454000]	B mag.	HJD [-2454000]	V mag.	HJD [-2454000]	R mag.	HJD [-2454000]	I mag.
184.9140602	8.3553	184.9427524	8.8469	184.9382265	8.9677	184.9434924	9.2307
184.9355416	8.451	184.9443953	8.8608	184.9398815	8.9651	184.9451363	9.1765
184.9371965	8.477	184.9460503	8.8857	184.9415254	8.9969	184.9467913	9.2009
184.9388515	8.4993	184.9477053	8.8739	184.9431804	9.0122	184.9484462	9.2045
184.9404954	8.5181	184.9493602	8.9325	184.9448233	9.036	184.9501012	9.2225
184.9421504	8.5089	184.9510042	8.95	184.9464783	9.0451	184.9517451	9.2237
184.9438054	8.5559	184.9526591	8.9564	184.9481342	9.0589	184.9534001	9.2984
184.9454483	8.5245	184.9543141	8.9908	184.9497892	9.0621	184.955055	9.2962
184.9471033	8.5753	184.955969	8.9988	184.9514321	9.0991	184.95671	9.3205
184.9487592	8.595	184.957624	9.0333	184.9530871	9.16	184.958365	9.2786
184.9504142	8.594	184.9592679	9.0564	184.9547421	9.1535	184.9600089	9.3093
184.9520571	8.6676	184.9609229	9.0822	184.956397	9.158	184.9616639	9.3697
184.9537121	8.6713	184.9625778	9.1047	184.958053	9.178	184.9633188	9.4099
184.955367	8.7098	184.9642328	9.1292	184.9596959	9.1593	184.9649618	9.3294
184.957022	8.7084	184.9658768	9.1549	184.9613509	9.2379	184.9666167	9.4574
184.958678	8.7402	184.9675427	9.1618	184.9630058	9.2553	184.9682717	9.4046
184.9603209	8.7842	184.9691867	9.1592	184.9646608	9.2722	184.9699276	9.4079
184.9619759	8.7724	184.9708416	9.1845	184.9663047	9.2827	184.9715826	9.4219
184.9636308	8.8153	184.9724846	9.1541	184.9679597	9.3229	184.9732376	9.4351
184.9652748	8.8485	184.9741515	9.1755	184.9696147	9.304	184.9748695	9.4243
184.9669297	8.8514	184.9757835	9.1544	184.9712696	9.3012	184.9765355	9.4173

Table B.2 cont.: *The photometric measurements of V752 Centauri.*

HJD [-2454000]	B mag.	HJD [-2454000]	V mag.	HJD [-2454000]	R mag.	HJD [-2454000]	I mag.
184.9685847	8.8646	184.9774734	9.1598	184.9729136	9.3176	184.9781564	9.4469
184.9702396	8.8837	184.9791164	9.1644	184.9745685	9.3073	184.9798114	9.4589
184.9718946	8.8301	184.9807833	9.1792	184.9762115	9.3079	184.9814543	9.4448
184.9735495	8.8515	184.9824273	9.1723	184.9778434	9.3089	184.9831093	9.4519
184.9751815	8.8638	184.9840933	9.1571	184.9794874	9.3188	184.9847762	9.4598
184.9768835	8.8562	184.9857372	9.1723	184.9811423	9.2998	184.9864312	9.4817
184.9785154	8.8452	184.9874032	9.1782	184.9827973	9.2874	184.9880751	9.4678
184.9801814	8.8494	184.9890471	9.1608	184.9844642	9.3002	184.9897301	9.4562
184.9818253	8.8609	184.9907021	9.1766	184.9861192	9.3364	184.9913851	9.4429
184.9834803	8.8562	184.992357	9.1638	184.9877622	9.2888	184.993028	9.4095
184.9851462	8.875	184.994001	9.115	184.9894171	9.2832	184.994683	9.4015
184.9868022	8.8482	184.9956559	9.083	184.9910721	9.2879	184.9963389	9.3787
184.9884451	8.8467	184.9973219	9.0696	184.992716	9.3068	184.9979939	9.4028
184.9901001	8.8437	184.9989659	9.0549	184.994371	9.2189	184.9996368	9.486
184.991744	8.8275	185.0006088	9.0148	184.9960259	9.2479	185.0013038	9.2942
184.993399	8.8456	185.0022758	8.9875	184.9976809	9.2061	185.0029587	9.3245
184.995054	8.775	185.0039197	8.9471	184.9993358	9.1958	185.0046017	9.2579
184.9967089	8.7487	185.0055747	8.9554	185.0009798	9.1441	185.0062577	9.251
184.9983639	8.7058	185.0072296	8.9153	185.0026458	9.1258	185.0079006	9.2503
185.0000078	8.7199	185.0088726	8.9033	185.0042897	9.1097	185.0095446	9.1924
185.0016738	8.6921	185.0105165	8.8759	185.0059447	9.1207	185.0111995	9.1767

Table B.2 cont.:*The photometric measurements of V752 Centauri.*

HJD [-2454000]	B mag.	HJD [-2454000]	V mag.	HJD [-2454000]	R mag.	HJD [-2454000]	I mag.
185.0033177	8.6779	185.0121715	8.8251	185.0075886	9.0686	185.0128425	9.173
185.0049727	8.6321	185.0138144	8.8302	185.0092316	9.0459	185.0144974	9.1533
185.0066276	8.5614	185.0154704	8.8005	185.0108865	9.0307	185.0161524	9.1461
185.0082706	8.6238	185.0171134	8.7999	185.0125305	9.0175	185.0177963	9.1377
185.0099146	8.5563	185.0193123	8.7635	185.0141854	8.9751	185.0199953	9.1307
185.0115695	8.524	185.0209673	8.7686	185.0158404	8.9754	185.0216502	9.1033
185.0132135	8.5261	185.0226342	8.7619	185.0174833	8.9498	185.0233052	9.0917
185.0148684	8.5227	185.0242892	8.7406	185.0196823	8.963	185.0249601	9.0775
185.0165114	8.477	185.0259441	8.7359	185.0213382	8.9185	185.0266151	9.0912
185.0187223	8.4592	185.0275881	8.7215	185.0229932	8.9029	185.0282591	9.0364
185.0203653	8.4406	185.029231	8.7269	185.0246592	8.9506	185.029914	9.0258
185.0220202	8.4525	185.030886	8.726	185.0263031	8.8843	185.031569	9.0686
185.0236872	8.4292	185.0325409	8.7261	185.0279461	8.908	185.0332129	9.0327
185.0253421	8.4134	185.0341849	8.7116	185.029601	8.8666	185.0348679	9.0577
185.0269861	8.4123	185.0358398	8.7044	185.031257	8.9103	185.0365108	9.0617
185.028629	8.4178	185.0374828	8.7032	185.0328999	8.8873	185.0381778	9.0359
185.030284	8.4102	185.0391498	8.696	185.0345549	8.8943	185.0398207	9.0385
185.031939	8.3696	185.0408047	8.6911	185.0362098	8.8686	185.0414647	9.0416
185.0335829	8.4068	185.0424257	8.6794	185.0378648	8.8623	185.0430967	9.028
185.0352379	8.3704	185.0440456	8.6832	185.0395087	8.8422	185.0447166	9.0206
185.0368928	8.3709	185.0456776	8.6987	185.0411637	8.8683	185.0463376	9.0279

Table B.2 cont.: *The photometric measurements of V752 Centauri.*

HJD [-2454000]	B mag.	HJD [-2454000]	V mag.	HJD [-2454000]	R mag.	HJD [-2454000]	I mag.
185.0385478	8.3763	185.0472975	8.6899	185.0427837	8.8603	185.0479695	8.9922
185.0402027	8.3432	185.0489295	8.6799	185.0444156	8.8305	185.0496005	8.9592
185.0418347	8.3426	185.0505504	8.6563	185.0460366	8.8273	185.0512214	9.0309
185.0434556	8.3012	185.0521814	8.6668	185.0476565	8.8414	185.0528414	8.9773
185.0450756	8.362	185.0538024	8.6688	185.0492885	8.8354	185.0544733	9.0046
185.0467076	8.3272	185.0554223	8.6485	185.0509204	8.8524	185.0560943	8.9876
185.0483275	8.3119	185.0570543	8.6342	185.0525404	8.8696	185.0577253	8.9635
185.0499595	8.3071	185.0586862	8.6229	185.0541614	8.8258	185.0593692	8.9918
185.0515804	8.2998	185.0619501	8.5979	185.0557933	8.7926	185.0625631	8.9253
185.0532124	8.3072	185.0635361	8.5792	185.0574253	8.7979	185.0641611	8.9605
185.0548323	8.3582	185.0651331	8.6253	185.0590562	8.7497	185.065758	8.9325
185.0564523	8.2685	185.066742	8.6365	185.0622511	8.7732	185.067355	8.9663
185.0580842	8.2758	185.068327	8.6089	185.0638481	8.7614	185.0689519	8.9508
185.0613372	8.2152	185.0699249	8.6473	185.065445	8.7471	185.0705379	8.9604
185.0629341	8.2157	185.0715099	8.5821	185.067043	8.7576	185.0721349	8.9628
185.0645311	8.1902	185.0731188	8.6496	185.06864	8.7835	185.0737438	8.9718
185.066128	8.2419	185.0747048	8.5974	185.0702249	8.7672	185.0753298	8.9751
185.067725	8.2582	185.0763017	8.6421	185.0718229	8.7605	185.0769267	8.9538
185.0693229	8.2707	185.0778987	8.6232	185.0734308	8.8146	185.0785237	8.9746
185.0709079	8.2638	185.0794957	8.6165	185.0750288	8.772	185.0801206	8.9729
185.0725059	8.2826	185.0810936	8.5962	185.0766137	8.7929	185.0817186	8.975

Table B.2 cont.:*The photometric measurements of V752 Centauri.*

HJD [-2454000]	B mag.	HJD [-2454000]	V mag.	HJD [-2454000]	R mag.	HJD [-2454000]	I mag.
185.0741138	8.2303	185.0826786	8.6165	185.0782117	8.7818	185.0833036	8.9892
185.0756998	8.2735	185.0842645	8.5837	185.0798087	8.7954	185.0848775	8.9829
185.0772967	8.279	185.1110458	8.6977	185.0814056	8.7724	185.1116708	9.0688
185.0788937	8.2695	185.1126428	8.6787	185.0829916	8.8052	185.1132677	9.0516
185.0804916	8.2855	185.1142287	8.7321	185.0845765	8.7986	185.1148537	9.0468
185.0820886	8.2749	185.1158257	8.7461	185.0861505	8.7902	185.1164507	9.0573
185.0836745	8.3013	185.1174236	8.7341	185.0877134	8.7911	185.1180486	9.0735
185.0852485	8.2629	185.1190206	8.7377	185.0892874	8.8192	185.1196456	9.0847
185.0868105	8.3181	185.1206055	8.7414	185.0908614	8.815	185.1212305	9.0795
185.0883844	8.3202	185.1222035	8.7723	185.1113588	8.8721	185.1228285	9.0941
185.0899584	8.2861	185.1238005	8.8042	185.1129558	8.8978	185.1244254	9.1303
185.0915213	8.2731	185.1253974	8.7307	185.1145417	8.8842	185.1260224	9.1358
185.1104438	8.3633	185.1269944	8.7928	185.1161387	8.9053	185.1276194	9.1419
185.1120418	8.3846	185.1285923	8.8552	185.1177356	8.8855	185.1292173	9.1711
185.1136267	8.3808	185.1301773	8.8542	185.1193326	8.9047	185.1308023	9.1783
185.1152237	8.408	185.1317862	8.8545	185.1209185	8.9083	185.1324112	9.2093
185.1168217	8.4199	185.1333722	8.9117	185.1225155	8.9325	185.1339852	9.1983
185.1184186	8.3976	185.1349462	8.9184	185.1241125	8.9669	185.1355481	9.2066
185.1200046	8.3944	185.1365201	8.9194	185.1257104	8.9542	185.1371331	9.2405
185.1216015	8.4266	185.1380941	8.9658	185.1273074	8.9986	185.1386961	9.2546
185.1231985	8.4725	185.139656	8.9624	185.1289043	9.0044	185.14027	9.2916

Table B.2 cont.: *The photometric measurements of V752 Centauri.*

HJD [-2454000]	B mag.	HJD [-2454000]	V mag.	HJD [-2454000]	R mag.	HJD [-2454000]	I mag.
185.1247954	8.4604	185.14123	8.9552	185.1304903	8.9862	185.141832	9.2899
185.1263924	8.4739	185.1428039	9.0412	185.1320982	9.0304	185.1434289	9.29
185.1279903	8.4888	185.1444019	9.0016	185.1336732	9.0344	185.1450269	9.3101
185.1295873	8.499	185.1459989	8.9891	185.1352472	9.0362	185.1466358	9.3775
185.1311733	8.4995	185.1475958	9.0505	185.1368211	9.0779	185.1482208	9.3817
185.1327812	8.5463	185.1491928	9.0069	185.1383951	9.1148	185.1498298	9.4171
185.1343442	8.5755	185.1519827	9.0655	185.139969	9.1099	185.1526077	9.3975
185.1359291	8.5697	185.1535797	9.1216	185.141531	9.1425	185.1542046	9.4396
185.1374921	8.5923	185.1142287	8.7321	185.1431169	9.1871	185.1557906	9.454
185.139066	8.6032	185.1158257	8.7461	185.1447139	9.1691	185.1573876	9.466
185.140629	8.5915	185.1174236	8.7341	185.1463109	9.2258	185.1589845	9.4481
185.142203	8.6511	185.1190206	8.7377	185.1479088	9.2115	185.1605815	9.4306
185.1437999	8.6883	185.1206055	8.7414	185.1495058	9.2461	185.1621784	9.4197
185.1453969	8.7301	185.1222035	8.7723	185.1522947	9.255	185.1637764	9.4602
185.1469938	8.7262	185.1238005	8.8042	185.1538916	9.2403	185.1653733	9.4269
185.1485918	8.7671	185.1253974	8.7307	185.1554776	9.2874	185.1669703	9.4741
185.1513807	8.7941	185.1269944	8.7928	185.1570746	9.3021	185.1685673	9.4096
185.1529777	8.7786	185.1285923	8.8552	185.1586725	9.306	185.1701652	9.4592
185.1545746	8.819	185.1301773	8.8542	185.1602695	9.3246	185.1717622	9.4796
185.1561606	8.8412	185.1317862	8.8545	185.1618664	9.2845	185.1733591	9.4701
185.1577695	8.843	185.1333722	8.9117	185.1634634	9.3013	185.1749331	9.4252

Table B.2 cont.:*The photometric measurements of V752 Centauri.*

HJD [-2454000]	B mag.	HJD [-2454000]	V mag.	HJD [-2454000]	R mag.	HJD [-2454000]	I mag.
185.1593545	8.8319	185.1349462	8.9184	185.1650603	9.2913	185.176496	9.4195
185.1609525	8.8606	185.1365201	8.9194	185.1666583	9.3101	185.17807	9.3564
185.1625494	8.8932	185.1380941	8.9658	185.1682553	9.3104	185.179644	9.3855
185.1641354	8.8555	185.139656	8.9624	185.1698522	9.3222	185.1812059	9.3521
185.1657323	8.8766	185.14123	8.9552	185.1714492	9.3078	185.1827799	9.341
185.1673413	8.8768	185.1428039	9.0412	185.1730471	9.2998	185.1843538	9.335
185.1689382	8.8393	185.1444019	9.0016	185.1746211	9.2851	185.1859168	9.3247
185.1705352	8.8519	185.1459989	8.9891	185.176195	9.2662	185.1874907	9.2912
185.1721212	8.8533	185.1475958	9.0505	185.177757	9.241	185.1890877	9.2729
185.1737181	8.8588	185.1491928	9.0069	185.179331	9.2414	185.1906847	9.2453
185.1752921	8.825	185.1519827	9.0655	185.1809049	9.2181	185.1942386	9.1826
185.176854	8.8262	185.1535797	9.1216	185.1824679	9.1731	185.1958355	9.2586
185.178428	8.7714	185.1551656	9.0918	185.1840418	9.1735	185.1974445	9.2682
185.1800029	8.7469	185.1567626	9.0588	185.1856158	9.1495	185.1990294	9.2934
185.1815769	8.7584	185.1583595	9.1114	185.1871777	9.1339	185.2006274	9.1098
185.1831389	8.6989	185.1599565	9.1431	185.1887757	9.1254	185.2022243	9.0496
185.1847128	8.6895	185.1615534	9.1054	185.1903727	9.1052	185.2038213	9.2388
185.1862758	8.6796	185.1631514	9.1194	185.1939256	9.0752	202.1205921	8.9561
185.1878607	8.683	185.1647364	9.1467	185.1955225	8.9673	202.123057	8.9662
185.1894587	8.6593	185.1663453	9.1088	185.1971205	9.0252	202.1047001	8.9371
185.1930226	8.6085	185.1679423	9.1033	185.1987174	9.0278	202.125522	8.9577

Table B.2 cont.: *The photometric measurements of V752 Centauri.*

HJD [-2454000]	B mag.	HJD [-2454000]	V mag.	HJD [-2454000]	R mag.	HJD [-2454000]	I mag.
185.1946085	8.6101	185.1695402	9.1044	185.2003144	8.9514	202.1067841	8.9578
185.1962055	8.5758	185.1711372	9.0674	185.2019114	9.0387	202.127987	8.9804
185.1978025	8.5612	185.1727341	9.1184	185.2035093	8.996	202.1096081	8.9595
185.1994004	8.5872	185.1743201	9.1129	202.1201061	8.7896	202.130453	8.9938
185.2009974	8.5457	185.1758821	9.119	202.122571	8.8001	202.1119811	8.9574
185.2025943	8.5657	185.177456	9.1281	202.1043991	8.7838	202.133763	9.0077
185.2041913	8.5202	185.179019	9.0994	202.125036	8.7943	202.1143991	8.9543
185.2057892	8.4896	185.1805929	9.0746	202.1064131	8.7743	202.136182	8.9997
185.2073742	8.3205	185.1821669	9.0499	202.127501	8.8161	202.1385889	9.0443
185.2089712	8.4531	185.1837408	9.0085	202.1091801	8.7906	202.1409849	9.0136
185.2105691	8.5762	185.1853028	9.0156	202.129967	8.8366	202.1433929	9.0565
202.1079761	8.286	185.1868778	8.9866	202.1115521	8.7736	202.1628368	9.1967
202.12595	8.3205	185.1884627	8.9999	202.133335	8.8275	202.1650588	9.2306
202.1052211	8.2731	185.1900597	8.9681	202.1139131	8.787	202.1675358	9.2413
202.123485	8.3086	185.1936136	8.9131	202.135754	8.8524	202.1697698	9.2958
202.1035081	8.2087	185.1952105	8.9241	202.1381609	8.858	202.1719918	9.2857
202.12102	8.3025	185.1968195	8.8297	202.1405569	8.8785	202.1770267	9.3634
202.1185551	8.3126	185.1984044	8.9238	202.1429639	8.889	202.1792607	9.4058
202.128404	8.3266	202.1195041	8.6234	202.1624668	9.0132	202.1814827	9.3984
202.1101291	8.2874	202.121969	8.6312	202.1646888	9.0555	202.1837167	9.4377
202.131795	8.3495	202.1040991	8.5674	202.1671078	9.0857	202.1859387	9.4521

Table B.2 cont.:*The photometric measurements of V752 Centauri.*

HJD [-2454000]	B mag.	HJD [-2454000]	V mag.	HJD [-2454000]	R mag.	HJD [-2454000]	I mag.
202.1124901	8.2733	202.124434	8.6455	202.1693878	9.1269	202.1914366	9.4575
202.134203	8.3597	202.1059271	8.6144	202.1716218	9.1398	202.1936696	9.4499
202.13661	8.3584	202.126899	8.6453	202.1766557	9.2098	202.1959036	9.4321
202.1390059	8.38	202.1086931	8.6255	202.1788897	9.2338	202.1981376	9.4365
202.1414129	8.3943	202.129353	8.6536	202.1811117	9.26	202.2003596	9.4634
202.1610308	8.5576	202.1110661	8.6276	202.1833457	9.301	202.2032306	9.4319
202.1632648	8.5875	202.132733	8.6752	202.1855797	9.3077	202.2054636	9.4541
202.1655568	8.6082	202.1134271	8.6255	202.1910776	9.3388	202.2076866	9.4016
202.1679638	8.6435	202.135152	8.6883	202.1932996	9.2976	202.2099315	9.3712
202.1701868	8.688	202.137559	8.7041	202.1955336	9.3005	202.2121655	9.336
202.1752207	8.7478	202.1399549	8.7102	202.1977556	9.3013	202.2150355	9.2889
202.1774547	8.782	202.1423619	8.7147	202.1999896	9.2994	202.2172575	9.2951
202.1796887	8.8236	202.1619808	8.8684	202.2028596	9.3086	202.2194915	9.241
202.1819107	8.8394	202.1642138	8.8972	202.2050936	9.3119	202.2217255	9.2084
202.1841447	8.8578	202.1665638	8.926	202.2073276	9.2517	202.2239595	9.2214
202.1896427	8.8812	202.1689018	8.9608	202.2095615	9.237	202.2263204	9.1998
202.1918646	8.8725	202.1711358	8.9897	202.2117945	9.2123	202.2285544	9.1575
202.1940986	8.8848	202.1761697	9.0546	202.2146655	9.1617	202.2307874	9.1629
202.1963206	8.8773	202.1784037	9.0934	202.2168875	9.1413	202.2330104	9.1029
202.1985546	8.8835	202.1806257	9.1215	202.2191215	9.1195	202.2352434	9.1068
202.2014126	8.8735	202.1828597	9.142	202.2213555	9.0949	202.2376974	9.073

Table B.2 cont.: *The photometric measurements of V752 Centauri.*

HJD [-2454000]	B mag.	HJD [-2454000]	V mag.	HJD [-2454000]	R mag.	HJD [-2454000]	I mag.
202.2036586	8.8498	202.1850937	9.1714	202.2235885	9.0737	202.2399314	9.0831
202.2058926	8.8163	202.1905916	9.1609	202.2259494	9.0794	202.2421654	9.0577
202.2081255	8.7893	202.1928136	9.1894	202.2281834	8.9928	203.823026	9.1446
202.2103595	8.7709	202.1950476	9.1826	202.2304174	9.0068	203.82585	9.2048
202.2132415	8.7389	202.1972696	9.1668	202.2326514	8.9142	203.828072	9.2115
202.2154525	8.7033	202.1995036	9.1594	202.2348734	8.9968	203.830306	9.2171
202.2176865	8.6698	202.2023616	9.1591	202.2373274	8.928	203.83254	9.2544
202.2199195	8.6511	202.2046076	9.1099	202.2395614	8.9184	203.834773	9.2765
202.2221535	8.6016	202.2068416	9.1032	202.2417944	8.9075	203.840109	9.3461
202.2245265	8.6125	202.2090745	9.1033	203.822655	9.0104	203.842343	9.3995
202.2267484	8.5843	202.2113085	9.0849	203.825479	9.0055	203.844565	9.4086
202.2289824	8.5626	202.2141795	9.0195	203.827702	9.068	203.846787	9.4239
202.2312164	8.533	202.2164015	9.0196	203.829947	9.0726	203.849021	9.4717
202.2334384	8.5204	202.2186355	8.9732	203.832169	9.1183	203.8522269	9.456
202.2359034	8.5017	202.2208685	8.9423	203.834403	9.1381	203.8544609	9.4686
202.2381254	8.5081	202.2231025	8.9031	203.839739	9.2151	203.8566829	9.4581
202.2403594	8.4638	202.2254635	8.8906	203.841961	9.2349	203.8589049	9.4557
203.8212201	8.5425	202.2276974	8.8772	203.844195	9.2572	203.8611389	9.4671
203.824044	8.5461	202.2299314	8.8601	203.846429	9.3047	203.8646809	9.463
203.826278	8.5622	202.2321654	8.834	203.848651	9.3057	203.8669149	9.4615
203.828512	8.608	202.2343874	8.8018	203.8518679	9.3179	203.8691369	9.4544

Table B.2 cont.:*The photometric measurements of V752 Centauri.*

HJD [-2454000]	B mag.	HJD [-2454000]	V mag.	HJD [-2454000]	R mag.	HJD [-2454000]	I mag.
203.830734	8.6345	202.2368524	8.8191	203.8540909	9.3265	203.8713709	9.442
203.832968	8.6641	202.2390744	8.7952	203.8563129	9.3119	203.8735929	9.4108
203.838315	8.7364	202.2413084	8.7884	203.8585469	9.3175	203.8823308	9.3119
203.840537	8.7523	203.8221691	8.85	203.8607689	9.3175	203.8845538	9.3156
203.84276	8.8042	203.824993	8.8835	203.8643099	9.3034	203.8867868	9.2419
203.844993	8.8264	203.827216	8.8958	203.8665439	9.3	203.8890098	9.2264
203.847216	8.8674	203.829461	8.9354	203.8687659	9.3139	203.8912428	9.1927
203.8504329	8.85	203.831683	8.9452	203.8710119	9.3054	203.8937548	9.1767
203.8526549	8.8609	203.833917	8.9679	203.8732229	9.2887	203.8959768	9.16
203.8548779	8.8579	203.839253	9.0491	203.8819488	9.1474	203.8982108	9.1352
203.8571109	8.8645	203.841486	9.1001	203.8841828	9.1309	203.9004448	9.1309
203.8593339	8.8761	203.843709	9.1222	203.8864048	9.111	203.9026668	9.0963
203.8628749	8.8646	203.845942	9.1498	203.8886388	9.0753	203.9053168	9.0837
203.8651089	8.872	203.848165	9.1661	203.8908728	9.0524	203.9074927	9.0735
203.8673309	8.8751	203.8513819	9.1612	203.8933848	9.0263	203.9096577	9.0802
203.8695649	8.8648	203.8536039	9.175	203.8956068	8.9941	203.9118337	8.9915
203.8717869	8.8658	203.8558269	9.1659	203.8978408	8.9626	203.9177937	9.0642
203.8805138	8.7081	203.8580599	9.1893	203.9000738	8.9677	203.9199587	9.0289
203.8827478	8.6891	203.8602829	9.1754	203.9023078	8.9457	203.9221347	9.005
203.8849698	8.6545	203.8638239	9.1656	203.9049468	8.9291	203.9242987	8.9898
203.8872038	8.6084	203.8660579	9.1698	203.9071227	8.9179	203.9264627	9.0014

Table B.2 cont.: *The photometric measurements of V752 Centauri.*

HJD [-2454000]	B mag.	HJD [-2454000]	V mag.	HJD [-2454000]	R mag.	HJD [-2454000]	I mag.
203.8894378	8.5784	203.8682799	9.171	203.9092867	8.8776	203.9293447	8.9709
203.8919488	8.5446	203.8705139	9.1719	203.9114627	8.9168	203.9315097	8.9695
203.8941828	8.5076	203.8727359	9.1421	203.9174237	8.8748	203.9336847	9.0342
203.8964048	8.497	203.8814628	9.0265	203.9195877	8.8351	203.9358496	8.9648
203.8986278	8.4703	203.8836968	8.9977	203.9217637	8.8425	203.9380256	8.96
203.9008728	8.4543	203.8859188	8.9681	203.9239287	8.8284	203.9407566	8.9611
203.9035228	8.4345	203.8881528	8.9215	203.9261037	8.8368	203.9429216	8.9348
203.9056878	8.4258	203.8903868	8.9054	203.9289747	8.8089	203.9451086	8.9605
203.9078517	8.4224	203.8929098	8.8661	203.9311507	8.81	203.9472846	8.9401
203.9100277	8.4358	203.8951208	8.842	203.9333147	8.8261	203.9494486	8.9776
203.9159997	8.3585	203.8973538	8.8259	203.9354906	8.8101	204.0065324	9.1273
203.9181527	8.4155	203.8995878	8.7886	203.9376546	8.8007	204.0039744	9.0666
203.9203287	8.3527	203.9018218	8.7857	203.9403866	8.7972	204.0086964	9.1354
203.9224927	8.3346	203.9044608	8.7671	203.9425626	8.7662	204.0108724	9.1445
203.9246687	8.328	203.9066367	8.7493	203.9447386	8.7898	204.0130484	9.1669
203.9275507	8.3285	203.9088127	8.7554	203.9469146	8.773	204.0152124	9.2273
203.9297157	8.3186	203.9109767	8.7346	203.9490786	8.7944	204.0274233	9.3545
203.9318797	8.2905	203.9169377	8.7119	204.0061614	8.9572	204.0300043	9.3829
203.9340557	8.301	203.9191017	8.6767	204.0036034	8.981	204.0325733	9.4154
203.9362196	8.2853	203.9212777	8.6772	204.0083264	8.9888	204.0351543	9.4277
203.9389516	8.2744	203.9234417	8.6697	204.0105024	9.0055	204.0377353	9.4452

Table B.2 cont.:*The photometric measurements of V752 Centauri.*

HJD [-2454000]	B mag.	HJD [-2454000]	V mag.	HJD [-2454000]	R mag.	HJD [-2454000]	I mag.
203.9411276	8.2741	203.9256177	8.6612	204.0126784	9.0271	204.0405943	9.4429
203.9432916	8.2901	203.9284887	8.649	204.0148424	9.0629	204.0431753	9.4825
203.9454786	8.2787	203.9306647	8.646	204.0269953	9.192	204.0457563	9.4472
203.9476436	8.2967	203.9328287	8.6418	204.0295763	9.2367	204.124958	8.9451
204.0047264	8.4798	203.9350046	8.6431	204.0321453	9.2539	204.127527	8.9617
204.0021684	8.4745	203.9371686	8.6511	204.0347263	9.2891	204.130108	8.94
204.0068904	8.4782	203.9399006	8.6269	204.0373193	9.2976	204.132701	8.9786
204.0090664	8.5285	203.9420766	8.6283	204.0401663	9.2941	204.135282	8.9487
204.0112424	8.5375	203.9442526	8.6202	204.0427473	9.3006	204.137851	8.9539
204.0134184	8.5463	203.9464286	8.6377	204.0453403	9.2928	204.140432	8.9544
204.0253283	8.7209	203.9485926	8.6311	204.124529	8.7757	204.143013	8.9378
204.0279093	8.7435	204.0056754	8.821	204.127099	8.7893	204.1455829	8.9584
204.0304903	8.7883	204.0031174	8.7817	204.12968	8.7961	204.1481639	8.9686
204.0330593	8.8231	204.0078404	8.824	204.132272	8.7966	204.1508949	8.9747
204.0356403	8.8558	204.0100154	8.8473	204.134853	8.7818	204.1534879	8.9851
204.0384993	8.8643	204.0121914	8.8921	204.137423	8.7718	204.1560569	8.9744
204.0410803	8.8752	204.0143674	8.8849	204.140004	8.7821	204.1586379	8.9829
204.0436613	8.8564	204.0263933	9.0492	204.142585	8.7986	204.1612189	9.0096
204.0627012	8.7269	204.0289743	9.0792	204.1451659	8.8028	204.1637889	8.9965
204.122874	8.2962	204.0315433	9.1067	204.1477349	8.8031	204.1663699	9.0209
204.125444	8.2994	204.0341243	9.1353	204.1504669	8.8298	204.1689509	9.0111

Table B.2 cont.: *The photometric measurements of V752 Centauri.*

HJD [-2454000]	B mag.	HJD [-2454000]	V mag.	HJD [-2454000]	R mag.	HJD [-2454000]	I mag.
204.128013	8.2947	204.0366943	9.1453	204.1530479	8.8062	204.1715319	9.0193
204.130606	8.3316	204.0395643	9.1602	204.1556289	8.8173	204.1741009	9.0472
204.133187	8.2989	204.0421453	9.1682	204.1582099	8.8149	204.1807908	9.0548
204.135768	8.295	204.0447263	9.1311	204.1607909	8.8437	204.1833598	9.0982
204.138337	8.2965	204.123928	8.6562	204.1633599	8.8333	204.1859528	9.0945
204.140918	8.2951	204.126497	8.6196	204.1659409	8.8569	204.1885218	9.1177
204.143499	8.3065	204.129078	8.6188	204.1685219	8.8552	204.1911028	9.1481
204.1460689	8.3118	204.131671	8.6275	204.1711029	8.8907	204.1936728	9.1722
204.1488119	8.3369	204.134252	8.6364	204.1736729	8.8719	204.1962538	9.2085
204.1513809	8.3286	204.136833	8.6151	204.1803628	8.9085	204.1988348	9.1969
204.1539619	8.3298	204.139402	8.6113	204.1829438	8.9458	204.2014158	9.2409
204.1565429	8.3372	204.141983	8.6126	204.1855248	8.9689	204.2039968	9.2689
204.1591239	8.358	204.1445639	8.6389	204.1880938	8.9659	204.2068787	9.3333
204.1617049	8.3559	204.1471339	8.6362	204.1906748	9.002	204.2094597	9.3505
204.1642749	8.3756	204.1498649	8.6443	204.1932558	9.012	204.2120407	9.3754
204.1668559	8.3887	204.1524459	8.6462	204.1958368	9.0448	204.2146217	9.4255
204.1694369	8.3855	204.1550269	8.6592	204.1984068	9.0685	204.2172027	9.4394
204.1720059	8.4166	204.1576079	8.6739	204.2009878	9.1167	204.2197717	9.486
204.1786958	8.4481	204.1601889	8.6581	204.2035688	9.1276	204.2223527	9.4516
204.1812768	8.4751	204.1627699	8.6862	204.2064508	9.1763	204.2249227	9.4749
204.1838468	8.4902	204.1653399	8.6763	204.2090317	9.2107	204.2275037	9.4743

Table B.2 cont.:*The photometric measurements of V752 Centauri.*

HJD [-2454000]	B mag.	HJD [-2454000]	V mag.	HJD [-2454000]	R mag.	HJD [-2454000]	I mag.
204.1864278	8.5087	204.1679209	8.6936	204.2116237	9.2486	204.2300847	9.4365
204.1890088	8.5166	204.1704899	8.6974	204.2141937	9.268	204.2333597	9.4734
204.1915898	8.5525	204.1730709	8.7245	204.2167747	9.3111	204.2359407	9.4163
204.1941588	8.587	204.1797608	8.7675	204.2193437	9.3413	205.8081133	8.9295
204.1967398	8.6072	204.1823418	8.7714	204.2219247	9.3267	205.8101743	8.9197
204.1993208	8.6538	204.1849228	8.7888	204.2244947	9.3292	205.8122223	8.9088
204.2019018	8.6995	204.1875038	8.797	204.2270757	9.334	205.8142713	8.9165
204.2047958	8.7317	204.1900728	8.8166	204.2296567	9.3436	205.8163313	8.9448
204.2073647	8.7373	204.1926538	8.8471	204.2329317	9.3242	205.8185183	8.9197
204.2099457	8.798	204.1952238	8.8767	204.2355127	9.3258	205.8205903	8.9341
204.2125267	8.8378	204.1978048	8.9016	205.8077433	8.7568	205.8261923	8.9714
204.2151077	8.8757	204.2003858	8.9343	205.8098033	8.7514	205.8280213	8.9471
204.2176887	8.9177	204.2029668	8.9669	205.8118523	8.7667	205.8298383	8.96
204.2202587	8.9231	204.2058598	9.0301	205.8139123	8.7589	205.8316673	8.9778
204.2228397	8.9074	204.2084297	9.0463	205.8159613	8.7627	205.8334843	8.9991
204.2254087	8.9228	204.2110107	9.1048	205.8181603	8.7657	205.8354173	8.9893
204.2279897	8.8955	204.2135917	9.1402	205.8202203	8.7768	205.8372453	8.9719
204.2312647	8.9392	204.2161727	9.1768	205.8258333	8.7773	205.8390743	9.0291
205.8064353	8.2465	204.2187417	9.1953	205.8276503	8.8048	205.8408913	9.0109
205.8084843	8.2505	204.2213227	9.2055	205.8294683	8.7978	205.8427203	9.0243
205.8105443	8.2268	204.2239037	9.1919	205.8312963	8.8211	205.8464703	9.0678

Table B.2 cont.: *The photometric measurements of V752 Centauri.*

HJD [-2454000]	B mag.	HJD [-2454000]	V mag.	HJD [-2454000]	R mag.	HJD [-2454000]	I mag.
205.8125933	8.2446	204.2264737	9.1781	205.8331133	8.818	205.8482413	9.0578
205.8146413	8.2503	204.2290547	9.1829	205.8350463	8.8225	205.8500003	9.0198
205.8168403	8.2426	204.2323417	9.1831	205.8368753	8.8328	205.8517823	9.0547
205.8188893	8.2516	204.2349107	9.2233	205.8387043	8.8417	205.8535423	9.0625
205.8247453	8.2901	205.8072683	8.5768	205.8405213	8.84	205.8575693	9.1354
205.8265623	8.2814	205.8093173	8.5846	205.8423493	8.857	205.8593863	9.1588
205.8283803	8.2766	205.8113663	8.5919	205.8460993	8.8815	205.8612153	9.1486
205.8302083	8.2918	205.8134263	8.5882	205.8478703	8.8778	205.8630323	9.1649
205.8320253	8.3123	205.8154743	8.6049	205.8496303	8.8974	205.8648733	9.1883
205.8339703	8.3059	205.8176743	8.6049	205.8514003	8.9102	205.8667133	9.184
205.8357873	8.3238	205.8197223	8.6242	205.8531713	8.9229	205.8685533	9.2144
205.8376163	8.339	205.8253473	8.6269	205.8571993	8.9648	205.8703703	9.2323
205.8394443	8.3462	205.8271643	8.6344	205.8590163	8.9704	205.8721993	9.2606
205.8412613	8.3548	205.8289813	8.6387	205.8608453	8.9869	205.8740283	9.2733
205.8450233	8.3642	205.8308103	8.6593	205.8626623	9.0109	205.8760423	9.3312
205.8467823	8.3876	205.8326273	8.6574	205.8645023	9.0274	205.8798963	9.3685
205.8485533	8.4065	205.8345603	8.6477	205.8663433	9.0369	205.8778593	9.3406
205.8503123	8.4286	205.8363893	8.6749	205.8681713	9.0756	205.8816783	9.3477
205.8520833	8.4197	205.8382183	8.6765	205.8700113	9.0926	205.8834373	9.3975
205.8560993	8.4476	205.8400353	8.6766	205.8718403	9.1186	205.8852083	9.4219
205.8579283	8.4735	205.8418633	8.682	205.8736573	9.1178	205.8869793	9.4061

Table B.2 cont.:*The photometric measurements of V752 Centauri.*

HJD [-2454000]	B mag.	HJD [-2454000]	V mag.	HJD [-2454000]	R mag.	HJD [-2454000]	I mag.
205.8597573	8.4853	205.8456133	8.7245	205.8756713	9.1602	205.8888083	9.4183
205.8615863	8.4767	205.8473843	8.7275	205.8795373	9.2053	205.8905793	9.4432
205.8634143	8.5173	205.8491553	8.7289	205.8774883	9.1834	205.8923613	9.4444
205.8652663	8.5465	205.8509143	8.7345	205.8812963	9.243	205.8941203	9.4415
205.8670833	8.5628	205.8526853	8.7613	205.8830673	9.241	205.8958803	9.4517
205.8689123	8.6226	205.8567133	8.7919	205.8848383	9.2723	205.8986233	9.4057
205.8707413	8.6371	205.8585303	8.8082	205.8865973	9.2816	205.9003933	9.4739
205.8725693	8.649	205.8603593	8.8146	205.8884373	9.2967	205.9021532	9.4685
205.8745833	8.6767	205.8621873	8.8332	205.8902083	9.2964	205.9039242	9.4845
205.8784263	8.7096	205.8640163	8.8512	205.8919793	9.2926	205.9056942	9.4376
205.8764123	8.6789	205.8658563	8.8802	205.8937503	9.2997	205.9077432	9.398
205.8802083	8.7418	205.8676853	8.9118	205.8955093	9.2991	205.9095142	9.3941
205.8819793	8.768	205.8695253	8.9213	205.8982523	9.3	205.9112852	9.3689
205.8837613	8.8087	205.8713433	8.9532	205.9000233	9.2935	205.9130552	9.3696
205.8855213	8.7838	205.8731713	8.9812	205.9017822	9.2961	205.9148382	9.3355
205.8873613	8.8176	205.8751743	9.0008	205.9035532	9.2911	205.9181712	9.299
205.8891203	8.8573	205.8790283	9.0456	205.9053242	9.2851	205.9199422	9.2638
205.8908913	8.8222	205.8770143	9.0242	205.9073732	9.2713	205.9232752	9.191
205.8926623	8.8407	205.8808103	9.0716	205.9091432	9.243	205.9250462	9.1859
205.8944213	8.8187	205.8825813	9.1078	205.9109262	9.2148	205.9268292	9.1729
205.8971763	8.8351	205.8843523	9.1221	205.9126972	9.1962	205.9286112	9.1627

Table B.2 cont.: *The photometric measurements of V752 Centauri.*

HJD [-2454000]	B mag.	HJD [-2454000]	V mag.	HJD [-2454000]	R mag.	HJD [-2454000]	I mag.
205.8989353	8.8535	205.8861233	9.1303	205.9144562	9.1529	205.9303932	9.1623
205.9007063	8.8419	205.8879513	9.1408	205.9178012	9.1372	205.9333562	9.1251
205.9024652	8.8373	205.8897223	9.1624	205.9195602	9.1137	205.9351392	9.1271
205.9042362	8.7968	205.8914933	9.1656	205.9229282	9.0579	205.9369212	9.1042
205.9062962	8.8148	205.8932643	9.1542	205.9246992	9.0484	205.9387042	9.0681
205.9080552	8.8081	205.8950233	9.1489	205.9264812	9.0262	205.9404862	9.0498
205.9098262	8.7682	205.8977663	9.1561	205.9282642	9	205.9427892	9.0428
205.9116092	8.7224	205.8995373	9.1609	205.9300462	8.9834	205.9444442	9.0519
205.9133682	8.7138	205.9012962	9.1453	205.9330092	8.9682	205.9460882	9.0331
205.9167242	8.65	205.9030672	9.1526	205.9347922	8.942	205.9477432	9.0531
205.9184842	8.6258	205.9048382	9.1242	205.9365742	8.934	205.9493982	9.0413
205.9218402	8.5903	205.9068862	9.1138	205.9383562	8.9046	205.9568172	9.0149
205.9236112	8.5791	205.9086572	9.1059	205.9401392	8.9002	205.9584612	8.9924
205.9254052	8.5351	205.9104282	9.0606	205.9424772	8.9139	205.9601272	8.9559
205.9271762	8.5275	205.9122112	9.0542	205.9441322	8.8938	205.9617822	8.9805
205.9289582	8.52	205.9139702	9.0396	205.9457752	8.8603	205.9634372	8.9402
205.9319212	8.4834	205.9173152	8.9784	205.9474302	8.8584	205.9698732	8.9416
205.9337042	8.476	205.9190742	8.9379	205.9490862	8.8672	205.9715622	8.9568
205.9354862	8.4451	205.9224422	8.9065	205.9565052	8.8176	205.9732412	8.9619
205.9372802	8.4101	205.9242242	8.9002	205.9581602	8.8474	205.9749422	8.9607
205.9390512	8.4023	205.9259952	8.8755	205.9598152	8.8365	205.9766432	8.9655

Table B.2 cont.:*The photometric measurements of V752 Centauri.*

HJD [-2454000]	B mag.	HJD [-2454000]	V mag.	HJD [-2454000]	R mag.	HJD [-2454000]	I mag.
205.9414582	8.422	205.9277782	8.8666	205.9614702	8.8194	205.9784142	8.9691
205.9431022	8.4038	205.9295602	8.827	205.9631252	8.8107	205.9800002	8.9352
205.9447572	8.4088	205.9325232	8.8178	205.9695252	8.7796	205.9815972	8.9341
205.9464002	8.3928	205.9343172	8.7708	205.9712152	8.7854	205.9831942	8.9239
205.9480672	8.3672	205.9360882	8.7768	205.9728932	8.7765	205.9847802	8.9647
205.9554742	8.3545	205.9378822	8.7669	205.9745952	8.765	205.9867362	8.9731
205.9571302	8.3303	205.9396532	8.7376	205.9762852	8.7655	205.9883332	8.9746
205.9587732	8.3249	205.9420492	8.7297	205.9781022	8.7718	205.9899192	8.9712
205.9604402	8.2957	205.9437042	8.7243	205.9796872	8.7783	205.9915282	8.9698
205.9620952	8.2944	205.9453592	8.7179	205.9812852	8.779	205.9931252	9.0027
205.9685302	8.2693	205.9470142	8.7197	205.9828822	8.7676	205.9952082	8.9504
205.9702202	8.2953	205.9486572	8.7055	205.9844682	8.7737	205.9968172	8.9148
205.9719102	8.3438	205.9560762	8.6876	205.9864242	8.7863	205.9984142	8.9542
205.9735992	8.267	205.9577312	8.6733	205.9880212	8.7704	206.0000112	8.9509
205.9752892	8.2627	205.9593862	8.6629	205.9896062	8.7852	206.0015972	8.9514
205.9771302	8.2614	205.9610532	8.6436	205.9912042	8.7869	206.0052202	8.9614
205.9787272	8.2609	205.9627082	8.6309	205.9928122	8.7989	206.0068172	8.9575
205.9803122	8.265	205.9691322	8.6152	205.9948962	8.7771	206.0084142	8.9264
205.9819102	8.2731	205.9708222	8.6111	205.9964932	8.7925	206.0100111	9.0107
205.9835072	8.272	205.9725112	8.5942	205.9981022	8.7779	206.0115971	9.0162
205.9854512	8.2725	205.9742012	8.6055	205.9996992	8.7901	206.0135071	8.9949

Table B.2 cont.: *The photometric measurements of V752 Centauri.*

HJD [-2454000]	B mag.	HJD [-2454000]	V mag.	HJD [-2454000]	R mag.	HJD [-2454000]	I mag.
205.9870492	8.2874	205.9758912	8.6133	206.0012962	8.7847	206.0151041	9.0213
205.9886462	8.287	205.9777312	8.6041	206.0049072	8.7973	206.0167131	9.0091
205.9902312	8.3113	205.9793292	8.6241	206.0065052	8.8262	206.0183101	9.0358
205.9918402	8.2926	205.9809142	8.6177	206.0081022	8.8255	206.0199071	9.0539
205.9939352	8.2953	205.9825112	8.6227	206.0096991	8.8168	206.0215741	9.0364
205.9955212	8.2848	205.9841092	8.6229	206.0112961	8.8423	206.0231711	9.0517
205.9971302	8.2735	205.9860532	8.6124	206.0132061	8.8141	206.0247681	9.033
205.9987272	8.2962	205.9876502	8.6252	206.0147921	8.8377	206.0263541	9.07
206.0003242	8.3128	205.9892362	8.5916	206.0163771	8.8564	206.0279631	9.0732
206.0039352	8.3147	205.9908332	8.6224	206.0179981	8.86	206.0296411	9.0323
206.0055322	8.3301	205.9924422	8.6077	206.0195951	8.8467	206.0312381	9.0415
206.0071302	8.3144	205.9945252	8.6194	206.0212611	8.87	206.0328361	9.1241
206.0087272	8.3178	205.9961232	8.621	206.0228591	8.8738	206.0344331	9.0958
206.0103121	8.3144	205.9977312	8.6275	206.0244561	8.8472	206.0360181	9.0757
206.0122221	8.314	205.9993292	8.6345	206.0260531	8.8891	206.0384721	9.104
206.0138191	8.3373	206.0009142	8.6424	206.0276501	8.8886	206.0400691	9.1673
206.0154171	8.3579	206.0045372	8.6365	206.0293291	8.9095	206.0416671	9.1471
206.0170251	8.3703	206.0061342	8.647	206.0309261	8.9107	206.0432641	9.1377
206.0186231	8.3368	206.0077312	8.6677	206.0325231	8.9297	206.0448611	9.1597
206.0203011	8.3648	206.0093291	8.6683	206.0341201	8.9278	206.0466091	9.1764
206.0218861	8.4029	206.0109261	8.6897	206.0357061	8.9253	206.0481941	9.1749

Table B.2 cont.:*The photometric measurements of V752 Centauri.*

HJD [-2454000]	B mag.	HJD [-2454000]	V mag.	HJD [-2454000]	R mag.	HJD [-2454000]	I mag.
206.0234841	8.3857	206.0128241	8.6598	206.0381601	8.9533	206.0497921	9.2147
206.0250811	8.3661	206.0144211	8.6775	206.0397571	8.9716	206.0513891	9.2358
206.0266781	8.4093	206.0160181	8.6961	206.0413541	8.9504	206.0529861	9.2821
206.0283681	8.4162	206.0176271	8.6703	206.0429511	8.9923	206.0546301	9.2826
206.0299651	8.4145	206.0192241	8.6952	206.0445491	9.0094	206.0562271	9.2784
206.0315511	8.4654	206.0208911	8.6909	206.0462851	8.992	206.0578241	9.3368
206.0331481	8.4495	206.0224881	8.7137	206.0478821	9.0287	206.0594211	9.3682
206.0347451	8.4586	206.0240971	8.6984	206.0494791	9.0296	206.0610181	9.3703
206.0371871	8.4654	206.0256831	8.7451	206.0510881	9.0791	206.0633561	9.3979
206.0387851	8.4785	206.0272801	8.7247	206.0526741	9.0929	206.0649421	9.3785
206.0403821	8.505	206.0289701	8.7428	206.0543171	9.1288	206.0667361	9.4239
206.0419791	8.5044	206.0305551	8.7564	206.0559141	9.1361	206.0683221	9.456
206.0435761	8.5153	206.0321531	8.7546	206.0575111	9.17	206.0699191	9.4466
206.0453361	8.5391	206.0337501	8.7663	206.0591091	9.1886	206.0715281	9.4975
206.0469101	8.5786	206.0353471	8.7898	206.0607061	9.202	206.0731251	9.4523
206.0485071	8.5859	206.0377891	8.8608	206.0630321	9.2313	206.0747221	9.4542
206.0501041	8.5998	206.0393861	8.7929	206.0646301	9.264	206.0763191	9.431
206.0517011	8.6221	206.0409841	8.8086	206.0664241	9.278	206.0779171	9.4719
206.0533451	8.6456	206.0425691	8.8475	206.0680211	9.2934	206.0795141	9.472
206.0549421	8.6761	206.0441781	8.8397	206.0696061	9.3062	206.0811111	9.4921
206.0565391	8.6791	206.0459261	8.8763	206.0712151	9.3078	206.0912611	9.4585

Table B.2 cont.: *The photometric measurements of V752 Centauri.*

HJD [-2454000]	B mag.	HJD [-2454000]	V mag.	HJD [-2454000]	R mag.	HJD [-2454000]	I mag.
206.0581481	8.7224	206.0475111	8.8842	206.0728121	9.3246	206.0928591	9.4281
206.0597341	8.7215	206.0491091	8.9102	206.0744101	9.3148	206.0944561	9.3669
206.0620721	8.7907	206.0507061	8.9021	206.0760071	9.3416	206.0960421	9.3464
206.0636691	8.7969	206.0523031	8.9408	206.0776041	9.3193	206.0976391	9.3514
206.0654511	8.8231	206.0539471	8.963	206.0792011	9.3177	206.0992361	9.3748
206.0670491	8.8351	206.0555551	8.9932	206.0807991	9.3416	206.1008331	9.348
206.0686341	8.8375	206.0571411	8.9829	206.0909611	9.3234	206.1024301	9.3234
206.0702311	8.8862	206.0587501	9.0276	206.0925461	9.3111	206.1040161	9.284
206.0718401	8.9024	206.0603361	9.0478	206.0941321	9.3061	206.1056131	9.2357
206.0734371	8.8601	206.0626621	9.0841	206.0957291	9.2944	206.1142241	9.1765
206.0750351	8.8965	206.0642711	9.1032	206.0973261	9.2379	206.1164001	9.1855
206.0766431	8.8815	206.0660531	9.1351	206.0989241	9.2182	206.1185651	9.1283
206.0782291	8.8791	206.0676501	9.1623	206.1005211	9.2132	206.1207291	9.1272
206.0798261	8.8369	206.0692361	9.1636	206.1021181	9.1832	206.1229171	9.1305
206.0899771	8.9004	206.0708451	9.1668	206.1037041	9.1664	206.1250811	9.1086
206.0915741	8.8577	206.0724421	9.1501	206.1053011	9.1185	206.1272681	9.0525
206.0931711	8.8401	206.0740391	9.177	206.1138541	9.0226	206.1294331	9.077
206.0947571	8.785	206.0756361	9.1811	206.1160301	9.0285	206.1316091	9.0416
206.0963541	8.777	206.0772341	9.1672	206.1181941	8.9864	206.1337731	9.1106
206.0979511	8.7696	206.0788311	9.1846	206.1203701	8.9323	206.1364241	9.0599
206.0995491	8.7659	206.0804281	9.1657	206.1225461	8.9765	206.138599	9.0534

Table B.2 cont.:*The photometric measurements of V752 Centauri.*

HJD [-2454000]	B mag.	HJD [-2454000]	V mag.	HJD [-2454000]	R mag.	HJD [-2454000]	I mag.
206.1011461	8.7454	206.0905791	9.1825	206.1247111	8.9205	206.140775	8.9318
206.1027431	8.6965	206.0921761	9.1485	206.1268981	8.8856	206.14294	9.0456
206.1043291	8.6681	206.0937731	9.1568	206.1290621	8.8965	206.145116	8.9769
206.1124881	8.5615	206.0953701	9.1439	206.1312381	8.9048	206.14728	9.0264
206.1146531	8.5308	206.0969561	9.1466	206.1334141	8.8681	206.149456	8.9963
206.1168171	8.4878	206.0985531	9.0964	206.1360651	8.8711	206.15162	8.9932
206.1189931	8.4848	206.1001501	9.0839	206.138229	8.8566	206.153785	8.9941
206.1211571	8.4567	206.1017481	9.0625	206.140405	8.8518	206.155961	8.9533
206.1233331	8.4352	206.1033331	9.0206	206.142569	8.8385	206.159248	9.0429
206.1255091	8.4303	206.1049301	8.9922	206.144745	8.8397	206.161424	9.0179
206.1276971	8.4379	206.1134261	8.9099	206.14691	8.8863	206.163599	8.9292
206.1298611	8.4113	206.1156021	8.8262	206.149086	8.7976	206.165764	8.9602
206.1320371	8.4206	206.1177661	8.8413	206.15125	8.8283	206.16794	8.9455
206.1346761	8.3498	206.1199421	8.8239	206.153426	8.8926	206.17912	8.9629
206.1368521	8.3639	206.1221181	8.7425	206.15559	8.8416	206.181169	8.9492
206.139028	8.3955	206.1242821	8.7729	206.158877	8.8209	206.183229	8.9693
206.141204	8.4716	206.1264701	8.7658	206.161053	8.9093	206.185289	8.9475
206.143368	8.3707	206.1286341	8.7568	206.163229	8.8242	206.187338	8.9693
206.145544	8.356	206.1308101	8.7385	206.165405	8.7705	206.189398	8.9191
206.147708	8.3374	206.1329861	8.787	206.167569	8.7593	206.191447	9.0625
206.149873	8.3863	206.1356251	8.7167	206.178808	8.7713	206.193507	8.9655

Table B.2 cont.: *The photometric measurements of V752 Centauri.*

HJD [-2454000]	B mag.	HJD [-2454000]	V mag.	HJD [-2454000]	R mag.	HJD [-2454000]	I mag.
206.152049	8.3335	206.137801	8.6962	206.180856	8.773	206.195567	8.9765
206.154213	8.3284	206.139977	8.7429	206.182917	8.7811	206.197616	8.9795
206.157511	8.3134	206.142153	8.6959	206.187025	8.7866	206.200289	9.0116
206.159676	8.3155	206.144317	8.6834	206.189086	8.8016	206.202338	9.0038
206.161852	8.265	206.146481	8.6768	206.191134	8.8097	206.204398	9.0119
206.164028	8.3055	206.148657	8.6209	206.193194	8.7924	206.206458	9.0044
206.166192	8.2603	206.150822	8.6649	206.195255	8.8176	206.208518	9.0135
206.17743	8.2658	206.152998	8.6922	206.197303	8.8376	206.210579	9.0665
206.179479	8.2727	206.155162	8.6278	206.199954	8.8218	206.212639	9.0261
206.181539	8.2693	206.158449	8.6461	206.202025	8.804	206.214699	9.0471
206.183599	8.2818	206.160625	8.6658	206.204074	8.8462	206.216759	9.0725
206.18566	8.2791	206.162801	8.6937	206.206146	8.8408	206.218808	9.0854
206.187708	8.2738	206.164977	8.6096	206.208206	8.8325	206.226366	9.1703
206.189768	8.302	206.167141	8.5985	206.210266	8.8676	206.228426	9.1922
206.191817	8.2823	206.17838	8.5981	206.212326	8.8767	206.230474	9.1543
206.193877	8.3001	206.180428	8.5893	206.214386	8.9048	206.232535	9.1866
206.195937	8.3344	206.182488	8.6028	206.216447	8.8994	206.234595	9.2167
206.198576	8.3298	206.184549	8.6004	206.218495	8.8738		
206.200648	8.3156	206.186609	8.6283	206.226053	8.9704		
206.202697	8.3448	206.188657	8.6045	206.228113	8.9823		
206.204768	8.356	206.190718	8.7203	206.230162	9.0527		

Table B.2 cont.:*The photometric measurements of V752 Centauri.*

HJD [-2454000]	B mag.	HJD [-2454000]	V mag.	HJD [-2454000]	R mag.	HJD [-2454000]	I mag.
206.206829	8.3701	206.192766	8.6246	206.232222	8.9599		
206.208877	8.3703	206.194826	8.6194	206.234282	9.103		
206.210949	8.3974	206.196886	8.6384				
206.213009	8.401	206.199525	8.6618				
206.215069	8.3953	206.201597	8.6537				
206.21713	8.4488	206.203646	8.6693				
206.224676	8.4732	206.205718	8.6678				
206.226736	8.5391	206.207778	8.6785				
206.228796	8.533	206.209838	8.7167				
206.230856	8.559	206.211898	8.7074				
206.232905	8.5751	206.213958	8.7345				
		206.216018	8.7484				
		206.218067	8.7274				
		206.225636	8.7919				
		206.227685	8.8265				
		206.229745	8.8432				
		206.231794	8.8642				
		206.233854	8.8746				

Table B.3: *The 1997 photometric measurements of V392 Carinae.*

HJD [-2450000]	Stromgren B	HJD [-2450000]	Stromgren Y
475.9785443	9.5602	475.9715889	9.459
475.9836829	9.5708	475.9764725	9.4843
475.9876066	9.5746	475.981901	9.4566
475.9911942	9.582	475.9858007	9.4554
475.9948279	9.5764	475.9892844	9.4679
476.0005914	9.5755	475.9929181	9.4738
476.0044331	9.5744	475.9986126	9.4743
476.0093987	9.5853	476.0025813	9.48
476.0153932	9.5735	476.006262	9.4904
476.0189109	9.5739	476.0115395	9.4909
476.0228925	9.5665	476.017117	9.4704
476.0264912	9.5764	476.0207047	9.458
476.0537929	9.5176	476.0247674	9.4827
476.0592894	9.5818	476.028424	9.4813
476.0627501	9.5564	476.0573916	9.4786
476.0664998	9.5865	476.0610142	9.4585
476.0702265	9.5804	476.0646829	9.4567
476.0739641	9.5567	476.0682586	9.4423
476.0852132	9.5832	476.0720783	9.4514
476.0897618	9.5877	476.0757	9.4486
476.0943104	9.5728	476.0830613	9.4714
476.1054314	9.5787	476.087574	9.5425
476.110049	9.5784	476.0918916	9.4822
476.1135787	9.5727	476.1010228	9.4821
476.1174904	9.5718	476.1081052	9.411
476.122027	9.5828	476.1117039	9.4723
476.1283235	9.5672	476.1158705	9.4653
476.1321421	9.5946	476.1197362	9.4808
476.1387626	9.5546	476.1303943	9.4536
476.1427312	9.5355	476.1369687	9.4551
476.1469099	9.6228	476.1408454	9.4915
476.1519674	9.572	476.144711	9.4902
476.1578809	9.5598	476.1500346	9.4588

Table B.3 cont.: *The photometric measurements of V392 Carinae.*

HJD [-2450000]	Stromgren B	HJD [-2450000]	Stromgren Y
475.9736838	9.576	476.1545592	9.4737
476.9059419	9.5719	476.0798666	9.4584
476.9093677	9.5761	476.9750331	9.4837
476.9128854	9.5766	476.9708434	9.4791
476.9161841	9.5716	476.9668978	9.4417
476.9193898	9.5843	476.963715	9.471
476.9232665	9.5769	476.9604513	9.4633
476.9272131	9.575	476.9570716	9.4504
476.9307778	9.5766	476.9536689	9.4542
476.9344345	9.575	476.9503822	9.4513
476.9377442	9.5776	476.9469805	9.4457
476.941043	9.5713	476.9429878	9.4427
476.9448046	9.5684	476.9394231	9.4472
476.9486353	9.572	476.9360894	9.4559
476.952037	9.5882	476.9323977	9.4533
476.9553817	9.5767	476.929088	9.453
476.9586685	9.5911	476.9256273	9.4453
476.9620832	9.5898	476.9211257	9.4488
476.9653229	9.5971	476.9178159	9.4422
476.9685526	9.5969	476.9145522	9.4452
476.9724753	9.5999	476.9111155	9.438
476.9769429	9.605	476.9076658	9.4437
476.9804496	9.6205	476.9040671	9.442
476.9843613	9.6283	476.8962668	9.4427
476.987532	9.6552	476.9785628	9.4952
476.9908417	9.6444	476.9824054	9.5004
476.9941284	9.645	476.9859581	9.5187
476.9973462	9.6577	476.9891639	9.5238
477.0006559	9.6574	476.9924736	9.5379
477.0044176	9.6636	476.9957143	9.5369
477.0076113	9.6789	476.998966	9.5412
477.011049	9.6929	477.0028197	9.5454
477.0142777	9.6954	477.0060024	9.5702

Table B.3 cont.: *The photometric measurements of V392 Carinae.*

HJD [-2450000]	Stromgren B	HJD [-2450000]	Stromgren Y
477.0176334	9.7116	477.0093361	9.5683
477.0218931	9.7056	477.0126569	9.5782
477.0256428	9.7219	494.9194096	9.4444
477.0291255	9.7117	494.9365615	9.454
477.0325282	9.7151	494.9418732	9.4609
477.0361619	9.7141	494.9482388	9.46
494.9276381	9.5612	494.9524745	9.4707
494.9393853	9.5667	494.9568372	9.4631
494.9455539	9.5728	494.961085	9.4644
494.9503566	9.5723	494.9651467	9.4626
494.9543494	9.5717	494.9691405	9.4593
494.9587821	9.574	494.9734912	9.4649
494.9630638	9.5714	494.9776929	9.4685
494.9670916	9.5772	494.9816507	9.4609
494.9714203	9.5785	494.9858864	9.4555
494.9755171	9.5815	495.0028643	9.4518
494.9795448	9.5742	495.007644	9.4602
494.9839425	9.577	495.0125867	9.445
494.9877733	9.5817	495.0164515	9.4405
495.0050752	9.5761	495.0203292	9.4631
495.0097739	9.547	495.024079	9.4562
495.0144846	9.5436	495.0281527	9.4415
495.0183504	9.555	495.0317405	9.4775
495.0222501	9.5579	495.0353863	9.4644
495.0261849	9.5554	495.039517	9.4647
495.0298996	9.5793	495.0444597	9.4681
495.0335684	9.5707	495.0505583	9.4661
495.0371682	9.5733	495.0545511	9.4574
495.0415199	9.586	495.0704181	9.4703
495.0469825	9.5736	495.0748158	9.4628
495.0525952	9.5732	495.0786935	9.4638
495.0609167	9.5497	495.0827553	9.4442
495.0726289	9.607	495.0884379	9.4703

Table B.3 cont.: *The photometric measurements of V392 Carinae.*

HJD [-2450000]	Stromgren B	HJD [-2450000]	Stromgren Y
495.0767147	9.5744	495.0925927	9.4424
495.0805334	9.5737	495.1681779	9.4535
495.0846422	9.6038	495.1725296	9.468
495.0906368	9.5736	495.871954	9.4391
495.0943986	9.5629	495.8768497	9.4491
495.1703308	9.5496	495.8806105	9.4474
495.1750065	9.5654	495.8844883	9.4527
495.0469825	9.5736	495.888353	9.4599
495.8748359	9.5612	495.8929947	9.4545
495.8787586	9.566	495.8969175	9.4602
495.8826474	9.5642	495.9006323	9.4537
495.8863051	9.5595	495.904278	9.4545
495.8903329	9.5772	495.9078658	9.4507
495.8949386	9.5606	495.9115116	9.4634
495.8987464	9.5725	495.9151574	9.4538
495.9024031	9.5714	495.9187451	9.4602
495.9060609	9.5718	495.9222289	9.4587
495.9096137	9.5753	495.9258277	9.4593
495.9133285	9.5762	495.9294045	9.457
495.9169163	9.568	495.9328533	9.4611
495.920446	9.5795	495.936811	9.4616
495.9240918	9.5714	495.9404338	9.4606
495.9275986	9.572	495.9440096	9.4595
495.9311404	9.5736	495.9476434	9.4672
495.9347861	9.5749	495.9511731	9.4529
495.9386169	9.5742	495.9547849	9.4579
495.9422387	9.5751	495.9582447	9.4547
495.9457575	9.5751	495.9620065	9.4579
495.9494372	9.5797	495.9655942	9.4569
495.95291	9.5825	495.969205	9.459
495.9564738	9.5826	495.9729548	9.4548
495.9600506	9.5736	495.9765076	9.4515
495.9638234	9.5699	495.9801073	9.4482

Table B.3 cont.: *The photometric measurements of V392 Carinae.*

HJD [-2450000]	Stromgren B	HJD [-2450000]	Stromgren Y
495.9674221	9.578	495.9839381	9.4559
495.9711379	9.5748	495.9881968	9.455
495.9746787	9.5796	495.9932895	9.4447
495.9782905	9.5775	495.9968883	9.4407
495.9819822	9.5757	496.0043998	9.449
495.986391	9.5732	496.0081606	9.4481
495.9900017	9.5784	496.0128593	9.4673
495.9950364	9.5776	496.0170261	9.4708
495.9994342	9.5788	496.0216318	9.4726
496.0062977	9.5725	496.0252546	9.477
496.0109154	9.5831	496.0288073	9.4865
496.0148852	9.5892	496.034548	9.5192
496.0196999	9.5917	496.0387727	9.5187
496.0234027	9.5991	496.0428115	9.5237
496.0269675	9.6103	496.0469662	9.5448
496.0319442	9.6182	496.050843	9.5479
496.0366429	9.6387	496.0554607	9.5738
496.0410636	9.6498	496.0591415	9.571
496.0451263	9.6542	496.0629842	9.5817
496.0488411	9.6562	496.066965	9.5828
496.0533088	9.6801	496.0714557	9.6005
496.0572316	9.6925	496.0752285	9.5958
496.0611554	9.6984	496.0793022	9.6016
496.0651021	9.7072	496.083214	9.6087
496.0693838	9.7178	496.0879707	9.6163
496.0735036	9.7247	496.0919635	9.6349
496.0811421	9.7236	496.0955512	9.6259
496.0858528	9.7231	496.099914	9.6233
496.0900766	9.7336	496.1054466	9.6041
496.0936993	9.7427	496.1139301	9.6045
496.0977151	9.7363	496.1177079	9.5851
496.1026228	9.7385	496.1224596	9.5909
496.1076105	9.7502	496.1267063	9.5859

Table B.3 cont.: *The photometric measurements of V392 Carinae.*

HJD [-2450000]	Stromgren B	HJD [-2450000]	Stromgren Y
496.1119852	9.7256	496.1310241	9.5567
496.11577	9.7251	496.1353638	9.5016
496.1204917	9.7159	496.1396805	9.5494
496.1242415	9.6997	496.1435343	9.5553
496.1289872	9.6877	496.14821	9.5121
496.1329099	9.6718	496.1531057	9.5232
496.1376896	9.6657	496.1577464	9.513
496.1417054	9.6659	496.1623871	9.4937
496.1458721	9.5912	496.1670138	9.4776
496.1506978	9.6184	496.1715076	9.4638
496.1557215	9.611	496.1739144	9.4701
496.1601883	9.6189	496.1794231	9.4634
496.16454	9.5963	496.1837638	9.4743
496.1695397	9.5854	496.1877446	9.4694
496.1817839	9.7887	496.1920963	9.4361
496.1857077	9.5738	508.1541429	9.4982
496.1899434	9.5719	508.1885735	9.5524
496.1938902	9.5728	508.0623759	9.4815
538.8581454	9.5709	508.129942	9.48
538.8627515	9.5693	508.1716182	9.4756
538.8662585	9.5714	508.0875478	9.5049
538.8695335	9.5697	508.0279444	9.4543
538.8726475	9.574	533.8445229	9.4596
538.8758306	9.577	538.8561774	9.4326
538.8789666	9.5891	538.8600894	9.4298
538.8836656	9.5332	538.8646155	9.4341
538.8870807	9.609	538.8680065	9.4429
538.8902867	9.6093	538.8710505	9.4487
538.8935277	9.6105	538.8743146	9.461
538.8966988	9.6215	538.8773466	9.4599
538.9001018	9.6368	538.8813746	9.4758
538.9033538	9.6326	538.8854257	9.4735
538.9092339	9.649	538.8887817	9.4854

Table B.3 cont.: *The photometric measurements of V392 Carinae.*

HJD [-2450000]	Stromgren B	HJD [-2450000]	Stromgren Y
538.9126589	9.6976	538.8917677	9.4869
538.9160619	9.6727	538.8950777	9.4947
538.9190719	9.6645	538.8985848	9.4946
538.925507	9.6887	538.9016638	9.5061
538.928678	9.7035	538.9048588	9.5265
538.9320811	9.7028	538.9109929	9.5176
538.9358421	9.7122	538.9145459	9.5178
538.9391871	9.7062	538.9175669	9.5181
538.9422662	9.702	538.920715	9.5656
538.9458422	9.7087	538.927058	9.624
538.9494302	9.7255	538.930356	9.5791
538.9529842	9.7233	538.9343491	9.5758
538.9561553	9.7281	538.9375321	9.5848
538.9593383	9.7182	538.9407031	9.5851
538.9634813	9.7245	538.9443612	9.5883
538.9667104	9.7179	538.9478452	9.6001
538.9697434	9.7181	538.9509582	9.5925
538.9729604	9.7119	538.9546393	9.5988
538.9769775	9.7015	538.9577873	9.5967
538.9801485	9.7159	538.9616413	9.5988
538.9833085	9.6767	538.9650094	9.5993
538.9879036	9.6818	538.9681924	9.5964
538.9909006	9.6689	538.9713404	9.6012
538.9944886	9.6578	538.9748014	9.5897
538.9977296	9.6642	538.9785285	9.5828
539.0007967	9.6456	538.9817455	9.6045
539.0045817	9.6378	538.9856345	9.5741
539.031202	9.5924	538.9893616	9.5576
539.03479	9.5816	538.9923936	9.5438
539.038019	9.5763	538.9962016	9.5515
539.041295	9.5761	538.9992347	9.5515
539.0448131	9.572	539.0022787	9.5348
539.0479501	9.5705	539.0295119	9.3498

Table B.3 cont.: *The photometric measurements of V392 Carinae.*

HJD [-2450000]	Stromgren B	HJD [-2450000]	Stromgren Y
539.0580422	9.5511	539.032823	9.4729
539.0615842	9.5649	539.036468	9.4442
539.0660983	9.5615	539.039802	9.4732
539.0699173	9.5597	539.0429731	9.448
539.0760404	9.579	539.0462601	9.453
557.9343113	9.5905	539.0498711	9.459
557.9382584	9.5963	539.0549872	9.4476
557.9421826	9.6078	539.0645593	9.4399
557.9455737	9.6116	539.0681933	9.4431
557.9503999	9.6354	539.0744893	9.4551
557.9665005	9.652	557.8527342	9.4583
557.9739428	9.5255	557.9363953	9.4895
557.9774039	9.6853	557.9399485	9.4825
557.9901584	9.7163	557.9439536	9.4982
557.9936775	9.7213	557.9478888	9.5077
557.9971266	9.7218	557.9520439	9.5169
558.0003908	9.718	557.9680855	9.5475
558.0043839	9.7221	557.9757018	9.5777
558.007601	9.7209	557.9885263	9.5904
558.0109122	9.7252	557.9917904	9.5826
558.0147433	9.716	557.9953326	9.5947
558.0177984	9.718	557.9988627	9.608
558.0212936	9.7173	558.0021148	9.6063
558.0258777	9.7003	558.006097	9.6126
558.032371	9.6944	558.0092451	9.6215
558.0370012	9.6807	558.0125432	9.5972
558.0436794	9.6636	558.0162474	9.6043
558.0471165	9.6685	558.0197195	9.6023
558.0509247	9.652	558.0243147	9.6021
558.0544668	9.6572	558.0275558	9.5895
558.0578579	9.6377	558.033922	9.5823
558.0614921	9.6398	558.0418273	9.5685
558.0649302	9.6274	558.0453455	9.5643

Table B.3 cont.: *The photometric measurements of V392 Carinae.*

HJD [-2450000]	Stromgren B	HJD [-2450000]	Stromgren Y
558.0680663	9.6064	558.0491656	9.5365
558.0715045	9.6019	558.0528118	9.5371
558.0749766	9.5982	558.0561449	9.5213
558.0783907	9.5879	558.059467	9.522
558.0818869	9.5708	558.0631942	9.5128
558.085128	9.5667	558.0665393	9.5137
558.0883801	9.5678	558.0697104	9.5133
558.0922803	9.5737	558.0731015	9.48
558.0954174	9.5826	558.0767707	9.4802
558.0988545	9.5693	558.0835419	9.4453
558.1020146	9.5648	558.086702	9.4827
558.1055678	9.5821	558.0900702	9.4769
558.1092029	9.5699	558.0938203	9.4547
558.112837	9.5858	558.0969454	9.4819
558.1163212	9.5785	558.1004986	9.4465
558.1197473	9.5961	558.1035077	9.4471
558.1233464	9.5701	558.1072578	9.4536
		558.110927	9.465
		558.1145851	9.4647
		558.1181842	9.4678
		558.1214134	9.4405

Appendix C

Radial Velocity Measurements

Table C.1: *Heliocentric Julian Date, radial velocities of component one and two of V392 Car.*

$HJD_{mid} - 2400000$	$RV_1(kms^{-1})$	$RV_2(kms^{-1})$
54232.835583143	-19.2548	51.5182
54234.061390523	109.9952	-74.6888
54234.084232116	107.4272	-72.1318
54234.960693373	-53.8038	84.9302
54235.065344339	-69.4558	99.2692
54235.811211581	-55.2738	86.1402
54274.888772668	117.2282	-80.6068
54276.054591195	-20.9928	53.1342
54277.040668752	-62.9368	94.0302
54277.062900817	-58.1858	90.6012
54277.240985496	-28.4768	60.2762
54278.021622036	114.2062	-77.0088
54278.105135733	119.2682	-81.8788
54278.159682564	121.9032	-86.4028
54278.185878545	122.6382	-86.1108
54278.212951647	123.7192	-87.0808
54307.014551109	114.1342	-79.8288
54307.047109735	112.4782	-77.6508
54307.095321037	109.4612	-73.7978

Table C.2: *Heliocentric Julian Date, radial velocities for the contact binary V752 Cen.*

$HJD_{mid} - 2400000$	$RV_1(kms^{-1})$	$HJD_{mid} - 2400000$	$RV_2(kms^{-1})$
54232.89207894	41.2782	54232.89207894	-170.3158
54232.91387871	19.2262	54232.91387871	-71.2278
54232.93661744	-63.7628	54232.93661744	21.5132
54232.95846194	20.7302	54232.98225889	190.6002
54232.98225889	-73.4018	54233.01366142	253.1332
54233.01366142	-85.7658	54233.07666409	176.5392
54233.07666409	-26.8578	54233.09819032	8.1752
54233.09819032	-73.8298	54233.12181471	-55.0758
54233.12181471	24.1862	54233.96670526	-270.6108
54233.14350644	15.7582	54233.98879723	-220.0748
54233.96670526	47.0952	54234.14560797	265.6632
54233.98879723	36.0372	54235.00528473	-172.8128
54234.14560797	-85.4798	54235.03457283	-257.0348
54235.00528473	-0.5928	54235.09720450	-227.0748
54235.03457283	10.3962	54235.12398422	-149.1488
54235.09720450	3.5582	54235.85037318	-191.8248
54235.12398422	7.4652	54235.87727418	-24.8208
54235.85037318	41.6942	54235.91610781	60.7712
54235.87727418	47.2922	54274.95030650	-19.8038
54235.91610781	-51.8078	54274.98629444	-143.4938
54274.95030650	20.8962	54275.78259558	-284.4848
54274.98629444	29.9392	54275.95840010	253.9112
54275.78259558	19.9202	54275.98416176	253.5652
54275.90367894	-18.9288	54276.01435837	200.5522
54275.95840010	-59.3418	54277.76645854	125.9592
54275.98416176	-43.9088	54277.82310389	256.7012
54276.01435837	-31.4578	54277.84935572	237.6502
54276.98496461	-29.1468	54277.99023680	-271.4998
54277.76645854	-50.8388	54278.79141956	-206.1038
54277.82310389	-54.4338	54278.87589264	133.9222
54277.84935572	-55.3818	54278.90137769	221.1592
54277.87963848	-42.4758	54278.95453974	245.2782
54277.90874379	-33.5688	54278.98253582	180.5542

Table C.2 cont.:*Heliocentric Julian Date, radial velocities for the contact binary V752 Cen.*

$HJD_{mid} - 2400000$	$RV_1(kms^{-1})$	$HJD_{mid} - 2400000$	$RV_2(kms^{-1})$
54277.93734630	-17.5718	54279.00949013	-9.5798
54277.99023680	10.9602		
54278.79141956	22.7642		
54278.81974859	11.5592		
54278.84541881	1.0992		
54278.87589264	-32.4188		
54278.90137769	-50.3318		
54278.95453974	-40.1848		
54278.98253582	-26.3728		
54279.00949013	-66.1268		

Table C.3: *The Heliocentric Julian Date and Radial Velocity measurements for the third component of V752 Cen.*

$HJD_{mid} - 2400000$	$RV(km/s^{-1})$	$HJD_{mid} - 2400000$	$RV(km/s^{-1})$
54232.892078936	24.4092	54274.986294442	32.8842
54232.913878709	25.9082	54275.782595583	2.5302
54232.936617439	26.3632	54275.903678938	-3.7678
54232.958461942	26.9182	54275.958400100	-6.5868
54232.982258893	27.7242	54275.984161762	-9.2568
54233.013661422	29.3152	54276.014358372	-11.1038
54233.076664093	30.3962	54276.984964611	-47.8278
54233.098190322	31.5942	54277.766458535	-42.0708
54233.121814708	32.0332	54277.823103885	-41.0468
54233.143506438	30.2982	54277.849355718	-39.9368
54233.966705256	29.6312	54277.879638478	-37.9578
54233.988797234	28.4072	54277.908743786	-37.7768
54234.145607970	23.8282	54277.937346299	-36.0288
54235.005284728	-18.5648	54277.990236796	-33.6698
54235.034572832	-20.2488	54278.791419558	5.2362
54235.097204496	-23.0768	54278.819748592	6.4902
54235.123984222	-25.2198	54278.845418813	8.1722
54235.850373180	-48.3938	54278.875892640	9.7672
54235.877274175	-49.5248	54278.901377689	11.3182
54235.916107808	-49.5818	54278.954539742	14.1852
54274.923787369	34.0992	54278.982535816	14.8642
54274.950306502	35.4152	54279.009490134	16.2742